AD NUMBER

AD487718

NEW LIMITATION CHANGE

TO

Approved for public release, distribution unlimited

FROM

Distribution authorized to U.S. Gov't. agencies and their contractors; Administrative/Operational use; 15 Apr 1966. Other requests shall be referred to Air Force Materials Laboratory, Research and Technology Division, Wright-Patterson Air Force Base, Ohio 45433.

AUTHORITY

AFML ltr, 7 May 1970

DMIC Report 227
April 15, 1966

COMPATIBILITY OF LIQUID AND VAPOR ALKALI METALS WITH CONSTRUCTION MATERIALS

DEFENSE METALS INFORMATION CENTER
Battelle Memorial Institute
Columbus, Ohio 43201

DMIC Report 227
April 15, 1966

COMPATIBILITY OF LIQUID AND VAPOR ALKALI METALS WITH CONSTRUCTION MATERIALS

by

J. H. Stang, E. M. Simons, J. A. DeMastry,
and J. M. Genco

to

OFFICE OF THE DIRECTOR OF DEFENSE
RESEARCH AND ENGINEERING

DEFENSE METALS INFORMATION CENTER
Battelle Memorial Institute
Columbus, Ohio 43201

TABLE OF CONTENTS

	Page
1. INTRODUCTION	1
2. SODIUM AND NaK	2
2.1. AUSTENITIC STAINLESS STEELS	2
2.1.1. Compatibility - General	2
2.1.2. Solubility Information	8
2.1.3. Detailed Loop-Test Data	8
2.1.3.1. Type 316 Stainless Steel; Inserts in and Hot Legs (1100 and 1200 F) of Pump Loops, With Type 316 or 2-1/4Cr-1Mo or 5Cr-1/2Mo-1/2Ti Alloys as the Cold Legs	8
2.1.3.2. Various Austenitic Steels: Inserts in 1110 and 1290 F Pump Loops Fabricated of 18Cr-9Ni-1Ti Steel	10
2.1.4. Carbon-Transport Behavior	10
2.1.4.1. General	10
2.1.4.2. Type 304 Stainless Steel; Equilibrium Reactions of 1000 to 1600 F Sodium-Immersed Material With Carbon	12
2.1.4.3. Various Austenitic Steels (and One Nickel-Base Alloy); Capsule-Insert Experiments to Investigate Carbon Transfer From Carbon Steels in 1200 F Sodium Environment	12
2.1.4.4. Combinations Involving Type 1043 Plain Carbon Steel	13
2.1.5. Multimetallic Loop System	13
2.1.5.1. Combination of Five Iron- and Nickel-Base Materials Incorporated Into Integral Pumping Loops Operated With 1300 to 1400 F NaK-78	13
2.1.6. Mechanical-Property Effects for Type 316 Stainless Steel	14
2.1.6.1. Type 316 Stainless Steel; Evaluation of Mechanical Properties After Sodium, Air, or Helium Exposure at 1200 F	14
2.1.6.2. Type 316 Stainless Steel; Recommended Design Stresses for Sodium Service	16
2.1.7. Nitrogen-Transport Behavior	16
2.1.7.1. Nitriding of Stainless Steel	16
2.1.7.2. Nitrogen Migration Via Dissimilar-Metal Mass Transfer	18
2.2. CHROMIUM ALLOY STEELS	19
2.2.1. Compatibility - General	19
2.2.2. Detailed Loop-Test Data	20
2.2.2.1. 2-1/4Cr-1Mo and 5Cr-1/2Mo-1/2Ti Alloys; Inserts in and Cold Legs of Pump Loops With the Same Material or Type 316 Stainless Steel as the Hot Legs	20
2.2.2.2. 2-1/4Cr-1Mo Alloy With Refractory Metal Additions; Inserts in a Thermal Loop Fabricated of Type 304 Stainless Steel	20
2.2.2.3. 12Cr-1Mo and 13Cr-1Mo Alloys; Inserts in Pump Loops Fabricated of 18Cr-9Ni-1Ti Steel	21
2.2.3. Mechanical-Property Effects	21
2.2.3.1. 2-1/4Cr-1Mo Alloy; Evaluation of Mechanical Properties After Sodium, Air, or Helium Exposure at 1100 F	21
2.2.3.2. 9Cr-1Mo Alloy; Evaluation of Mechanical Properties After Decarburization in a Type 316 Stainless Steel NaK-78 Loop at 1425 F (Isothermal) for 600 Hours	22
2.2.3.3. 9Cr-1Mo Alloy Steel; Recommended Design Stresses for Sodium Service	23

TABLE OF CONTENTS (Continued)

	Page
2.3. NICKEL- AND COBALT-BASE ALLOYS	23
2.3.1. Compatibility - General	23
2.3.2. Inconel Pump-Loop Experiments Encompassing Several Corrosion Parameters	27
2.3.2.1. Effect of Temperature	27
2.3.2.2. Effect of Temperature Differential	27
2.3.2.3. Effect of Time	27
2.3.2.4. Effect of Flow Rate	28
2.3.2.5. Effect of Sodium Versus NaK	28
2.3.2.6. Effect of Cold-Trap Operation	28
2.3.2.7. Effects of Various Oxygen-Level-Control Methods	28
2.4. ZIRCONIUM AND ZIRCONIUM ALLOYS	28
2.4.1. Compatibility - General	28
2.4.2. Zirconium Inserts Exposed to Flowing or Static Sodium and NaK for Periods up to About 2300 Hours	29
2.4.2.1. Oxidative Weight Gains	29
2.4.2.2. Dissolution Weight Losses	30
2.4.3. Zirconium and Zirconium-Alloy Inserts Exposed to Static Sodium	30
2.4.3.1. Materials	30
2.4.3.2. Oxidative Weight Gains	30
2.5. BERYLLIUM	31
2.5.1. Compatibility - General	31
2.5.2. Beryllium Exposed to 1000 F Static Sodium	31
2.5.3. Beryllium Inserts Exposed to Flowing NaK-78 or Sodium	31
2.5.3.1. Corrosion in NaK (Cold Trapped at 248 F)	31
2.5.3.2. Corrosion in NaK With Calcium or Thorium Additions	31
2.5.3.3. Corrosion in Sodium With Calcium Additions	32
2.5.4. Beryllium in Multi-metallic Loop Systems	32
2.5.4.1. General Corrosion	32
2.5.4.2. Intermetallic Compound Formation	32
2.5.4.3. Effect of Spacing	32
2.6. COLUMBIUM AND COLUMBIUM-BASE ALLOYS	33
2.6.1. Compatibility - General	33
2.6.2. Static Exposures of Columbium at 1700 and 1800 F	33
2.6.3. Exposures of Columbium and Cb-1Zr in Sodium and NaK Loops Fabricated of Another Material	33
2.6.4. Exposures of Cb-1Zr (and three other Cb-base alloys) In Monometallic Systems With Boiling (2000 to 2380 F) Sodium; Exposures Conducted in Chambers With Vacuum Levels From 10^{-6} to 10^{-9} torr	37
2.6.4.1. Loop Experiments (Cb-1Zr)	37
2.6.4.2. Refluxing Capsule Experiments (Cb-1Zr)	37
2.6.4.3. Refluxing Capsule Experiments (Cb-10W-10Ta, Cb-10W-1Zr-0.1C, Cb-5W-3Zr-0.1C)	39
2.7. VANADIUM AND VANADIUM-BASE ALLOYS	39
2.8. TANTALUM- AND TANTALUM-BASE ALLOYS	40
2.9. MOLYBDENUM	41

TABLE OF CONTENTS (Continued)

Page

2.10. TUNGSTEN 42

2.11. URANIUM, THORIUM, AND THEIR ALLOYS 42

2.12. BRAZE ALLOYS 44

2.13. GRAPHITE 44

2.14. CERMETS AND CERAMIC MATERIALS 48

3. POTASSIUM 51

3.1. COLUMBIUM ALLOYS 51

3.1.1. Compatibility - General 51
3.1.2. Cb-1Zr in Monometallic Systems 52
3.1.3. Columbium Alloys Other Than Cb-1Zr 52
3.1.4. Columbium Alloys in Heterometallic Systems 56
3.1.4.1. Cb-1Zr - Hastelloy X 56
3.1.4.2. Cb-1Zr - Austenitic Stainless Steel 58
3.1.4.3. Cb-1Zr - TZM (Mo-0.5Ti-0.08Zr) 58
3.1.4.4. Cb-1Zr - PWC-11 (Cb-1Zr-0.1C) 59
3.1.4.5. Cb-1Zr - PWC-533 (Cb-5Mo-3Ti-3Zr-0.1C) 59

3.2. MOLYBDENUM ALLOYS 59

3.2.1. Compatibility - General 59
3.2.2. Corrosion and Mass-Transfer Tests 60
3.2.3. Effects of Exposure on Mechanical Properties 61

3.3. TANTALUM ALLOYS 63

3.4. ZIRCONIUM, TITANIUM, AND HAFNIUM 64

3.5. NICKEL-, AND IRON-, AND COBALT-BASE ALLOYS 65

3.5.1. Compatibility - General 65
3.5.2. Nickel-Base Alloys 66
3.5.2.1. Inconel (78Ni-15Cr-7Fe) 66
3.5.2.2. Hastelloy X (45Ni-24Fe-22Cr-9Mo) 66
3.5.3. Steels 66
3.5.3.1. Stainless Steel 66
3.5.3.2. Carbon Steels 68
3.5.4. Haynes No. 25 (or L-605) Alloy (50Co-20Cr-15W-10Ni-3Fe-1Si-1Mn) . . . 68

3.6. BEARING MATERIALS 69

4. LITHIUM 76

4.1. GENERAL COMPATABILITY OF MATERIALS 76

4.2. COLUMBIUM ALLOYS 77

4.2.1. Compatibility - General 77
4.2.2. Unalloyed Columbium 77
4.2.3. Columbium-1 Zirconium Alloys 77
4.2.4. Loop Tests of Cb-1Zr 80
4.2.5. Miscellaneous Columbium Alloys 87

TABLE OF CONTENTS (Continued)

Page

4.3. TANTALUM 87

4.4. MOLYBDENUM ALLOYS 88

4.5. TUNGSTEN ALLOYS AND RHENIUM 88

4.6. IRON-BASE ALLOYS 89

4.7. NICKEL-BASE ALLOYS 89

5. CESIUM 91

5.1. INTRODUCTION 91

5.2. NICKEL-BASE ALLOYS 91

5.3. IRON-BASE ALLOYS 91

5.4. REFRACTORY METALS (GENERAL) 97

5.5. COLUMBIUM-BASE ALLOYS 97

5.6. MOLYBDENUM-BASE ALLOYS 99

5.7. TANTALUM-BASE ALLOYS 101

5.8. TUNGSTEN-BASE ALLOYS 103

5.9. MISCELLANEOUS MATERIALS 103

6. REFERENCES 104

COMPATIBILITY OF LIQUID AND VAPOR ALKALI METALS
WITH CONSTRUCTION MATERIALS

J. H. Stang, E. M. Simons, J. A. DeMastry, and J. M. Genco*

1. INTRODUCTION

For the past decade, the amount of research and the volume of literature on alkali metals as heat-transfer media and working fluids have been increasing exponentially. Prominent among the liquid-metals research efforts are studies directed toward finding the best containment material for a given alkali metal under a given set of operating conditions.

As early as 1950, Argonne published a report on the "Resistance of Materials to Attack by Liquid Metals", which covered 174 references on 17 liquid metals from aluminum to zinc.[1] A slightly modified version of this report was published soon thereafter, as the corrosion chapter of the first edition of a Liquid Metals Handbook. As is the case today, the compatibility data available for sodium and NaK systems were far more extensive than those for any other liquid metal. In fact, in 1951, Epstein and Weber presented a very thorough treatment (151 references) on the use of molten sodium as a heat-transfer fluid.[2]

Since that time, there has been an accelerating interest in alkali metals as:

- Coolants for fast-breeder nuclear reactors
- Coolants in space power plants
- Rankine-cycle working fluids in high-temperature nuclear reactors
- Propellants in ion-propulsion engines
- Seeding materials in magnetohydrodynamic generators
- Space-charge dissipating media in thermionic generators
- High-temperature hydraulic fluids.

While research on sodium and NaK has continued unabated, these broadened applications have been involving other alkali metals (potassium, lithium, and cesium) on an increasing scale. Many of the compatibility results have, until recently, been classified. They are presented in a diverse assortment of project reports, meeting papers, periodical publications, theses, and state-of-the-art reviews.

This compilation attempts to present the highlights of what has been ascertained about the interactions of liquid and vapor sodium, NaK, potassium, lithium, and cesium with solid materials of potential use in practical liquid-metal systems. This is an extremely complex subject when one considers the multitude of variables possible, and there is still much that is unknown. Data for inclusion were selected by the authors on the basis of their practical utility to designers and research workers. No attempt was made to include the entire body of information available.

In many cases, data from a variety of sources were combined to illustrate a conclusion. Where data were conflicting, the authors attempted to explain the differences or to eliminate those which were questionable. In a few instances, it was necessary to present the contradictory findings and point out that no plausible explanations had been found.

*Associate Chief, Fellow, Associate Chief, and Senior Technician, respectively, Experimental Physics and Environmental Engineering Divisions, Battelle Memorial Institute, Columbus, Ohio.

2. SODIUM AND NaK

2.1 AUSTENITIC STAINLESS STEELS

2.1.1 Compatibility - General

Corrosion attack of austenitic stainless steels by sodium (or NaK) can take the forms of:

(1) Surface reactions which produce hot-to-cold zone transfer of corrosion products in a nonisothermal flow system

(2) Matrix attack, usually distinguished by grain-boundary deterioration

(3) Pickup of carbon, nitrogen, or hydrogen from the environment or through migration from hot-to-cold zones.

Investigation of these processes with temperature, time, flow velocity, contamination level, etc., as variables has been intensive for nearly 20 years, and the amount of diverse information generated is staggering. Experience ranging from laboratory experiments to the operation of large nuclear plants has led to the conclusion that the common austenitic steels (specifically, Types 304, 316, and 347), can be utilized up to 1000 F in sodium flow systems with virtually unlimited life, provided the oxygen and the carburizing potential of the fluid are maintained at low levels. However, departures from these conditions, involving higher temperatures or increased contamination levels, often produce compatibility-oriented questions which still cannot be answered without qualification.

Static-test data, which demonstrate austenitic steel-sodium compatibility, are many and varied; typical results are:

Negligible weight change [< -0.1 mg/(cm^2) (month)] at 932 F

Slight weight change [$\sim +0.1$ mg/(cm^2) (month)] at 1100 F

Substantial weight change [$\sim +40$ mg/(cm^2) (month)] at 1832 F.

More definitive, however, are data from polythermal-loop experiments. Tables 2.1 and 2.2 describe several of these operated over a broad temperature range. The results show:

(1) Little or no low-temperature attack.

(2) Enough corrosion in relatively short exposures at 1500 F and above to challenge the feasibility of long-time operation.

(3) A dearth of pumping-loop information in the 1300 to 1400 F range. Thermal-convention-loop results show very little attack, but the effects of flow velocity, known to be important as outlined below, cannot be ascertained.

(4) Moderate attack in the 1000 to 1200 F range, which, at least in recent years, has received major emphasis.

Considerable attention has been given to defining the mechanisms associated with austenitic steel-sodium compatibility. Among the well-established facts is that the amount of corrosion and mass transfer is strongly dependent on the level of oxygen impurity in the sodium. The tabulation below illustrates this, as well as the typical nonuniform leaching of constituents by sodium from hot stainless-steel surfaces. In this study, radiotracer techniques were used to measure the removal rates of individual constituents from Type 347 stainless steel in a flowing, isothermal sodium loop at 925 F.[3]

Element	Ratio of Rate of Leaching by Na Containing 100 PPM O_2 to Rate of Leaching by Na Containing 30 PPM O_2
Iron	17
Cobalt	54
Tantalum	5
Manganese	4

The exact role of oxygen has not been determined, but it may accelerate dissolution and/or participate directly in a corrosion reaction involving compounds of the form, $Na_xM_yO_z$, where M is a structural-metal constituent. It is generally accepted that mass transfer of iron is dominated by reaction rather than dissolution, with a hot-zone reaction as follows:

$$Fe + 3Na_2O \longrightarrow 2Na + (Na_2O)_2 \cdot FeO.$$

In cold zones, the reverse reaction occurs, liberating free iron which crystallizes out. This particular sodium-iron complex was isolated and identified several years ago.[18]

In the case of constituents other than iron, dissolution may be more important than chemical reactions. This conjecture stems from meager and controversial solubility data which suggest that the order of solubility in sodium is chromium> nickel>iron.

From many "corrosion-mechanism" studies, the rate of diffusion of reaction products through the boundary layer at the hot surface has emerged as the most likely controlling step in the

TABLE 2. 1. DATA FOR PUMP-LOOP EXPERIMENTS TO EXAMINE THE CORROSION OF AUSTENITIC STAINLESS STEELS BY SODIUM AND NaK

Site	Fluid	Material	T_{max}, F	ΔT, F	V, fps	Oxygen Level[a]	Time, hr	Special Comments	Corrosion Findings
Harwell[4]	Na	18:8:1	730	~200	4,8, and 10	Cold trap at 275 F	350	--	Maximum insert weight loss = 0.03 mg/(cm^2) (month)
General Electric, Knolls[5]	Na NaK	Type 347	700, with some operation at higher levels	~225	~10	Less than 220 ppm by analysis of samples	3 years of experimental operation	Large system used principally for heat-transfer studies Primary – Na (950 F design) Secondary – NaK (900 F design) Final – Water (760 F superheated steam)	Neither structural or insert material exhibited significant corrosion
Los Alamos[6]	Na	Type 316 (primary and intermediate heat exchanger and superheater); Type 304L (special parts throughout system); 1-1/4 Cr-1/2 Mo steel (evaporator and tempering heat exchanger); transition welds made with Inco Rod A filler	1100	~250	~5	Very low; plugging temperature at 220 F	~18 months	200-kw test facility	Type 316 increased slightly in hardness and tensile strength; decreased slightly in ductility; no intergranular penetration. SS-to-chromium alloy steel transition welds were undamaged. Chromium-alloy steel decarburized to an average depth of 9 mils and lost tensile strength accordingly. Materials failures occurred in a Type 316 thermocouple well and in a Type 304 mixing section, but these were apparently unrelated to sodium corrosion.

TABLE 2.1. (Continued)

Site	Fluid	Material	T_{max}, F	ΔT, F	V, fps	Oxygen Level[a]	Time, hr	Special Comments	Corrosion Findings
Babcock & Wilcox[7]	Na	Type 304, Type 316, and Type 316 welded with 19-9 Cb rod	1100	Isothermal except for cold-trap bypass	~55 (see comments)	Cold trap at 400 F or below	1000	Samples were rotated at top speeds of about 55 fps in sodium circulated through a loop system.	Test materials showed little or no attack regardless of structure (sensitized structures, weld structures both presensitized and sensitized during the exposure, heat-affected zones, etc.).
GE, Vallecitos[8]	Na	Type 316	1100 and 1200	250 and 500	To 30	10 and 50 ppm from plugging-meter data	To 30,000	Loop investigation in which Type 316 stainless steel, and 2-1/4 Cr-1 Mo and 5 Cr-1/2 Mo-1/2 Ti alloy steels were investigated singly and in combination.	Main results for Type 316 stainless steel in four categories (see Section 2.1.3.1): 1. Weight loss expressed by empirical equation 2. Intergranular penetration 3. Carbon transport 4. Austenitic-to-ferritic transformation (surface effect).
Soviet Laboratory[9]	Na	Inserts of various steels in loops fabricated of 18 Cr-9 Ni-0.45 Ti	1150 and 1290	--	--	Variable	To 5,500	Emphasis in program on evaluating corrosion and mechanical-property behavior with various oxygen levels (20 to 50 ppm, 60 to 80 ppm, 200 to 400 ppm, 200 to 400 ppm plus cadmium addition).	Main results in two categories (see Section 2.1.3.2): 1. Corrosion attack 2. Mechanical-property behavior after sodium exposure.

TABLE 2.1. (Continued)

Site	Fluid	Material	T_{max}, F	ΔT, F	V, fps	Oxygen Level(a)	Time, hr	Special Comments	Corrosion Findings
ORNL(10-12)	Na	Type 316	1500	300	--	Cold trap at 300 F	1,000	--	Results for Types 316, 304, and 347 were essentially identical; very little mass transfer occurred; hot-zone intergranular penetration was found to a maximum of 2 mils with some slight porosity to as much as 5 mils below sodium-exposed surfaces.
	Na	Type 304	1500	300	--	Cold trap at 300 F	1,000		
	Na	Type 347	1500	300	--	Cold trap at 300 F	1,000		
	Na	Type 310	1500	300	--	Cold trap at 300 F	1,000	--	Results for Type 310 included intergranular attack and void formation to 13 mils; cold-zone deposits were as heavy as 9 mils, but the total weight of scraped material was quite low, only 2-1/4 g.
	Na	Type 316	1650	300	--	Cold trap	1,000	--	Hot-zone intergranular attack in Type 316 to 2 mils with small voids appearing to a depth of 5 mils; cold-zone-deposit clusters 3 to 5 mils thick appeared; the weight of scrapings was about 2 g.
Pratt & Whitney, Canel(13,14)	NaK	Type 316	1600 and 1660	130 and 400	To 35	~100 to 1000 ppm by analysis of samples	To 515	--	Hot-zone solution attack to 3-1/2 mils; intergranular attack to 4 mils; cold-zone deposits to about 4 mils. Although not entirely consistent, high-oxygen-level systems showed the more aggravated attack. In some systems, carbon depletion and sigma phase occurred in hot-zone walls; a corresponding carbide network pattern was found throughout cold-zone walls.

(a) The solubility of sodium oxide in sodium (or in NaK) increases with increasing temperature. This property presents the opportunity of removing oxide from a flowing stream by circulating part of the flow through a bypass line maintained at a relatively low temperature. In this cold zone, that fraction of the oxide above the solubility level precipitates out. The plugging indicator device for oxygen monitoring takes advantage of this principle. The temperature of flow through a restriction is reduced until oxides precipitate and cause plugging. The measurement involves essentially a determination of the temperature at which the flow rate begins to decrease.

The difficulty with these precipitation-sensitive devices is definition of the absolute oxide solubility with temperature. Many data exist along this line, but owing largely to inherent experimental difficulties, individual sets of values can differ significantly. In Tables 2.1 and 2.2 cold-trap and plugging-indicator temperatures or numerical values for oxygen levels reported by the data sources are listed. Where the numerical values were assigned on the basis of the former, the correlations were apparently taken from the relations appearing in Figure 2.1 or from similar ones.

TABLE 2.2. DATA FOR THERMAL-CONVECTION-LOOP EXPERIMENTS TO EXAMINE THE CORROSION OF AUSTENITIC STAINLESS STEELS BY SODIUM AND NaK

(Typical $\Delta T \cong 400$ F)

Site	Fluid	Material	T_{max}, F	Oxygen Level	Time, hr	Special Comments	Corrosion Findings
Harwell[4]	NaK (22 Na 78 K)	18:8:1	1110	Cold trap at 212 F	500		Specimen weight loss = 0.14 mg/(cm^2)(month)
Atomics International[15]	NaK (22 Na 78 K)	Type 304 Type 316 Type 347	1200 and 1400	<20 ppm from plugging-meter data	To 4000	Experiments conducted in Type 304 and Inconel loops; inserts of several materials other than austenitic stainless steel were also evaluated and are reported in Table 2.15.	

	Duration, hr	At 1200 F	At 1400 F
Type 304	1,500	No attack	No attack
	2,500	~1-1/2-mil intergranular corrosion	~1-1/2-mil pitting
	4,500	~1-1/2-mil pitting	~1-1/2-mil intergranular corrosion: some decarburization
Type 316	1,000	High corrosion rates not considered realistic owing to possible contamination	No attack
	2,000		Some decarburization
	3,000		~1-mil light general attack
Type 347	1,500	~1-mil intergranular corrosion	~1/2-mil intergranular attack
	2,500	--	Ditto
	4,500	--	"

TABLE 2.2. (Continued)

Site	Fluid	Material	T_{max}, F	Oxygen Level	Time, hr	Special Comments	Corrosion Findings
American Standard[16]	Na	Type 316	1540 to 1640	Cold trap at 410, 440, and 190 F	To 2600	Closely spaced inserts were located throughout the loop circuits.	Inserts showed regular patterns of weight losses and gains, depending on position, and consequently temperature level; a set of values for a system with highly purified sodium is given below; values for higher oxygen cases are not appreciably different. Hot leg - Mg/(Cm²)(Month) 1600 to ~1400 F: -1.5 to 0 ~1400 to 1200 F: 0 to 0.4 Cold leg - 1200 to ~1450 F: +0.5 to 0 ~1450 to 1600 F: 0 to -1.0
Oak Ridge[10]	Na	Type 316	1630	20 to 35 ppm by analysis of samples	1080	--	Hot-zone surface attack to 3-1/2 mils, austenitic-to-ferritic transformation to about 1/2 mil; sparse cold-zone deposits.
	Na	Type 348	1490	20 ppm by analysis of samples	To 740	Sodium boiling at 1490 F.	No cold-zone mass transfer was found but heavy intergranular cracking occurred (up to 40 mils) in condenser section.

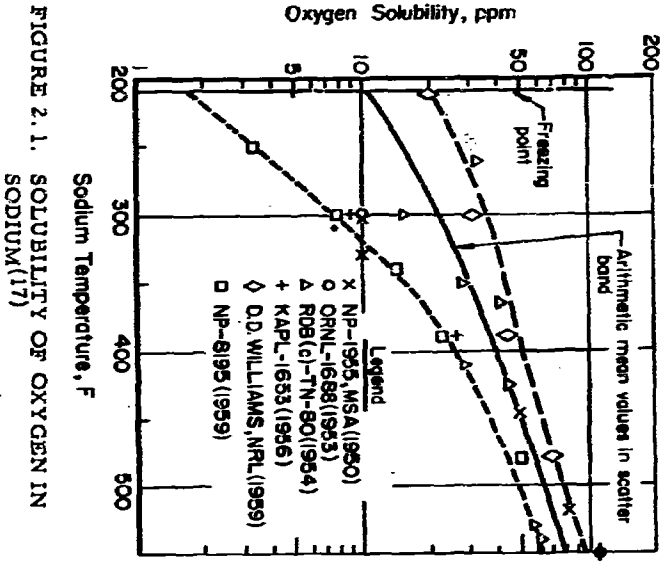

FIGURE 2.1. SOLUBILITY OF OXYGEN IN SODIUM[17]

SODIUM AND NaK AUSTENITIC STAINLESS STEELS

corrosion process in ordinary flow-loop situations. This is based on such observations as the direct influence of fluid-flow velocity on corrosion rates. Velocity affects boundary-layer turbulence and thickness, which in turn influence the ability of reaction products to diffuse into the main stream.

Transfer of interstitial elements to and from sodium-exposed austenitic steels has been observed under many conditions. Carbon migration has received the most attention, primarily because of the interest in using austenitic and ferritic steels in the same sodium heat-transfer system. The former provides needed strength for high-temperature (~ 1200 F) piping and components, while the latter offers economy and other desirable traits for low-temperature (~900 F) sections. However, ferritic-to-austenitic migration of carbon can occur, with consequent decrease in strength of the carbon-depleted material, and embrittlement of the carbon-enriched one. The mechanisms relating to this migration are understood only in a qualitative way. Weeks[19] observed that the safest way to minimize problems from dissimilar-metal interaction is to avoid mixing structural alloys in a liquid-metal system unless the major metallic constituents of all alloys are known to be essentially insoluble and the activities of all possible nonmetal transferring species (O, N, C, H) are equalized in all alloys by gettering.

2.1.2 Solubility Information

In a nonisothermal liquid-metal system, material which is dissolved from hot-zone surfaces and transported in flowing fluid to colder zones can, owing to differential solubility with temperature, precipitate and deposit in solid form on the cooler surfaces. The mass transfer of constituents of stainless steels as well as those of nickel- and cobalt-base alloys) by sodium or NaK has long been thought to depend to some degree on solution phenomena. Consequently, assorted studies have been carried out in attempts to measure, with some degree of confidence, the solubility in sodium of the elements which combine to make up these alloys. For reasons which are often obscure, data which should be directly comparable are in considerable disagreement. Undoubtedly, the extreme difficulties involved in the measurement techniques are partially responsible.

Table 2.3 shows some experimental values of solubility for iron in sodium, and one value in NaK. It is immediately apparent that the 1956 data of Baus are three orders of magnitude lower than those of the other investigators. In spite of substantial efforts to resolve this discrepancy, the exact cause remains a mystery. As can be seen in Table 2.4, the same situation exists for the solubility of nickel in sodium. Values for cobalt, tantalum, and columbium are listed in Table 2.5.

2.1.3 Detailed Loop-Test Data

2.1.3.1 Type 316 Stainless Steel; Inserts in and Hot Legs (1100 and 1200 F) of Pump Loops, With Type 316 or 2-1/4Cr-1Mo or 5Cr-1/2Mo-1/2Ti Alloys as the Cold Legs*(8,27)

Loss of Metal by Corrosion. Data obtained from inserts removed periodically from experimental loops operated up to 30,000 hours provide the basis for the following empirical steady-state equation:

$$100\ R = V^{0.884} O^{1.156} \exp\left(12.845 - \frac{23,827}{T+460} - 0.00676\ \frac{L}{Di} + \frac{2.26}{t+1}\right),$$

where

R = removal of hot-zone metal, mg/(cm^2) (month)
V = velocity, fps
O = oxygen level, ppm
T = temperature, F
L/Di = distance ratio downstream from hot leg
t = exposure time, months.

Note:

(1) The absence of a term referring to the hot-to-cold zone temperature differential, since a variation from 250 to 500 F did not produce significant changes in metal-removal rates.

(2) An effect of exposure time which initially is strong, but ultimately is weak.

(3) An L/Di effect which describes gradually diminishing insert weight loss with distance, in isothermal sections downstream from the hot zone. This observation has given considerable credence to the concept of diffusion-controlled corrosion. If diffusion of reaction products from the boundary layer must build up with L/Di, the diminishing surface-to-boundary layer concentration gradient must produce a corresponding decrease in the rate of formation of these products at the reacting surface.

* Conditions listed in Table 2.1.

TABLE 2.3. SOLUBILITY OF IRON IN SODIUM

Temperature, F	Baus, et al[20](a) In Na	Baus, et al[20](a) In Na Saturated With Na_2O	Rodgers et al[21](b)	Epstein[22](c)
445	0.0024	-	6	6
530	-	0.0016	-	-
580	0.0037	-	8	8
660	-	0.0010	-	-
735	-	0.0017	-	-
760	0.0050	-	10	10
835	-	0.0025	-	-
970	0.0091	-	-	-
980	-	0.0041	-	-
990	-	-	12	12
1290[d]	-	-	-	-

(a) By radiotracer technique.
(b) By chemical analysis of equilibrated samples, S_{ppm} (400-1000 F) = 0.5 + 0.0122 T (F).
(c) By chemical analysis of equilibrated samples, S_{ppm} (450-900 F) = 1.47 + 0.02 T (C).
(d) Single value by Drugos et al[23] = 15 ± 3 ppm in NaK-78.

TABLE 2.4. SOLUBILITY OF NICKEL IN SODIUM

Temperature, F	Solubility, ppm Baus, et al[24](a)	Solubility, ppm Rodgers, et al[21](b)
392	0.005(50)(c)	-
572	0.006(40)	10
662	0.006(30)	12
752	0.004(50)	14
932	0.009(20)	17
1112	0.012(30)	-
1112	0.038(430)	-
1112	0.014(770)	-
1112	0.022(1130)	-

(a) By radiotracer technique.
(b) By chemical analysis of equilibrated samples, S_{ppm} (400-1000 F) = -1.3 + 0.0199 T (F).
(c) Number in parenthesis following solubility value is ppm of oxygen in the sodium.

TABLE 2.5. SOLUBILITY OF COBALT, TANTALUM, AND COLUMBIUM IN SODIUM

Temperature, F	Solubility, ppm Cobalt[25]	Tantalum[25]	Columbium[26]
689	0.028	0.032	-
798	0.021	0.19	-
977	1.00	2.9	-
1846	-	-	7.4
2185	-	-	35
2518	-	-	243

SODIUM AND NaK AUSTENITIC STAINLESS STEELS

For illustrative purposes, a set of values for V = 10 fps, O = 50 ppm, and L/Di = 0 (situation for maximum weight loss) is given below.

T_F	Weight Loss, mg/(cm²)(month) 1-Month Exposure	Weight Loss, mg/(cm²)(month) 12-Month Exposure	Equivalent Removal of Metal From Exposed Surface, mils/yr 1-Month Exposure	Equivalent Removal of Metal From Exposed Surface, mils/yr 12-Month Exposure
1000	0.7	0.3	0.4	0.2
1100	1.7	0.7	1.0	0.4
1200	4.2	1.9	2.5	1.5
1300	11.0	5.2	7.0	4.5

Intergranular Penetration. The inserts did not show intergranular penetration.[27] However, this type of attack, to about 1.7 mils/yr (specifically, about 7 mils after nearly 30,000 hours), was observed in approximately isothermal sections of Type 316 stainless steel and occurred between heat-input and heat-extraction zones. The following discussion is provided.

"The results of electron microscope fractographic examination show:

(1) The stainless steel piping was heavily sensitized in the cross-over region. Chromium carbides precipitated in all the grain boundaries.

(2) There is no attack of the grain-boundary precipitates themselves.

(3) Chemical attack by solution of metal at the interface with the grain-boundary precipitate.

"A preliminary interpretation of this effect is that attack results from a high effective-oxide-impurity level created at the entrance to the cold leg on the beginning of supersaturation, and subsequent nucleation of metal precipitates with the accompanying liberation of oxygen to sodium oxide. This causes attack in grain-boundary areas which are suspected to be depleted in chromium by the precipitation of $Cr_{23}C_6$ at the grain boundaries."[27]

Materials Transfer. Type 316 stainless steel was approximately neutral to carbon transfer in a monometallic system. However, it carburized to several mils when combined with 2-1/4Cr-1Mo or 5Cr-1/2Mo-1-1/2Ti steels. The carbon profile of inserts in a Type 316/2-1/4Cr-1Mo system was as follows:

Temperature, F	Approximate Gross Carbon Content of Inserts, percent	
	Type 316 SS	2-1/4Cr-1Mo
Pretest	0.045	0.105
1200	0.05	--
1100	0.08	0.05
1000	0.08	0.10
700	--	0.105

This transfer was not dependent on the oxygen content of the sodium (from 10 to 50 ppm). In addition, selective transport of chromium and nickel from austenitic surfaces was found to occur in low-oxide-level systems above 1000 F. This was sufficient to produce a noticeable ferritic layer (for example, 5 to 8 microns thick after 2800 hours at 1200 F). In the case of high-oxide-level systems, iron was selectively removed.

2.1.3.2 Various Austenitic Steels: Inserts in 1110 and 1290 F Pump Loops Fabricated of 18Cr-9Ni-1Ti Steel[9]

Corrosion Behavior. After 5500 hours in 1110 F sodium containing 60 to 80 ppm oxygen, indications of corrosion were as follows:

No Attack

15Cr-15Ni-3Mo

Up to 5 mils Intergranular Attack

12Cr-16Ni-4Si-0.5Cb
14Cr-15Ni-1Cb
14Cr-20Ni-2W-1Cb
15Cr-15Ni-3Mo-0.7Cb
18Cr-9Ni-0.45Ti

After 1500 hours in 1110 F sodium containing 200 to 400 ppm oxygen, indications of corrosion were as follows:

Up to 4 mils Intergranular (Plus Some Transgranular) Attack

14Cr-20Ni-2W-1Cb
14Cr-15Ni-1Cb
15Cr-36Ni-3W-0.3Cb
18Cr-9Ni-0.45Ti
20Cr-14Ni-2Si

Strength and Ductility. Exposure to 1110 F sodium, containing 60 to 80 ppm oxygen, for 5500 hours did not strongly affect either strength or ductility of any of the above six steels evaluated under these conditions. However, 1500 hours' exposure to 1110 F sodium containing 200 to 400 ppm oxygen did produce noticeable increases in strength and decreases in ductility. This occurred in all five of the above steels which were evaluated under the latter conditions, but gettering the sodium with calcium significantly reduced the observed changes. Data for 18Cr-9Ni-0.45Ti, the alloy exhibiting the greatest variation, are:

	Tensile Strength, psi	Elongation, percent
Original material	74,000	41
Inert-atmosphere control sample	81,000	40
Ungettered sodium exposure	96,000	4
Calcium-gettered sodium exposure	70,000	36

The effects of exposure to 1290 F, 20 to 50-ppm-oxygen sodium for 5000 hours on the strength and ductility of the four steels listed in Table 2.6 were not appreciably different from those produced by inert-atmosphere exposures.

2.1.4 Carbon-Transport Behavior

2.1.4.1 General

Atomics International[28,29] has investigated the nature of carbon in sodium and the reactions of "dissolved" carbon with Type 304 stainless steel. Although it is fairly well accepted that carbon can exist in four different forms in sodium, the factors governing its distribution among these four states are open to considerate conjecture. The four conditions in which carbon is thought to exist are:[29]

(1) Dissolved Carbon - A true solution, similar to sugar in water

(2) Suspended Carbon - A state in which carbon particles are suspended in the sodium, as in a colloidal suspension

(3) Sodium Carbide - A compound (Na_2C_2), resulting from the chemical reaction of carbon with sodium

(4) Other Carbon Compounds - Where the carbon exists as a carbonate, cyanide, acetylide, or some other complex salt.[32]

The latter two forms, i.e., sodium carbide and and carbon compounds, exist in only very small concentrations, relative to the amounts of "dissolved" and "suspended" carbon, and thus play only minor roles in any carburization-decarburization

TABLE 2.6. STRENGTH AND DUCTILITY OF INSERT MATERIALS EXPOSED TO 1290 F, 20 TO 50-ppm-OXYGEN SODIUM FOR 5000 HOURS IN LOOP CIRCUIT[9]

	As-Received		Inert Atmosphere Exposure		Sodium Exposure	
Material	Tensile Strength, psi	Elongation, percent	Tensile Strength, psi	Elongation, percent	Tensile Strength, psi	Elongation, percent
14Cr-14Ni-4Si-0.6Cb	85,000	38	94,000	19	99,500	26
15Cr-15Ni-3Mo-0.7Cb	84,000	34	65,400	4	82,500	5
20Cr-14Ni-2.5Si	94,000	25	102,000	13	98,000	13
18Cr-9Ni-0.45Ti	108,000	39	104,000	25	99,500	30

processes occurring in stainless steel-sodium-carbon systems. In fact, it has been postulated that only the carbon which is in true solution (dissolved carbon) is available for carburizing stainless steel.[29] Hence, the term "effective" carbon has been introduced to distinguish between the total carbon content (all four forms) of the sodium and that dissolved carbon which effectively contributes to the carburization process.

Currently, only one experimental study has given the concentration of dissolved carbon in sodium, and little work has been reported concerning the nature of suspended or colloidal carbon. J. G. Gratton of Knolls[30] determined the solubility of carbon in sodium at elevated temperatures, Figure 2.2, by exposing a spectroscopically pure graphite electrode to commercial-grade sodium. He sampled the sodium at various temperature levels through a 5-micron filter and then analyzed for carbon by the wet-oxidation method of Pepkowitz and Porter.[33] The results of this investigation indicate that the solubility of carbon in low-oxygen (40 ppm) sodium varied between 32 ppm and 74 ppm in the temperature range 297 to 1292 F, and was dependent upon the oxygen concentration in the sodium. The functional dependence of carbon solubility (S = ppm) with temperature (K) was expressed by the relationships:

$$\ln S = 2.96 - 6.21 \times 10^2/T \text{ at 40 ppm oxygen}$$

$$\ln S = 5.61 - 3.76 \times 10^2/T \text{ at 260 ppm oxygen.}$$

Luner, Johnson, Cosgarea, and Feder,[34] in attempting to verify Gratton's results, found an abnormal amount of scatter for a given set of conditions and no smooth variation with temperature. Filtration studies and centrifugation experiments led them to the tentative conclusion that the carbon exists in so fine a suspension in sodium that there

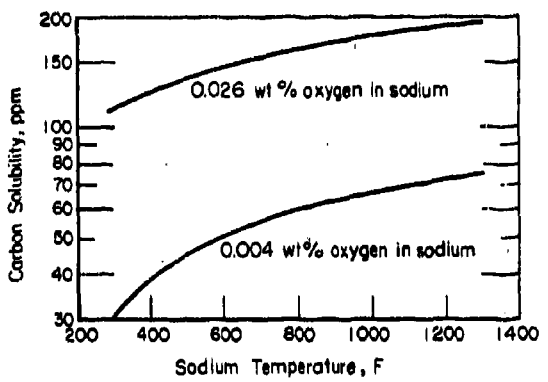

FIGURE 2.2. SOLUBILITY OF CARBON IN SODIUM[30]

is no "readily measurable equilibrium solubility in the graphite sodium system". These studies are continuing.

Goldmann and Minuskin[31] present a concise discussion of carbon transport in sodium-stainless steel-carbon systems. Since carbon is more or less soluble in sodium and occurs in varying forms and amounts in container materials, it tends to migrate from one region to another in molten sodium systems. This carbon-transport behavior can be rationalized on the basis of simple thermodynamic considerations. In most systems, the initial activity (free energy) of carbon in the sodium is different from that in the containment materials. Thus, "when carbon or carbon alloys with different carbon activities (free energies) are in contact with sodium in the same system, or when a single metal or alloy is in contact with sodium at different temperatures, carbon migrates via the sodium from regions with the higher activity (free energy) to those with the lower activity (free energy). The

SODIUM AND NaK AUSTENITIC STAINLESS STEELS

carbon transfer tends toward an equilibrium at all surfaces in contact with the sodium. The resulting carbon concentration in the metal or alloy may reach very different values from the original ones".[31] The driving force for the carbon migration process is this difference in activities or partial molal free energies between the carbon existing in the container materials and that in the sodium.

2.1.4.2 Type 304 Stainless Steel; Equilibrium Reactions of 1000 to 1600 F Sodium-Immersed Material With Carbon[35]

Carbon at Steel Surface. In sodium saturated with carbon, the equilibrium carbon content at the surface of Type 304 stainless steel was measured as:

Temperature, F	Equilibrium Surface Carbon Concentration, wt%
1000	2.68
1200	3.1
1400	3.6
1600	4.35

The equilibrium carbon content at the surface of Type 304 stainless steel with sodium of varying carbon content at 1200 F is:

Carbon in Sodium, ppm	Equilibrium Surface Carbon Concentration, wt%
15	0.04
18	0.30
25	1.0
60	3.0
70 (saturation level at 1200 F)	3.1

This implies that sodium containing 15 ppm carbon would be in equilibrium with normal Type 304 stainless steel (0.04 to 0.08 C) at 1800 F.

Carbon Within Case. Case depth as a function of time and temperature is shown in Figure 2.3. The case depth is defined by a concentration of 0.31 weight percent, which is the limit that can be detected metallographically.

The equilibrium carbon level in the case is greater than the level of carbon solubility in the steel. The excess carbon reacts to form an iron-chromium-carbon compound, $(Fe, Cr)_7C_3$, containing 75 percent chromium which precipitates and, in effect, removes chromium from the alloy.

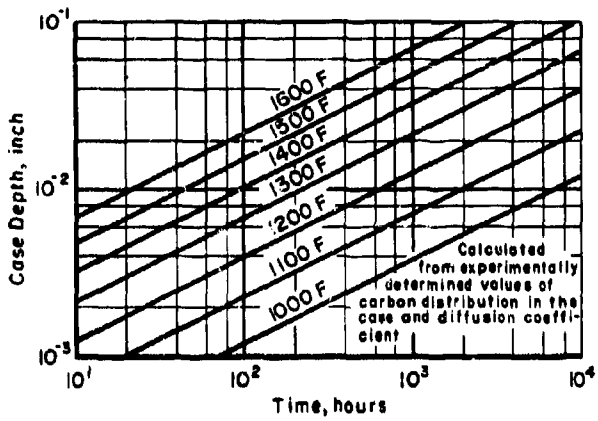

FIGURE 2.3. METALLOGRAPHICALLY DETERMINED DEPTH OF VOLUME CARBURIZATION VERSUS TIME AT TEMPERATURE, FROM CARBURIZATION OF TYPE 304 STAINLESS STEEL IN CARBON-SATURATED SODIUM[35]

2.1.4.3 Various Austenitic Steels (and One Nickel-Base Alloy); Capsule-Insert Experiments to Investigate Carbon Transfer From Carbon Steels in 1200 F Sodium Environment[36]

Materials

Austenitic Steels

18Cr-11Ni-0.64Ti-0.08C
20Cr-15Ni-1Mn-2.5Si-0.14C
14Cr-20Ni-2.7W-1Cb-1.5Mn-0.12C

Nickel-Base Alloy

75Ni-20Cr-0.21Ti-0.09C

Carbon Steels

0.73, 0.83, and 0.99C

Carbon Transfer (From Carbon Steel Crucibles to Inserts; 1200 F, 2000 and 4000 Hours). As indicated below, considerable carbon transfer occurred between carbon steel and several austenitic stainless steels. This mass-transfer effect was found to depend somewhat on the oxygen level in the sodium.

Insert Material	Carbon Content, wt%, in 0.2 MM-Thick Surface Layer After 4000 Hours' Exposure to Sodium of Indicated Oxygen Content		
	50 PPM O_2	500 PPM O_2	1000 PPM O_2
18Cr-11Ni	2.34	2.59	3.0
20Cr-15Ni	1.66	1.70	1.76
14Cr-20Ni	1.85	1.80	2.1
21Cr-75Ni	--	1.33	1.18

Additions of zirconium inserts, which gettered both oxygen and carbon, reduced the carbon transfer by approximately 25 percent; columbium in the sodium was less effective.

Not only was carbon transferred to the insert materials, but when the oxygen levels in the sodium were abnormally high (to about 6000 ppm), carbon also appeared in a fine layer on the sodium-contacting crucible walls. Insert specimens located above the liquid sodium were carburized, but only about one-fourth as much as submerged specimens.

Anodic polarization of the carbon steel increased the degree to which it decarburized, while cathodic protection gave the opposite result. The interpretation was that the carbon-transfer process involves ionic oxygen rather than molecular sodium oxide.

These various observations led to the hypothesis that the carbon carrier is carbon monoxide which is formed by chemical reaction of ionic forms of carbon and oxygen. Dissociation of monoxide molecules on metal surfaces would liberate carbon.

Property Changes Owing to Carburization. Insert materials were embrittled severely as a result of carburization, as indicated in the following tabulation.

Material	4000-Hour Exposure at 1200 F to Inert Atmosphere		4000-Hour Exposure at 1200 F to Sodium of Indicated Oxygen Content					
			50 PPM O_2		500 PPM O_2		1000 PPM O_2	
	Hardness, VHN	Elongation, percent	Hardness, VHN	Elongation, percent	Hardness, VHN	Elongation, percent	Hardness, VHN	Elongation, percent
18Cr-11Ni	220	22	637	0	724	0	700	0
20Cr-15Ni	222	18	425	0	460	0	440	0
14Cr-20Ni	144	24	427	0	457	0	478	0
21Cr-75Ni	185	21	265	1	263	9	255	11

2.1.4.4 Combinations Involving Type 1043 Plain Carbon Steel[10]

Table 2.7 presents results of 1830 F static-capsule experiments which demonstrate the decarburization of sodium-exposed Type 1043 steel in contact with Armco iron and with Type 304 ELC stainless steel. The findings in the latter case also indicate transfer of nickel to the carbon steel from the austenitic steel employed as the containment material.

2.1.5 Multimetallic Loop System

2.1.5.1 Combination of Five Iron- and Nickel-Base Materials* Incorporated Into Integral Pumping Loops Operated With 1300 to 1400 F NaK-78.[37-39]

Table 2.8 summarizes corrosion data for NaK-78 pumping-loop experiments involving materials located in series, as follows, in the flow circuits:

Hastelloy N (Chromized) - Heater section

Types 316 and 347 stainless steel and Croloy 9M - Heater-cooler connecting section

Croloy 9M - cooler section

Croloy 9M, Hastelloy C, and Type 316 stainless steel - Cooler-heater connecting section.

Corrosion and Mass Transfer. The corrosion of Hastelloy N and stainless steel was dependent on the presence of oxygen in the NaK. Hastelloy N exhibited the greater degree of attack, but its corrosion rate was not as sensitive to oxygen as that of the stainless steels. Slight weight gains which were observed for the Croloy 9M resulted from nickel pickup by dissimilar-metal transfer. In the high-oxygen loops, mass-transfer products containing sodium chromite ($NaCrO_2$) were found.

* The simulated reactor-materials situation is as follows:

Hastelloy N (Chromized) - fuel cladding
Hastelloy C - lower grid plate
Type 347 stainless steel - BeO moderator cladding
Type 316 stainless steel - reactor vessel and primary piping system
Croloy 9M - mercury boiler material.

TABLE 2.7. DATA FOR EXPOSURES OF TYPE 1043 PLAIN CARBON STEEL IN 1832 F SODIUM[10]

Material	Carbon, wt %		Weight Loss, mg/cm²		Nickel, wt %	
	Original	After 100-Hour Exposure	After 400-Hour Exposure	After 100-Hour Exposure	After 400-Hour Exposure	Original	After 400-Hour Exposure
Armco Iron Capsule							
Type 1043 steel	0.43	0.121	0.054	0.03	6.1		
Armco iron	0.019						
Vapor zone		0.019	0.016				
Bath zone		0.035	0.024				
Type 304 ELC Stainless Steel Capsule							
Type 1043 steel	0.43	0.100	0.074	0.03	4.7	0.008	0.090
Type 304 ELC stainless steel	0.022					11.12	
Vapor zone		0.022	0.162				10.32
Bath zone		0.128	0.200				9.98

TABLE 2.8. EFFECT OF TIME, TEMPERATURE, HYDROGEN, AND OXYGEN ON CORROSION OF MATERIALS IN NaK-78 PUMPING LOOPS (Δt = 200 F)

Peak Temperature, F	Time, hours	Hydrogen Present	Oxygen Content in NaK (Regulated by Cold Trapping), ppm	Corrosion, mg/cm²		
				Hastelloy N (Chromized)	Type 347 Stainless Steel	Croloy 9M
1300	2000	No	< 30	-3	+0.8	+0.1
1400	2000	No	< 30	-8	-1	+0.3
1400	2000	No	~ 80	-8	-3	-1.5
1400	5100	No	< 30	-20	-2	-0.3
1300	2000	Yes	< 30	-3	+0.8	0

Effect of Hydrogen. One objective in the program was to determine the effect of hydrogen, introduced into the liquid-metal stream, on compatibility. Pertinent experiments led to the conclusion that hydrogen has no effect on either corrosion rates or carbon migration.

Carbon Migration. At temperatures as low as 1200 F, Croloy 9M experienced significant carbon depletion, while in other sections at lower temperatures, it was carburized. Variations in oxygen level in the NaK appeared to have little effect on the carbon-migration rates.

2.1.6 Mechanical-Property Effects for Type 316 Stainless Steel

2.1.6.1 Type 316 Stainless Steel; Evaluation of Mechanical Properties After Sodium, Air, or Helium Exposure at 1200 F.[40-43]

Carbon Transfer. Exposure of Type 316 stainless steel to high-carbon* sodium resulted in carburization of the surface layer - typically, from an original 470 ppm to nearly 7000 ppm in 4000 hours. Exposure to normal-carbon sodium (both low and high oxygen) increased the surface carbon level to about 1000 ppm.

* Low-oxygen sodium = ~30 ppm oxygen
High-oxygen sodium = ~ 300 ppm oxygen
High-carbon sodium = generally, in the 30 to 60-ppm range (saturated or nearly so).

Several materials tested were found to gain carbon in the following order:

Type 321 > Type 304 > Type 310 > Type 317 > Type 309 > Type 330 > Incoloy 800 > 2-1/4Cr-1Mo > Inconel 600 > Nickel > Armco iron.

As shown below, stress was found to promote carburization in Type 316 stainless steel exposed at 1200 F sodium.

Exposure Time, hour	2,489	4,000
Stress Level, psi	18,500	0
Average Carbon Content, ppm		
0-2 mils below surface	3,211	1,063
2-4 mils below surface	1,516	491
4-6 mils below surface	686	561
6-8 mils below surface	806	471
Original Carbon Content, ppm	458	458

Creep-Rate Behavior. See Figures 2.4 and 2.5. The deformation-time curves for Type 316 stainless steel in 1200 F high-carbon sodium showed inflections and only brief second-stage creep periods.

Creep-Rupture Behavior. See Figure 2.6.

Cyclic-Strain* Behavior. See Figures 2.7 and 2.8.

Tensile-Strength Behavior. Variations of tensile strength after the following 1200 F exposures were 5 percent or less:

(1) Air

(2) Helium

(3) 400 hours in low-oxygen sodium; tested in helium.

Typical values for sodium-exposed specimens were:

Tensile Strength
1200 F - 48,470 psi
RT - 92,850 psi

* Defined as the ratio of specimen thicknesses to the radius of the mandrel over which the specimen was bent.

SODIUM AND NaK AUSTENITIC STAINLESS STEELS

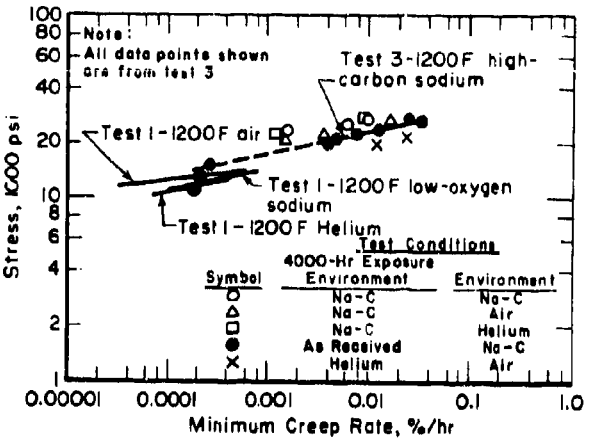

FIGURE 2.4. MINIMUM CREEP RATE OF TYPE 316 STAINLESS STEEL IN AIR, HELIUM, AND SODIUM AT 1200 F[41]

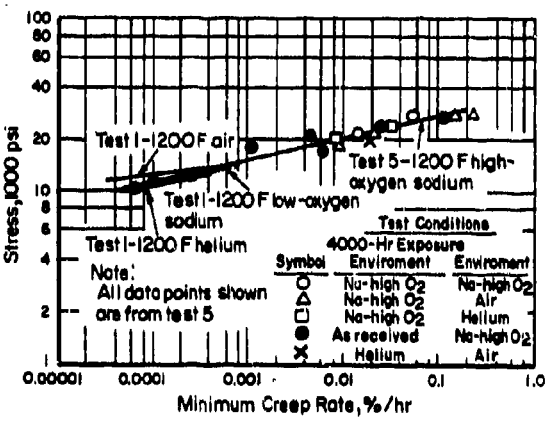

FIGURE 2.5. MINIMUM CREEP RATE OF TYPE 316 STAINLESS STEEL IN AIR, HELIUM, AND SODIUM AT 1200 F[41]

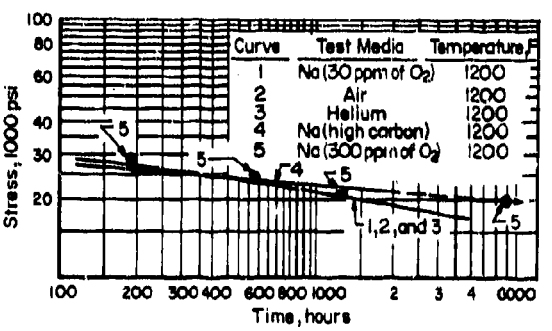

FIGURE 2.6. CREEP TO RUPTURE OF TYPE 316 STAINLESS STEEL SPECIMENS IN AIR, HELIUM, AND SODIUM AT 1200 F[42]

SODIUM AND NaK AUSTENITIC STAINLESS STEELS

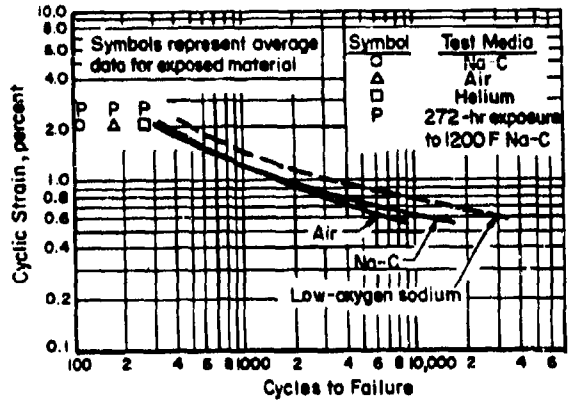

FIGURE 2.7. FATIGUE TESTS OF 316 STAINLESS STEEL IN AIR, LOW-OXYGEN SODIUM, AND HIGH-CARBON-SODIUM ENVIRONMENTS AT 1200 F[41]

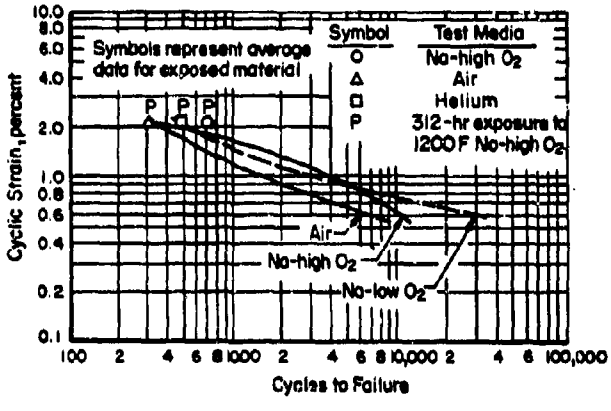

FIGURE 2.8. FATIGUE TESTS OF TYPE 316 STAINLESS STEEL IN AIR, LOW-OXYGEN SODIUM, AND HIGH-OXYGEN SODIUM ENVIRONMENTS AT 1200 F[41]

Offset (0.2%) Yield Strength
1200 F - 25,870 psi
RT - 43,930 psi

Elongation
1200 F - 43 percent
RT - 48 percent

Impact-Strength Behavior. Exposures of 4000 hours at 1200 F resulted in the following reductions in impact strength:

(1) 47 percent in helium

(2) 65 percent in sodium (high oxygen)

(3) 82 percent in sodium (high carbon)

(Original material had impact strengths between 9 and 10 ft-lb for 0.098-inch-thick specimens.)

2.1.6.2. Type 316 Stainless Steel; Recommended Design Stresses for Sodium Service[44]

Figure 2.9. presents recommended stress curves "developed by applying the following factors to the stress levels reduced by the extended life and environmental considerations for each of the materials:

(1) 100 percent of the average stress to produce 1 percent creep in 210,000 hours

(2) 100 percent of the stress to produce rupture in 210,000 hours.

"Figure 2.9 includes all of the factors for extended life (210,000 hours) and the nonoxidizing environment effect. The extended life does not affect the design stresses until approximately 1150 F. This effect reaches 10 percent between 1200 and 1250 F and a maximum of 33 percent at 1400 F. The nonoxidizing environment effect, which was reported by MSA Research Corporation, shows a 20 percent reduction of creep strength at 210,000 hours. Applying this effect to the creep curve, it now becomes the controlling factor at approximately 1050 F.

"Not included in the design stress curve are the effects of carburization and of nickel and chromium transport. Although carburization tends to strengthen, it also tends to embrittle the material.[44]

2.1.7. Nitrogen-Transport Behavior

2.1.7.1. Nitriding of Stainless Steel[45,46]

Although nitrogen is considered to be practically insoluble in sodium, early experiments at Knolls[46] have demonstrated that ferrous alloys and beryllium are readily nitrided in sodium when confined under a nitrogen cover gas. Results of static capsule tests, performed at 900 F for 7 days, and static container tests, conducted at 1100 F for 30 days, are presented in Table 2.9. These results indicate that (1) the ferrous alloys (with the possible exception of 2-1/4Cr-1Mo) and beryllium will nitride in sodium when in the presence of nitrogen, either dissolved or carried as Ca_3N_2, and (2) the nitride reaction occurs at 900 F. The boundary between the nitride layer and the base material in the austenitic stainless steels had the same sharp delineation that is

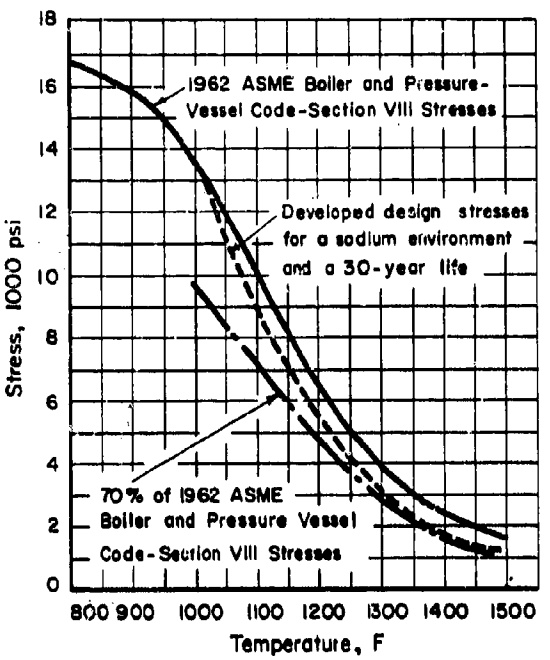

FIGURE 2.9. DEVELOPED DESIGN STRESSES FOR TYPE 316 STAINLESS STEEL IN A SODIUM ENVIRONMENT AND A 30-YEAR LIFE[44]

prominent in commercially nitrided steels. Also apparent in these tests was a noticeable decrease in hardness of the nitrided materials. This decrease in hardness was attributed, by the authors, to a combination of two factors: first, nitride layers that are maintained at elevated temperatures for long periods of time tend to soften, and second, nitriding may be incomplete under the reaction conditions during the tests. It was postulated, from the thermodynamics of the reaction, that nitrogen transport in sodium (via diffusion, entrainment, or in Ca_3N_2 as a carrier) could conceivably be the rate-controlling step in the nitriding process.

The results observed in the Knolls study were confirmed several years later for Type 304 stainless steel at Atomics International.[45] In this more extensive investigation, nitriding of Type 304 stainless steel occurred in sodium loop tests at 1000 F. The experiments consisted of exposing Type 304 stainless steel specimens to low-oxygen-content (10 ppm) sodium in a low-velocity (0.1 to 0.2-ft/sec) test loop employing nitrogen as a cover gas. The specimens were positioned in the loop so that a portion of each extended above the surface of the sodium into the nitrogen atmosphere. One specimen was completely submerged 18 inches below the surface of the sodium. Specimens were removed from the loop after exposures of 660, 1100, and 1400 hours and examined metallographically. The results of

TABLE 2.9. NITRIDING OF VARIOUS MATERIALS IN SODIUM UNDER A NITROGEN COVER GAS[46]

Test	Material	Surface Area, dm^2	Weight Change, mg (Average, of 3 Specimens)	Thickness of Nitride Layer, mils	Knoop Hardness		X-Ray Diffraction Data
					Nitride Layer	Base Material	
Static Capsule Tests 900 F, 7 days O_2 = 0.003 wt % Ca = 10 ppm	Be	0.072	+ 0.4[a]	None[b]	-	-	Film identified as Be_3N_2
	347 SS	0.074	+ 1.0	0.25	285	178	None taken[c]
Static Container Tests 1100 F, 30 days O_2 = 0.003 wt % Ca = 10 ppm	347 SS	0.196	+ 9.0	0.4	243	182	None taken[c]
	304 SS	0.163	+ 9.0	1.0	350	156	Layer identified as γCrN
	410 SS	0.163	+18.0	2.25	263	154	Layer identified as γCrN
	2.5Cr-1Mo	0.163	0.0	None	155[d]	131	-
	18-4-1 tool steel	0.102	+ 2.0	1.5	310	243	None taken[c]
	6-6-2 tool steel	0.163	+ 7.0	1.5	277	212	None taken[c]

(a) After descaling; film weight (per specimen) 1.6 mg.
(b) No visible nitride effect on descaled surface, except remaining nitride film caught in narrow irregularities owing to incomplete descaling.
(c) Structure similar between this film and X-ray identified films, plus the increase in hardness, are taken as evidence that this film carries a nitride.
(d) Too small an increase to be significant in the absence of a visible film.

these tests, Table 2.10, indicate that Type 304 stainless steel will nitride in a 1000 F sodium flow loop. It is evident from Table 2.10 that nitriding is relatively rapid immediately below the sodium-nitrogen interface, and the degree of nitriding decreases with increasing distance from the sodium side of the boundary. Exposure for 1140 hours or more was sufficient to produce some nitriding on the gas side of the interface. For the completely submerged specimen, 18 inches below the sodium surface, a very thin case was found to exist after 1400 hours' exposure.

Also, to ascertain the effects of nitriding on the mechanical properties of Type 304 stainless steel, tensile, stress-rupture, and flexural-fatigue tests were performed on specimens which had been nitrided by commercial techniques employing ammonia gas.[45] Table 2.11 summarizes the results of these tensile tests. An increase in the yield strength and a marked decrease in both ultimate strength and ductility (elongation) were exhibited by the light (1 to 2-mil case) and the heavy (4 to 6-mil case) nitrided Type 304 stainless steel. These effects occurred from room temperature to 1000 F. From the stress-rupture tests, it was determined that at 1000 F, the nitrided material has an appreciably shorter life at a given stress than does mill-annealed Type 304 stainless steel. For example, it is evident from Figure 2.10 that at a stress of 40,000 psi, the life of the "as received" specimens is approximately 50 times that of specimens with a 1 to 2-mil case. Furthermore, the heavier the case the shorter the rupture life at a given stress.

2.1.7.2. Nitrogen Migration Via Dissimilar-Metal Mass Transfer[43]

In refractory metal-stainless steel-sodium systems, the transfer of interstitial nitrogen (similar to carbon) from stainless steel to the refractory-metal surface (where more stable nitrides are formed) has been observed. The system Type 316 stainless steel-columbium-sodium was extensively investigated in the 1500

TABLE 2.10. NITRIDE-CASE THICKNESS FOR TYPE 304 STAINLESS STEEL EXPOSURE TO 1000 F SODIUM-NITROGEN SYSTEM[45]

Exposure Time, hours	Nitride-Case Thickness, mils			
	Specimen Position			
	Sodium-Side Interface		Nitrogen-Side Interface	
	Slightly Below	3 Inches Below	Slightly Above	3 Inches Above
660	0.9	0.1	None	None
1140	1.5	0.1	0.1	0.1
1400	2.0	0.3	-	0.4

TABLE 2.11. TENSILE DATA FOR NITRIDED TYPE 304 STAINLESS STEEL[45]

	As Received	1 to 2-Mil Case	4 to 6-Mil Case
Yield Strength, psi			
RT	35,300	34,000	39,500
500 F	22,500	28,400	29,800
1000 F	18,800	26,900	29,800
Ultimate Strength, psi			
RT	93,100	74,000	60,000
500 F	67,900	53,500	41,600
1000 F	61,900	48,100	41,700
Elongation, percent			
RT	65.2	35.6	17.5
500 F	34.9	19.6	10.5
1000 F	32.8	18.3	6.5

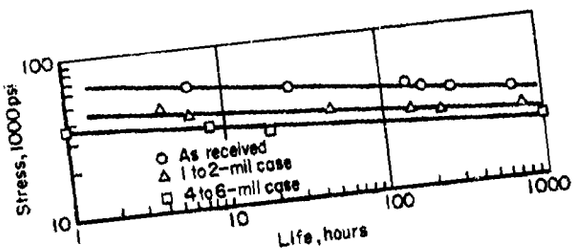

FIGURE 2.10. STRESS-RUPTURE DATA AT 1000 F FOR NITRIDED TYPE 304 STAINLESS STEEL(45)

to 1800 F temperature range.(47) The results of this investigation, shown in Table 2.12 indicate that time, temperature, and surface-area ratio all affect the amount of interstitial nitrogen (and carbon) transfer. For example, when the surface-area ratio of stainless steel to columbium was 6.5 or greater, nitrogen (also carbon) was transferred from the stainless steel to the columbium. This produced an increase in ultimate tensile strength and a decrease in ductility of the columbium. When the surface-area ratio of stainless steel to columbium was reduced to 0.1, no significant increase of nitrogen in the columbium was observed. However, some evidence of Cb_2N was observed on the surface of the Type 316 stainless steel.

In these tests, the increases in nitrogen concentration of the columbium were determined by chemical analyses and verified by metallographic and X-ray examinations. These analytical investigations revealed that the surface layer existing on the columbium consisted of Cb_2N.*

* A layer of CbC was also shown to have formed.

2.2 CHROMIUM ALLOY STEELS

2.2.1 Compatibility - General

Chromium alloy steels, as substitutes for austenitic steels, have been widely investigated as containment materials for sodium and NaK in the 1000 F temperature range. These materials are characterized by reasonable strength at such temperatures and low cost. In addition, when compared with austenitic stainless steels, these alloys exhibit high thermal conductivities and low coefficients of thermal expansion, which facilitate a reduction in thermal stress and fatigue in large-scale plumbing systems.

When chromium-alloy steels are exposed to sodium, the principal problem encountered is loss of carbon and consequent loss of strength. Compatibility studies have invariably given emphasis to this particular aspect of the problem. The general conclusions from a broad spectrum of laboratory investigations include:

(1) Within the range of permissible strength, up to about 1200 F, the resistance of chromium-alloy steels to attack by high-purity sodium is roughly equivalent to that of the austenitic steels. However, high concentrations of oxygen in sodium markedly reduce the corrosion resistance of chromium alloy steels. In this regard, these materials are considerably more sensitive than the austenitic alloys.

TABLE 2.12. EFFECT OF MASS TRANSFER OF CARBON AND NITROGEN ON ROOM-TEMPERATURE TENSILE PROPERTIES OF COLUMBIUM[a] TESTED IN SODIUM IN TYPE 316 STAINLESS STEEL[b] CONTAINERS(47)

Temperature, F	Time, hours	Surface-Area Ratio of Stainless Steel to Columbium	Change in Concentration in Columbium, ppm		Ultimate Tensile Strength, psi		Room-Temperature Tensile Properties: Elongation in 2.5 Inches, percent	
			Carbon	Nitrogen	Before Test	After Test	Before Test	After Test
1700	1000	0.1	+100	- 20	22,800	48,200	17.5	5
1700	500	6.5	+240	+ 660	22,800	46,200	17.5	11
1700	500	6.5	+420	+1920	22,800	50,400	17.5	6
1800	500	20	+790	+ 860				

(a) All specimens used in these tests were annealed for 2 hours at 1600 C in vacuum prior to exposure; specimen thickness, 0.040 inch.

(b) 18Cr-13Ni-2.5Mo-1.8Mn-0.06C-0.03N.

(2) At temperatures up to about 900 F, chromium alloy steels do not suffer loss of carbon as a result of sodium exposure. At higher temperatures, particularly when a carbon sink is present, carbon losses do occur and can progress to the point where the material is seriously weakened. In practical heat-exchange systems, this sink usually consists of some austenitic steel component.

(3) Resistance to decarburization is a direct function of the chromium content in chromium alloy steels. This is illustrated by the following observations on insert specimens exposed to sodium in pump loops fabricated of austenitic stainless steels and operated with oxygen levels below 100 ppm.

Alloy	Exposure Temperature in Loop System, F	Decarburization
1/2Cr	1100	Nearly complete
1Cr-1/2Mo	750	None
	1020	Nearly complete
1-1/4Cr-1Mo	1050	About 50 percent
	1100	Nearly complete
2-1/4Cr-1Mo	750	None
	950	None
	1020	Slight
	1050	About 50 percent
	1100	Nearly complete
5Cr-0.5Mo	1050	Slight
5Cr-0.5Mo-0.39Ti	1050	None
5Cr-0.5Mo-1-1/2Si	950	None
7Cr-0.5Mo	1050	None
9Cr-1Mo	1050	Slight
12Cr	930	None

(selected from References 4, 8, 9, 27, 48-50.)

(4) The resistance of low-chromium alloys to decarburization can be significantly improved through the addition of refractory metals which function as carbon stabilizers.

2.2.2 Detailed Loop-Test Data

2.2.2.1. 2-1/4Cr-1Mo and 5Cr-1/2Mo-1/2Ti Alloys; Inserts in and Cold Legs of Pump Loops With The Same Material or Type 316 Stainless Steel as the Hot Legs[8,27]

Nominal Sodium Conditions.

T_{max} = 1100 and 1200 F

ΔT = 250 and 500 F

V = to 30 fps

Time = to 30,000 hours

Oxygen in sodium = 10 and 50 ppm (by cold trapping).

2-1/4Cr-1Mo Steel. This material decarburized in both monometallic and bimetallic (Type 316 stainless steel hot leg) systems and suffered a corresponding loss of tensile strength. In the monometallic case, the carbon migration occurred from the high-temperature (~1200 F) to the low-temperature zone; in the bimetallic case, the migration occurred from zones have temperatures greater than 1000 F to the austenitic regions. Data pertinent to these studies are listed below:

Type of Loop	Insert Exposure Temperature, F	Insert Exposure Time, hours	Carbon Level, percent	Room-Temperature Strength of 2-1/4Cr-1Mo Insert, psi: Yield	Ultimate
None (original stock)	-	-	0.10	52,000	98,000
Bimetallic (O_2 ≯ 50 ppm)	1000	2800	0.10	59,000	85,000
Monometallic (O_2 ≯ 10 ppm)	1000	1400	0.09	51,000	80,000
Bimetallic (O_2 ≯ 10 ppm)	1100	700	0.04	35,000	68,100
Bimetallic (O_2 ≯ 10 ppm)	1100	1400	0.04	30,000	61,000
Monometallic (O_2 ≯ 10 ppm)	1200	700	0.05	32,000	63,000

5Cr-1/2Mo-1/2Ti Steel. In both the monometallic and bimetallic systems, this material was largely unaffected by carbon transport. However, it did suffer intergranular attack up to 1 mil after 2800 hours' exposure in the 1000 to 1200 F range (~50 ppm oxygen in the sodium).

2.2.2.2 2-1/4Cr-1Mo Alloy With Refractory Metal Additions; Inserts in a Thermal Loop Fabricated of Type 304 Stainless Steel[50]

Nominal Sodium Conditions

T_{max} = 1200 F

ΔT = 750 F

V = 0.1 fps

Time = to 4000 hours

Oxygen in Sodium = approximately 60 ppm.

Materials

2-1/4Cr-1Mo
2-1/4Cr-1Mo-0.037Cb (4S3)*
2-1/4Cr-1Mo-0.73Cb (4S7)
2-1/4Cr-1Mo-0.32Ti (4S2)
2-1/4Cr-1Mo-0.4Ti-0.1Cb (4S5)
2-1/4Cr-1Mo-0.4Ti-0.4Cb (4S1)
2-1/4Cr-1Mo-0.4Ti-0.4Cb-1.3Ni (5S2)
2-1/4Cr-1Mo-0.6V (4S4)
2-1/4Cr-1Mo-0.6V-0.1Cb (4S8)
2-1/4Cr-1Mo-0.6V-0.25Cb (4S9)
2-1/4Cr-2Mo-0.4Ti-0.4Cb (5S1)
5Cr-1Mo-0.4Ti-0.4Cb (7S1)

Corrosion Behavior. The resistance to corrosion was improved by refractory-metal additions. Typical specimen weight changes were as follows:

* Laboratory designation.

2-1/4Cr-1Mo steel: -0.11 mg/(cm^2)(month)*

Refractory-metal-alloyed steels: -0.03 to -0.07 mg/(cm^2)(month)

Type 304 stainless steel (comparison material): -0.02 mg/(cm^2)(month).

Carbon Transfer. Improved resistance to carbon transfer was also obtained through the addition of refractory metals. This observation is illustrated by the following variations in carbon concentration resulting from 1000 to 4000-hour exposures.

Material	Approximate Pre-exposure Carbon Level, wt%	Approximate Change, wt%
2-1/4Cr-1Mo	0.11	-0.06
4S3, 4S2, 4S4, 4S8	0.14	-0.03 to 0.07
4S7, 4S5, 4S1, 5S2, 4S9	0.14 to 0.16	0 to -0.02
5S1, 7S1	0.15 to 0.17	to +0.02
Type 304 stainless steel (comparison material)	0.06	+0.01

2.2.2.3 12Cr-1Mo and 13Cr-1Mo Alloys; Inserts in Pump Loops Fabricated of 18Cr-9Ni-1Ti Steel[9]

Nominal Sodium Conditions

T_{max} = 1292 F

V = to 15 fps

Time = to 6,500 hours

Oxygen in Sodium = 20 to 50 ppm.

Materials

12Cr-1Mo-0.3W-0.42V
12Cr-1Mo-0.59W-0.31V-0.42Cb
13Cr-1Mo-1Si-0.37Cb

Carbon Transfer

12Cr-1Mo-0.59W-0.31V-0.42Cb changed from an initial carbon concentration of 0.20 percent to a final carbon concentration of 0.14 percent in 5100 hours.

12Cr-1Mo-0.3W-0.42V changed from an initial carbon concentration of 0.14 percent to a final carbon concentration of 0.13 percent.

13Cr-1Mo-1Si-0.37Cb did not vary in carbon level.

Strength and Ductility. The strength and ductility of sodium-exposed inserts (5100 to 6500 hours) were approximately the same as those of inert-atmosphere control samples exposed for 5000 hours.

Material	Original Properties: Ultimate Tensile Strength, psi	Original Properties: Elongation at Fracture, percent
12Cr-1Mo-0.59W-0.31V-0.42Cb	132,000	11
12Cr-1Mo-0.3W-0.42V	78,200	17
13Cr-1Mo-1Si-0.37Cb	108,000	13

Material	5000 Hours Inert Atmosphere Exposure at 1292 F: Ultimate Tensile Strength, psi	5000 Hours Inert Atmosphere Exposure at 1292 F: Elongation at Fracture, percent
12Cr-1Mo-0.59W-0.31V-0.42Cb	81,000	22
12Cr-1Mo-0.3W-0.42V	79,500	16
13Cr-1Mo-1Si-0.37Cb	96,500	12

Material	Sodium Exposure at 1292 F: Ultimate Tensile Strength, psi	Sodium Exposure at 1292 F: Elongation at Fracture, percent
12Cr-1Mo-0.59W-0.31V-0.42Cb	81,000(a)	24
12Cr-1Mo-0.3W-0.42V	75,500(a)	18
13Cr-1Mo-1Si-0.37Cb	95,000(b)	12

(a) Exposed for 6500 hours.
(b) Exposed for 5100 hours.

2.2.3 Mechanical-Property Effects

2.2.3.1 2-1/4Cr-1Mo Alloy; Evaluation of Mechanical Properties After Sodium, Air, or Helium Exposure at 1100 F[43,51]

Carbon Transfer. Sodium-exposed specimens lost carbon approximately as follows:

Time, hours	Average Carbon Level, ppm: Low-Oxygen[a] Sodium	Average Carbon Level, ppm: High-Oxygen Sodium
Original	870	870
2000	550	400
4000	450	350
6000	350	-

(a) Low-oxygen sodium = ~30 ppm oxygen
High-oxygen sodium = ~300 ppm oxygen
High-carbon sodium = generally, in the 30 to 60-ppm-carbon range (saturated or nearly so).

* A weight loss of 1 mg/(cm^2)(month) is approximately equivalent to the uniform removal of 0.6 mil per year of surface.

SODIUM AND NaK CHROMIUM ALLOY STEELS

In high-carbon sodium at 1100 F, specimens rapidly absorbed carbon to an equilibrium value of approximately 0.5 percent.

Creep-Rate Behavior. See Figure 2.11.

Samples exposed to both helium and high-oxygen sodium indicated earlier third-stage creep than samples exposed to air.

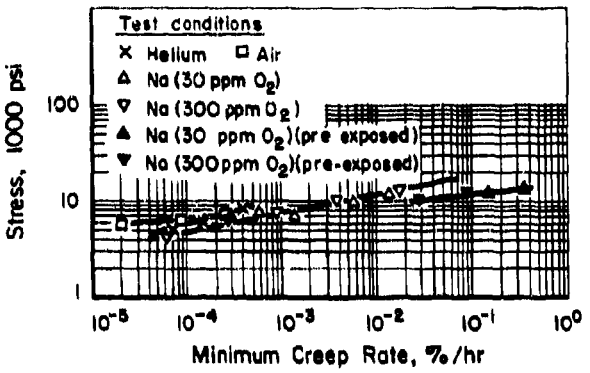

FIGURE 2.11. MINIMUM CREEP RATE OF 2-1/4Cr-1Mo ALLOY STEEL IN AIR, HELIUM, AND SODIUM AT 1100 F[51]

Creep-Rupture Behavior. See Figure 2.12.

The high-oxygen sodium introduced surface cracking and a faster rate of decarburization, which might lead to additional deleterious effects over long periods of time.

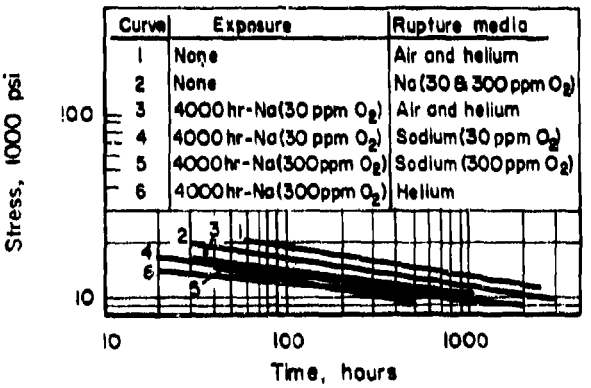

FIGURE 2.12. CREEP TO RUPTURE OF 2-1/4Cr-1Mo ALLOY SPECIMENS IN AIR, HELIUM, AND SODIUM AT 1200 F[51]

Cyclic Strain Behavior. The fatigue life at 1100 F varied approximately as follows:

Cyclic Strain, percent	Approximate Cycles to Failure: Air and Helium	Approximate Cycles to Failure: Sodium (30 and 300 ppm Oxygen)
2	400	2,500
0.6	2000	30,000

Tensile-Strength Behavior. The tensile strength of sodium-exposed specimens was significantly reduced from that of specimens in helium and air. Average 1100 F tensile properties following 400-hour exposures were as follows:

	Air	Helium	Sodium (low oxygen)[a]
Tensile Strength, psi	55,120[b]	38,550[b]	26,150
Offset (0.2%) Yield Strength, psi	27,990	23,700	17,100
Elongation, percent	31	33	45

(a) Exposure to high-oxygen sodium reduced the tensile strength to approximately 22,000 psi.
(b) The difference between air and helium exposures was labeled as "inexplicable".

2.2.3.2 9Cr-1Mo Alloy: Evaluation of Mechanical Properties After Decarburization in a Type 316 Stainless Steel NaK-78 Loop at 1425 F (Isothermal) for 600 Hours[52]

Carbon Transfer. Specimens were decarburized from an original carbon concentration of 0.12 percent to less than 0.01 percent.

Mechanical-Property Behavior

Temperature, F	Ultimate Strength, psi: Control[a]	Ultimate Strength, psi: Decarburized
78	71,200	55,100
500	64,900	48,900
1100	27,600	22,000
1300	10,200	8,130
1400	6,080	4,320

Temperature, F	Yield Strength (0.2% Offset), psi: Control[a]	Yield Strength (0.2% Offset), psi: Decarburized	Carbon Content of Decarburized Specimen, percent
78	45,300	35,500	0.008
500	36,600	24,550	0.007
1100	19,070	16,330	0.005
1300	9,590	7,800	0.004
1400	5,810	3,920	0.004

(a) Control specimens were given same thermal history as decarburized specimens, i.e., fully annealed and heated 600 hours at 1425 F.

2.2.3.3 9Cr-1Mo Alloy Steel; Recommended Design Stresses for Sodium Service[44]

Figure 2.13 presents recommended design stress curves for 9Cr-1Mo alloy steel. These curves were developed in a manner analogous to those for Type 316 stainless steel, presented in Figure 2.9 on page 16.

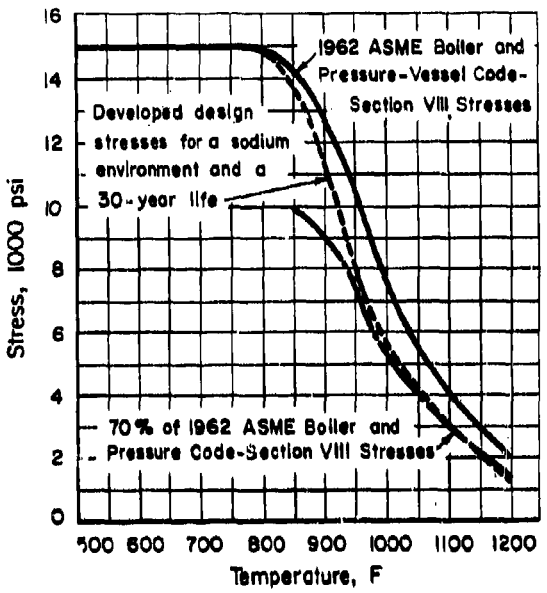

FIGURE 2.13. DEVELOPED DESIGN STRESSES FOR CROLOY 2-1/4 ALLOY STEEL IN A SODIUM ENVIRONMENT AND A 30-YEAR LIFE[44]

2.3 NICKEL- AND COBALT-BASE ALLOYS

2.3.1 Compatibility - General

Nickel- and cobalt-base alloys have been examined for sodium and NaK service, with emphasis at temperatures above 1200 F, the approximate temperature at which the usefulness of austenitic stainless steels may be limited by mechanical strength. However, these materials have not been subjected to the intensive multilaboratory types of investigation which are associated with the stainless steels. The underlying reason is that their resistance to corrosion and mass transfer (in the temperature realm where their strength would give them the advantage) is insufficient to assure long trouble-free life for a nonisothermal system.

Corrosion-loop data for nickel-base alloys are included in Tables 2.13 and 2.14 (pump loops), in Table 2.15 (thermal convection loops), and in the section at the end of the discussion (Inconel pump loops encompassing several variables). It is seen that below 1300 F, nickel-base alloys suffer very little corrosion in sodium environments. Above this temperature, however, corrosion and mass transfer in pump-loop experiments occur in amounts several times greater than for stainless steel experiencing the same thermal conditions. The corrosion is characterized by the selective leaching of nickel and, to a lesser degree, chromium. A typical composition of material deposited by mass transfer of Inconel is 90Ni-8Cr-0.5Fe.

It is generally accepted that the solubility process dominates the mass-transfer behavior of nickel-base alloys in flowing nonisothermal systems, and that the rate-controlling step in the process is the rate of diffusion of reaction products through the boundary layer at the hot zones. These characteristics can be deduced on the basis of the particularly distinct pattern of mass-transfer dependency on temperature, temperature differential, and flow velocity. The effect of velocity is especially well illustrated by a comparison of thermal-convection-loop data, indicating sparse mass transfer, with pump-loop data, indicating fairly copious deposits, under similar conditions of temperature and time.

Only a scant amount of information exists relative to carburization of nickel- and cobalt-base materials during sodium exposure. The data in Tables 2.16 and 2.17 show that a carburizing environment will result in carburization, although generally to a lesser degree than for the austenitic stainless steels. The conditions under which decarburization might occur, however, are less clear. On the one hand, evidence of decarburization is reported as a part of the information from the thermal-convection-loop experiments listed in Table 2.15; a low oxygen level (<20 ppm) was maintained. On the other hand, an Oak Ridge source[56] outlines evidence of decarburization of Inconel by sodium exposure in instances where the sodium apparently had a higher-than-normal oxygen level. A link between this decarburization and the oxygen level was suggested, inasmuch as decarburization of Inconel was not observed as a result of exposure to sodium of higher purity.

The decarburization of Inconel from the Oak Ridge Source[56] was cited as the reason for some loss of creep strength of the specimens

TABLE 2.13. DATA FOR PUMP-LOOP EXPERIMENTS INVOLVING SELECTED NICKEL-BASE ALLOYS[12,53]

Material of Loop Construction	Corrosion Findings
T_{max} = 1500 F; ΔT = 300 F; t = 1000 hours	
Inconel	Hot-zone attack to 2 mils; heavy cold-zone deposits to 18 mils
Incoloy	Almost identical to that for Inconel
Hastelloy B[a]	Heavy hot-zone surface pitting to 1-1/2 mils; slightly more cold-zone deposits than for Inconel
Hastelloy W	Hot-zone intergranular attack to 1-1/2 mils; about 17 percent greater cold-zone deposits than for Hastelloy B
T_{max} = 1700 F; ΔT = 650 F; t = 305 hours	
Hastelloy X (as heater leg with pump cell of Inconel and remaining sections of Type 316 stainless steel	Hot-zone attack; characterized by large subsurface voids, to 3-1/2 mils (Hastelloy X); intergranular attack to ~ 1 mil at entrance to cooler (Type 316 stainless steel); deposits up to 32 mils in cooler; no observation regarding interactions among construction materials

(a) A 1300 F peak-temperature, Hastelloy-B system (ΔT = 300 F, t = 1000 hours) showed very sparse mass-transfer deposits. The depth of intergranular attack however, was about the same as in the 1500 F system.

TABLE 2.14. DATA FOR PUMP-LOOP EXPERIMENTS INVOLVING HAYNES ALLOY NO. 25 AND NaK-56[54]

T_{max},	ΔT, F	Time, hours	Flow (Hot Leg), fps	Pretest Oxygen Level, ppm	Corrosion Findings: Attack in Hot Zone, mils	Corrosion Findings: Mass-Transfer Deposit, mils
1800	400	275	14.7	< 50	2.5 to 3.5	6.0
1800	400	500	14.7	< 50	3.0 to 5.0	10.0
1650	400	497	14.4	<100	1.0 to 1.5	8.0
1650	400	1000	14.4	<100	2.5 to 4.0	5.0

TABLE 2.15. DATA FOR THERMAL-CONVECTION-LOOP EXPERIMENTS INVOLVING NICKEL- AND COBALT-BASE ALLOYS[11,15,55]

Fluid	Material	T_{max}, F	Time, hr	Special Comments	Corrosion Findings
NaK-78 (<20 ppm O_2)	Inconel X Hastelloy C Hastelloy N Haynes Alloy No. 25	1400	To 4500	Experiments listed for NaK exposure conducted in Type 304 SS and Inconel; evaluations were made on insert specimens; austenitic stainless steels were also evaluated as outlined in Table 2.2.	Inconel X - 1000 hr - No apparent attack 2000 hr - Very slight general corrosion 3000 hr - Very slight pitting Hastelloy C - 1000 hr - 1 mil pitting 2000 hr - 1.7 mil decarburization Hastelloy N - 1500 hr - Slight evidence of intergranular attack 2500 hr - General corrosion to 1/2 mil 4500 hr - 2-1/2 mils of decarburization Haynes Alloy No. 25 - 1000 hr - 0.2 mil pitting 2000 hr - Very slight evidence of general corrosion 3000 hr - 1.1 mil decarburization
Sodium	Hastelloy B	1600	1008		Slight amount of mass transfer; 1 to 2 mils' intergranular attack
Sodium	Hastelloy X	1500	1000		No hot-zone attack or evidence of metallic deposits in cold zones
Sodium	Hastelloy W	1500	1000		No hot-zone attack but scattered nickel deposits in the cold zones
Sodium	Nickel-molybdenum experimental alloys				
	Ni-11Mo-2Al Ni-17Mo-2W Ni-15Mo-3Nb-0.5Al-3W Ni-16Mo-5Cr-1.5Ti-1Mn Ni-20Mo-1Nb-2Ti-0.8Mn	1500	1000		Average hot-zone attack about 1 mil, appearing as subsurface voids and pits, rather than intergranular attack; sparse deposits in cold zone.

TABLE 2.16. CARBON-PICKUP DATA FOR VARIOUS ALLOYS AFTER EXPOSURE TO GRAPHITE AND SODIUM, 100 HOURS, 1500 F[11]

Material	Carbon in Sodium, wt %	Carbon Found in 3-Mil Surface Layer, wt %	Depth of Carburization, mils
Hastelloy B	1	0.68	5
	5	0.58	8
	10	1.12	8
Type 310 Stainless Steel	1	0.39	2
	5	0.99	4
	10	1.43	4
Type 316 Stainless Steel	1	0.61	2
	5	1.09	4
	10	2.35	4
Type 430 Stainless Steel	1	0.27	4
	5	1.30	10
	10	1.47	24

TABLE 2.17. CARBON-PICKUP AND MECHANICAL-PROPERTY DATA FOR VARIOUS ALLOY SAMPLES ROTATING IN SODIUM (~25 FPS, 1500 HOURS, 1110 F) OIL VAPOR PRESENT IN THE COVER GAS[57]

Material	After 700 Hours Inert Atmosphere Exposure at 1110 F		After 1500-Hour Sodium Exposure at 1110 F		
	Ultimate Tensile Strength, psi	Elongation at Fracture, percent	Ultimate Tensile Strength, psi	Elongation at Fracture, percent	Approximate Thickness of Carbide Layer, mils
20Cr-65Ni (Nichrome)	127,000	29	90,000	45	2
20Cr-75Ni-1Al-1Ti (Nimonic)	106,000	40	104,000	35	0
16Cr-60Ni-2Al (Nimonic)	174,000	13	132,000	25	1
Nickel	89,000	25	61,000	50	1
20Cr-14Ni-2Si	113,000	37	94,000	14	7
18Cr-14Ni-1Ti	123,000	28	104,000	0.5	16
18Cr-12Ni-2Mo-1Ti	104,000	32	94,000	5	8

involved. The information in Figure 2.14* and Table 2.15, however, indicates that deterioration of mechanical properties of Inconel owing to sodium exposure does not constitute a problem of special significance, as is the case for austenitic stainless steel.

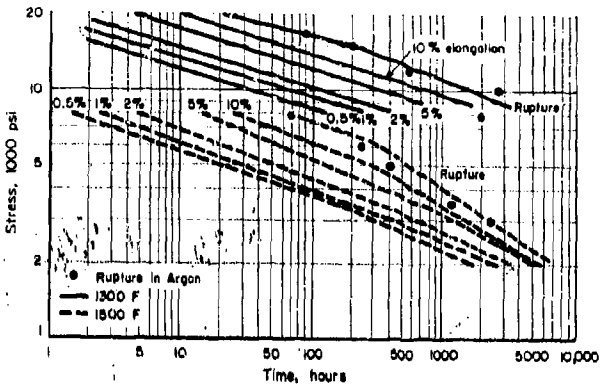

FIGURE 2.14. DESIGN CURVES FOR AS-RECEIVED INCONEL TESTED IN SODIUM AT 1300 and 1500 F[58]

On the basis of relative solubilities of nickel and cobalt (see Tables 2.4 and 2.5), and assuming that mass transfer of nickel- and cobalt-base materials is solubility dependent, the conclusion might be reached that the resistance of the latter to attack by sodium or NaK should be superior to that of the former. However, the few pertinent compatibility data which exist lead to the conclusion that this is not actually the case. Rather, as indicated by the Haynes Alloy No. 25-NaK data presented in Tables 2.14 and 2.15, the corrosion and mass-transfer behavior of the two types of materials appears to be about equal at comparable temperature levels.

2.3.2. Inconel Pump-Loop Experiments Encompassing Several Corrosion Parameters[10,11,12]

2.3.2.1 Effect of Temperature

Fluid = Sodium
T = 200 or 300 F
t = 1000 hours

Peak Loop Temperature, F	Corrosion Findings
1000	Original oxide film on tubing was undisturbed; no hot-zone attack or cold-zone deposits
1350	Hot-zone intergranular attack to 1/2 mil; scattered cold-zone deposits to 3 mils thickness
1500	Hot-zone attack to 2 mils; heavy cold-zone deposits to 18 mils thickness.

Conclusion: Temperature produced a significant effect on corrosion.

2.3.2.2 Effect of Temperature Differential

Fluid = Sodium
T_{max} = 1500 F
t = 1000 hours

Temperature Differential, F	Cold-Zone Mass Transfer
150	12 mils thick, 5-1/2 g[a]
300	18 mils thick, 13-1/2 g
400	20 mils thick, 21 g

(a) Weight of deposit (approximately 90 percent nickel and 10 percent chromium) scraped from wall.

Conclusion: Plot of ΔT versus weight of deposit shows almost linear relation.

2.3.2.3 Effect of Time

Fluid = Sodium
T_{max} = 1500 F
ΔT = 300 F

Length of Run, hours	Weight of Cold-Zone Deposit, g
500	7
1000	13-1/2
2000	20

Conclusion: Rate of mass transfer between 1000 and 2000 hours appears to decrease somewhat from almost linear variation below 1000 hours.

* Testing of Inconel in both argon and sodium at 1300 and 1500 F reveals very little difference between the creep-rupture properties in the two environments

SODIUM AND NaK ZIRCONIUM AND ZIRCONIUM ALLOYS

2.4.2.2 Dissolution Weight Losses

At 740 F, zirconium inserts in NaK-78 containing approximately 15 ppm oxygen lost about 0.2 mg/cm^2 during 500-hour exposures.

At 1020 F, sparse cold-trap and heat-exchange deposits were observed[4] in a sodium system where the oxygen level was maintained in the 15 to 25 ppm range by cold trapping. This dissolution effect for zirconium is illustrated in Figure 2.17.

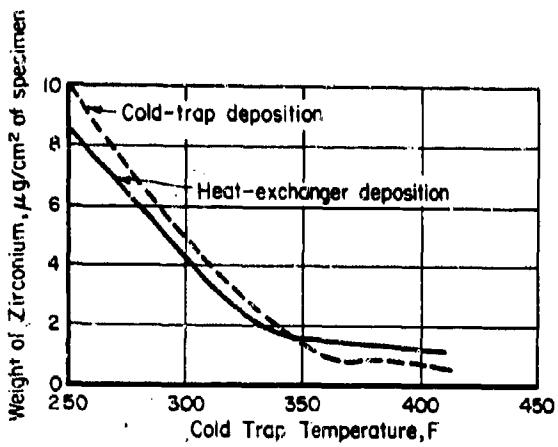

FIGURE 2.17. MASS TRANSFER OF ZIRCONIUM IN FLOWING SODIUM AS A FUNCTION OF COLD-TRAP TEMPERATURE (1020 F; 1000-HOUR TEST)[4]

2.4.3. Zirconium and Zirconium-Alloy Inserts Exposed to Static Sodium[60]

The oxidation of zirconium and several zirconium alloys was investigated at Atomics International[60] in a static sodium system with oxygen concentration of approximately 10 ppm. The materials investigated were:

2.4.3.1 Materials

Zirconium
Zr-1.5Al
Zr-1.5Al-1.5Sn
Zr-1.5Al-3Sn
Zr-1.5Al-1.5Mo
Zr-1.5Al-1Sn-1Mo
Zr-3Al
Zr-3Al-1.5Sn
Zircaloy-2

2.4.3.2 Oxidative Weight Gains

The slopes of log (weight gain) versus log (time), which are the values of 1/n in Equation (2), for these materials are:

	Value of 1/n at Indicated Temp		
	1030 F	1105 F	1175 F
Zirconium	0.45	0.45	0.46
1.5Al	0.41	0.46	0.52
1.5Al-1.5Sn	0.50	0.50	0.50
1.5Al-3Sn	0.42	0.46	0.50
1.5Al-1.5Mo	0.41	0.45	0.49
1.5Al-1.0Sn-1.0Mo	0.45	0.45	0.48
3.0Al	0.41	0.48	0.46
3.0Al-1.5Sn	0.40	0.45	0.50
Zircaloy-2	0.41	0.46	0.50

The rate constants for the above materials are presented in Figure 2.18 and are based on n = 2.

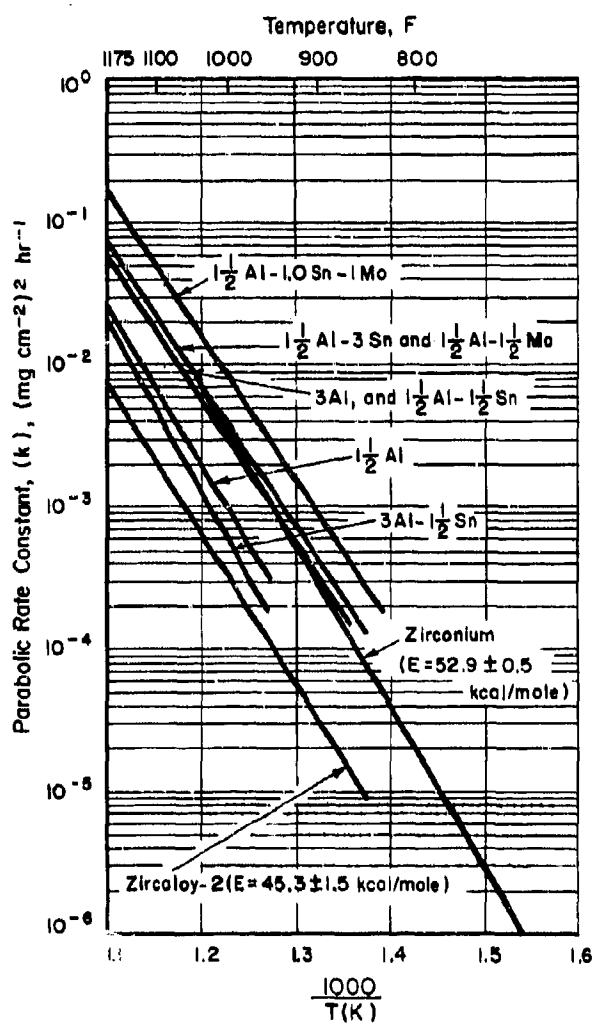

FIGURE 2.18. OXIDATION-REACTION RATE CONSTANTS FOR ZIRCONIUM AND ZIRCONIUM ALLOYS IN SODIUM AS A FUNCTION OF TEMPERATURE[60]

2.5 BERYLLIUM

2.5.1 Compatibility - General

Beryllium like zirconium, forms a much more stable oxide than sodium* and, consequently, BeO will form at the surface of a beryllium sample exposed to sodium containing oxygen. The reaction occurring is:

$$Be + Na_2O = BeO + 2Na. \quad (1)$$

In contrast to ZrO_2 films, however, the BeO films are nonadherent and readily dislodged by flowing sodium. Thus, they are nonprotective. Control of the oxidation rate has been realized through reductions of the oxygen level in beryllium-sodium systems by gettering with either calcium or thorium, which are stronger oxide formers than beryllium.

Another corrosion characteristic is the migration of beryllium to other materials in a composite system. While there is no evidence that this occurs to any significant degree at temperatures of 1000 F or lower, it has been noted repeatedly at 1200 F and higher.

2.5.2 Beryllium Exposed to 1000 F Static Sodium(62)

No intergranular attack or stress corrosion was observed in the samples involved in the stress-rupture tests summarized in Figure 2.19.

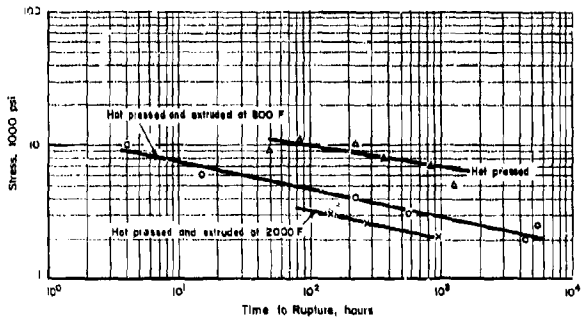

FIGURE 2.19. RUPTURE STRENGTH OF BERYLLIUM IN 1000 F SODIUM ENVIRONMENT(62)

2.5.3 Beryllium Inserts Exposed to Flowing NaK-78 or Sodium(63)

2.5.3.1 Corrosion in NaK (Cold Trapped at 248 F)

Figure 2.20 presents values from 250-hour experiments. A dependency on temperature and flow rate is apparent; the latter points to increased spalling of nonadherent oxide with increased NaK flow velocity.

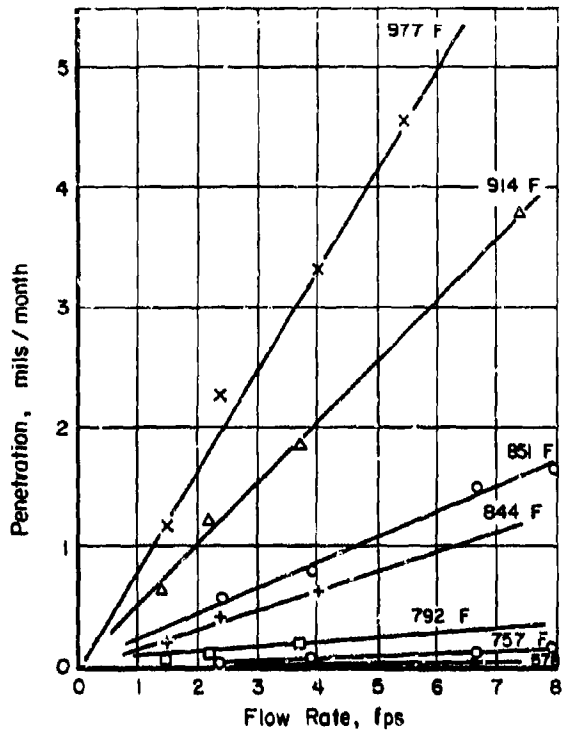

FIGURE 2.20. BERYLLIUM CORROSION RATE VERSUS NaK VELOCITY AND TEMPERATURE(63)

2.5.3.2 Corrosion in NaK With Calcium or Thorium Additions

Calcium. Large quantities of added calcium decreased the oxidation of the beryllium about in proportion to the quantity of added calcium. In fact, the following loop operations produced beryllium samples exhibiting slight weight gains.

Procedure A

(1) Batch cold trap at 212 F, followed by standard cold trapping at 248 F.

(2) Isolate cold trap and introduce calcium (2 kilograms).

(3) Maintain calcium at 980 F and beryllium samples at 928 F.

Procedure B

Same as above except 4 kilograms of calcium, maintained at 1022 F, was utilized to protect the beryllium at 968 F.

* For example, at 1000 K (1338 F), the free energy of formation of BeO by means of Reaction (1) is calculated to be $\Delta F = -54{,}150$ cal/mole.

Thorium. Additions of thorium were less effective in reducing oxidative corrosion than additions of calcium, and the gettering efficiency of the thorium decreased at an impractical rate. Some evidence was noted of hot-to-cold-zone mass transfer of the thorium.

In these exposures with added calcium and thorium, there was no evidence of:

(1) Nitriding of the beryllium, although nitrogen was utilized as a cover gas

(2) Reaction between beryllium and nickel from the stainless steel.

On the other hand, contrasting results were obtained:

(1) In beryllium-sodium experiments where nitriding was observed as outlined below

(2) In higher temperature dissimilar-metal systems where nickel-beryllium interactions were observed, as outlined in the subsequent section.

2.5.3.3 Corrosion in Sodium With Calcium Additions[64]

Seven types of hot-pressed beryllium samples, from different starting powders (virgin, blend, recycling), were exposed to sodium under the following conditions:

(1) 47 hours at 900 F, followed by 520 hours at 1000 F

(2) Flow velocity = 20 fps

(3) Low oxygen level maintained by cold trapping and calcium gettering (1 percent addition).

The specimen weight losses were less than 1 mg/(cm^2)(month), without evidence of erosion or flaking. Black films, about 50 microns in thickness, appeared on the sample. The identification made was Be_3N_2. The source of nitrogen was presumed to be an impurity in the argon cover gas or in the calcium.

2.5.4 Beryllium in Multi-metallic Loop Systems[10-12,55]

2.5.4.1 General Corrosion

Thermal-convection-loop exposures were conducted with sodium for 1000 and 1500 hours each with a beryllium insert positioned in the hot zone so that a few mils separated its surfaces from the surface of a nickel base alloy. Selected corrosion results are listed below.

Loop Material	Hastelloy B	Hastelloy B
Temperature, F	1200	1300
Corrosion, mils		
Loop material in hot leg	1	1
Beryllium insert	3	3

Loop Material	Inconel	Inconel[a]	Inconel
Temperature, F	1200	1300	1500
Corrosion, mils			
Loop material in hot leg	1	1	1
Beryllium insert	3	6	12

(a) These conditions resulted in very low concentrations of beryllium on the inconel walls; specifically about 6×10^{-3} mg/cm^2 in the hot zones and about 1×10^{-3} mg/cm^2 in the cold zones.

Conditions	Distance Between Sodium-Immersed Hastelloy B and Beryllium, mils	Equivalent Concentration of Beryllium in Hastelloy B Surface, 10^{-3} mg/cm^2
1200 F, 1000 hours	0	8800
	5	6.3
	20	1.06
	50	0.63
	100	0.74

Conditions	Distance Between NaK-44 Immersed Type 304 Stainless Steel and Beryllium, mils	Equivalent Concentration of Beryllium in Type 304 Stainless Steel Surface 10^{-3} mg/cm^2
1470 F, 500 hours	2	4950
	5	2300
	10	800
	15	310
	25	170
	50	140

2.5.4.2 Intermetallic Compound Formation

Compounds, identified as BeNi or $Be_{21}Ni_5$, were observed:

(1) At beryllium-nickel base alloy surfaces in contact in the 1300 F range; a reaction zone nearly 20 mils thick occurred during a 1000-hour exposure. Chromium plate was evaluated as a barrier, but Be_2Cr formation rendered it impractical.

(2) As a layer to about 3 mils thick on the surface of the inserts in the loops described above.

2.5.4.3 Effect of Spacing

The distance between the beryllium and the third material was found to control the transfer of beryllium strongly. Relevant data from static experiments are as follows:

2.6 COLUMBIUM AND COLUMBIUM-BASE ALLOYS

2.6.1 Compatibility - General

The behavior of sodium-exposed columbium- and columbium-base alloys has been found to be sensitive to variations in oxygen level in the range that would ordinarily be considered as very low, i.e., from nominally zero to as high as perhaps 30 ppm. Both dissolution and chemical reactions involving impurities must enter into columbium-sodium compatibility. According to free-energy data, columbium forms a more stable oxide than sodium. For example, at 1000 K (1340 F), the following reactions favor the reduction of Na_2O by columbium:

$$2Cb + 4Na_2O \rightarrow Cb_2O_4 + 8Na; \quad \Delta F = -32,800 \text{ cal/mole} \qquad (1)$$

$$2Cb + 5Na_2O \rightarrow Cb_2O_5 + 10Na; \quad \Delta F = -22,100 \text{ cal/mole} \qquad (2)$$

Solubility data for columbium in sodium over the temperature range 1846 to 2518 F are given on page

Columbium- and columbium-alloy inserts have been exposed to sodium and NaK contained in third-material (usually an austenitic stainless steel) systems at temperatures up to 1800 F. Both static and loop exposures have been involved. Some of the results clearly indicate high corrosion rates, appearing as specimen weight losses, and a sensitivity of these rates to the oxygen content of the liquid metal. However, others obtained under seemingly similar conditions indicate that the principal corrosion effect is one involving the migration of interstitials from the containment to the exposed refractory metal. Specimen weight loss is not an identified problem. There is no apparent explanation for this divergent pattern of behavior.

In another type of experiment, selected columbium-base materials have been exposed to boiling sodium at temperatures above 2000 F. These experiments have featured single-metal systems totally enclosed in high-vacuum enclosures. In such cases, fairly good corrosion performance has been consistently demonstrated.

SODIUM AND NaK — COLUMBIUM AND COLUMBIUM-BASE ALLOYS

2.6.2 Static Exposures of Columbium at 1700 and 1800 F[47]

Static experiments involving columbium inserts in Type 316 stainless steel containers are discussed under "Nitrogen Migration Via Dissimilar Metal Mass Transfer". Briefly, the principal finding was the transfer of carbon and and nitrogen from the steel to the refractory metal in sufficient quantity to alter the mechanical properties of the latter. Pertinent information is presented in Table 2.12. The carbon was confined to the surface, but the nitrogen penetrated the entire distance across the 40-mil-thick inserts. Surface layers were identified by X-ray analysis as CbC and Cb_2N.

Transfer of columbium to the stainless steel also occurred. At 1700 F, 40-mil-thick stainless steel inserts picked up about 0.5 percent columbium as a CbC surface layer.

2.6.3 Exposures of Columbium and Cb-1Zr in Sodium and NaK Loops Fabricated of Another Material[4,39,65-68]

Pertinent data are listed in Tables 2.18, 2.19, and 2.20. Note that the first four listings in Table 2.18 refer to experiments where the corrosion findings are reported mostly in terms of specimen weight losses, and that these weight losses are related directly to the oxygen level in the liquid metal. Perhaps the most surprising evidence from this group is the extensive corrosion attack of both columbium and columbium alloys observed, even though the oxygen level in the sodium was maintained at approximately 15 ppm by zirconium gettering.

This latter result is in some contrast to those obtained from the experiments referred to in the final three listings of Table 2.18. These experiments appear to have been conducted with an oxygen level possibly slightly higher than 15 ppm. Weight losses are not reported. Rather, the findings emphasize interstitial migration and indicate that corrosion, per se, was not especially severe. No apparent explanation exists for this considerable divergence in degree of corrosion obtained from experimental conditions which seem to be comparable, at least as far as the variable of oxygen in low concentration is concerned.

TABLE 2.18. DATA FOR EXPOSURES INVOLVING COLUMBIUM OR Cb-1Zr IN PUMP LOOPS FABRICATED OF ANOTHER MATERIAL

Ref	Fluid	Materials Arrangement	T_{Max}, F	Time, hr	Regulation of Oxygen Level in Liquid Metal	Corrosion Findings
4	NaK-78 and -70	Cb inserts in high-velocity austenitic-stainless steel systems	698-932	500	Oxygen level regulated only by cold trapping at 284 F	Inserts suffered high weight losses; see Table 2.19 for selected values; sensitivity to flow velocity points to a nonadherent, nonprotective oxide corrosion product
4	NaK-78 and sodium	Ditto	32-1112	To 350	Oxygen level regulated by cold trapping plus deoxidants of magnesium, titanium, and zirconium	Corrosion was markedly reduced by the deoxidants; selected values are included in Table 2.20.
66	Sodium	Cb and Cb-alloy inserts in low-velocity (~2 fps) austenitic stainless steel systems	1202	21 days	Oxygen level maintained in 1 to 5 ppm Na_2O range by gettering with uranium	Corrosion was generally light; selected values are included in Table 2.20.
67	Sodium	Ditto	1202	To 13 days	Oxgen level maintained in 15-ppm range by gettering with zirconium; this level originally thought to be in the 150 to 200-ppm range but later study indicated a considerably lower level	Very high degrees of attack were observed; selected values are included in Table 2.20.
65	NaK-78	Cb-1Zr inserts in high-velocity (~7 fps) Type 316 stainless steel system	1250	3000	<30 ppm of oxygen	Carbide layers built up on Cb-1Zr to a maximum thickness of 0.1 mil in 1000 hr; surface carbon increased by about 300 ppm in 1000 hr and then remained constant; nitrogen increased periodically by about 300 ppm; oxygen did not change; Cb-1Zr showed no change in microstructure, hardness, or ductility.

TABLE 2.18 (Continued)

Ref	Fluid	Materials Arrangement	TMax, hr	Time, hr	Regulation of Oxygen Level in Liquid Metal	Corrosion Findings
39	NaK-78	Cb-1Zr hot zone with remainder of high-velocity (to 11-1/2 fps) loop fabricated of Type 316 stainless steel; inserts of both materials throughout system	1257	2000	Oxygen concentration controlled to <20 ppm by cold trapping	Small quantities of carbon and nitrogen transferred to the Cb-1Zr; layers to 0.1 inch thick showed CbC-Cb_2N composition; no significant insert weight changes
68	NaK	Cb-1Zr inserts in hot zones of high-velocity (to 25 fps) loops fabricated of Type 316 stainless steel or of Haynes Alloy No. 25	1570 to 1650 for stainless steel systems; 1800 for Haynes Alloy No. 25 systems	To 1608	No mention made of the oxygen-regulation technique	Corrosion mainly involved transfer of carbon and nitrogen to the Cb-1Zr; the Haynes Alloy No. 25 systems exhibited cold-zone deposits to 10 mils thick, consisting mostly of carbides and nitrides of columbium. The Cb-1Zr: Haynes Alloy No. 25 combination was designated as being slightly more susceptible to corrosion at 1800 F than the Cb-1Zr:Type 316 stainless steel system at 1650 F; tensile and elongation properties at 1600 F for Cb-1Zr and for Haynes Alloy No. 25 were unaffected by the exposure; similar properties of Type 316 stainless steel were changed, presumably as a result of loss of carbon and nitrogen.

TABLE 2.19. BEHAVIOR OF COLUMBIUM IN SODIUM OR NaK CIRCULATING IN AUSTENITIC STAINLESS STEEL PUMPING LOOPS[4]

Temperature, F	Flow Velocity, fps	Weight Change[a] mg/(cm^2)(month)
	Cold Trap at 284 F; NaK-78; 500-Hour Duration	
698	1.3	- 0.9
	11.3	- 0.9
761	1.3	- 15.7
	11.4	- 52.1
852	11.3	- 77.7
	11.4	- 52.1
932	11.3	-175
	11.8	completely corroded
	Cold Trap at 257 F; NaK-30; 336-Hour Duration	
1112	16.2	-333
	29.5	-716
	Pretest Cold Trapping; 10 Percent of Flow Through Magnesium Dispenser at 752 F; NaK-78; 250-Hour Duration	
932	1.3	- 0.3
	11.5	- 1.4
	Pretest Cold Trapping; Hot Trap With Titanium at 1202 F; Sodium; Approximately 300-Hour Duration	
1022	30	- 1.1
1112	5.5	- 7.0
	Pretest Cold Trapping; Hot Trap With Zirconium at 1112 F; Sodium; Approximately 200-Hour Duration	
1112	30	- 0.6 to 63.4

(a) The uniform removal of 1 mil/yr from the exposed surface is approximately equivalent to a weight loss of 2 mg/(cm^2)(month).

TABLE 2.20. BEHAVIOR OF COLUMBIUM-BASE MATERIALS IN 1202 F SODIUM CIRCULATING IN STAINLESS STEEL PUMPING LOOPS[66,67]

Alloy Composition, weight percent	Weight Change,[a] mg/(cm²)(month)
21-Day Exposures; 1 to 5 PPM of Na_2O in Sodium, Regulated by Uranium Gettering	
Unalloyed Cb	- 0.33
Cb-1.84Cr	± 0.00
Cb-3.21Cr	± 0.00
Cb-4.33Zr	+ 0.01
Cb-20Ti-4.28Cr	+ 0.33
Cb-5Mo	- 0.04
Cb-1V	+ 0.30
Cb-3V	- 0.09
Cb-5V	- 0.10
7- or Approximately 13-Day Exposures; Approximately 15 PPM of Oxygen in Sodium, Regulated by Zirconium Gettering	
Unalloyed Cb	- 41, - 52
Cb-1Zr	-136, -364
Cb-5Zr	- 31, -220
Cb-5Mo	- 26, - 62
Cb-39V-1Ti	- 41, - 93
Cb-2.37Cr	-128
Cb-10Ti-5Zr	- 17, - 80
Cb-18Ti-4V	- 50, - 66
Cb-10W-2.5Zr	- 13, - 38
Cb-9Mo-9Ti	- 67, - 73

(a) Double listings indicate two exposures: one of stress-relieved and the other of recrystallized material.

2.6.4 Exposures of Cb-1Zr (and three other Cb-base alloys) In Monometallic Systems With Boiling (2000 to 2380 F) Sodium; Exposures Conducted in Chambers With Vacuum Levels From 10^{-6} to 10^{-9} torr

2.6.4.1 Loop Experiments (Cb-1Zr)[69,70]

Table 2.21 summarizes results from loop systems operated as indicated above. All experiments indicated a very high degree of compatibility of Cb-1Zr with sodium under the operating conditions.

2.6.4.2 Refluxing Capsule Experiments (Cb-1Zr)[70-72]

Table 2.22 summarizes data from various refluxing capsule exposures of Cb-1Zr with sodium carried out in the 2200 to 2300 F range for periods up to 8000 hours. On the basis of findings such as these, the following conclusion has been drawn:

> "In tests where less than 3000 ppm O_2 was found in the Cb-1Zr capsules, little or no corrosion was detected. This attack was limited to a slight roughening at the liquid-vapor interface (~0.001 inch maximum). When more than 3000 ppm O_2 was found in Cb-1Zr capsules, intergranular corrosion to a depth of 4 mils was observed. Postweld heat treatment of 2210 F for 1 hour had no effect on the corrosion of Cb-1Zr containing >2000 ppm O_2."[71]

TABLE 2.21. MONOMETALLIC LOOP EXPOSURES OF Cb-1Zr WITH BOILING SODIUM; HIGH VACUUM (10^{-6} to 10^{-9} TORR) IN ENCLOSURES

Type of Loop	Maximum Temperature, F	Cold Leg Temperature, F	Duration, hours	Corrosion Findings	Reference No.
Thermal	2100	1200	1330	No corrosion or deposition was apparent	70
Thermal	2000	1780	5003	No corrosion after routine shutdown	70
Thermal	2380	1350	1000	The maximum corrosion was less than 1 mil. Almost no migration of interstitial elements occurred.	69
Pumping (7-1/2-fps flow velocity)	2065	650	2650	Metallographic examination and bend tests indicated no corrosion or loss of ductility of the Cb-1Zr. The principal corrosion effect appeared to be some minor transfer of oxygen from peak-temperature to low-temperature material.	69

TABLE 2.22. REFLUXING CAPSULE EXPOSURES (UP TO 5000 HOURS) OF Cb-1Zr WITH SODIUM; HIGH VACUUM (10^{-6} to 10^{-9} TORR) IN ENCLOSURES

Reference No.	Temperature, F	Additive	Corrosion Findings
72	2282	None	Specimen weight changes ranging from +0.7 to -0.1 mg/cm^2 (5000-hour exposure)
70	2200	None, 75 ppm O,[a] 300 ppm O, Ta insert or Mo insert	No corrosion
70	2200	150 ppm O	~2-mil transgranular and intergranular attack in ~ liquid region
70	2200	500 ppm Ba	~3-mil intergranular attack in vapor region
70	2200	Cb insert	~5-mil intergranular attack in vapor region of insert
70	2310	None, 500 ppm Ca, 500 ppm Mg, 500 ppm Ba, Y, 150 ppm O, 600 ppm O, 150 ppm C, 600 ppm C	No corrosion
70	2310	600 ppm O	~1-mil transgranular and intergranular attack at liquid interface

(a) Oxygen added as Na_2O_2 in all cases.

2.6.4.3 Refluxing Capsule Experiments[70] (Cb-10W-10Ta, Cb 10W-1Zr-0.1C, Cb-5W-3Zr-0.1C)

Exposures at 2310 F produced:

(1) No corrosion of Cb-10W-1Zr-0.1C or of Cb-5W-3Zr-0.1C after 8000 hours

(2) Severe attack (to as much as about 30 mils) of Cb-10W-10Ta after 5000 hours.

2.7 VANADIUM AND VANADIUM-BASE ALLOYS

Evaluation of the corrosion behavior of sodium-exposed vanadium and vanadium alloys has been in close alliance with the corresponding evaluation of columbium and columbium alloys. As a result, it has been common to draw comparisons between the performances of the two types of materials. As might be expected from thermodynamic considerations,* it has been found that the corrosion behavior of unalloyed vanadium is similar to that of unalloyed columbium. However, vanadium alloys have demonstrated corrosion resistance superior to that of columbium alloys.

Table 2.23 presents pumping-loop corrosion data for vanadium; the corresponding data for columbium appear in Table 2.19. Each presents evidence of high corrosion rates in cold-trapped circuits and reduced corrosion rates through the use of strong oxygen getters.

* For example, at 1000 K (1340 F), the thermodynamics of the following reactions indicate that vanadium is capable of reducing sodium oxide (Na_2O):

$V + Na_2O \rightarrow VO + 2Na; \Delta F = -13{,}500$ cal/mole (1)

$2V + +Na_2O \rightarrow V_2O_3 + 6Na; \Delta F = -38{,}000$ cal/mole (2)

TABLE 2.23 BEHAVIOR OF VANADIUM IN SODIUM OR NAK-78 CIRCULATING IN AUSTENITIC STAINLESS STEEL PUMPING LOOPS[4]

Temperature, F	Flow Velocity, fps	Weight Change,[a] mg/(cm²)(month)
Cold Trap at 284 F; 500-Hour Duration; NaK-78		
632	1.8	- 8.3
	15.9	- 5.2
742	0.8	- 27.8
	7.8	- 94.2
762	1.88	- 54.6
	16.5	-219
860	0.9	- 77
	7.5	-231
Cold Trap at 248 F; 350-Hour Duration; NaK-30		
1112	5.5	- 91.2
Pretest Cold Trapping; 0.01 Percent Magnesium Added; 350-Hour Duration; NaK-78		
1112	5.5	- 0.72
Pretest Cold Trapping; Hot Trap With Titanium at 1292 F; Sodium; 136-Hour Duration		
1112	25	- 0.19
Pretest Cold Trapping; Hot Trap With Zirconium at 1112 F; Sodium; 127-Hour Duration		
1112	25	- 3.0

(a) The uniform removal of 1 mil/yr from the exposed surface is approximately equivalent to a loss of 2 mg/(cm²)(month).

Table 2.24 presents pumping loop data for vanadium alloys; Table 2.20 is the columbium-alloy counterpart. A comparison of results from the experiments with approximately 15 ppm of oxygen in the sodium shows a substantially better performance for the vanadium-base materials.

SODIUM AND NaK — VANADIUM AND VANADIUM-BASE ALLOYS

TABLE 2.24 BEHAVIOR OF VANADIUM-BASE MATERIALS IN 1202 F SODIUM CIRCULATING IN STAINLESS STEEL PUMPING LOOPS[66,67]

Alloy Composition	Weight Change, mg/(cm²)(month)
21-Day Exposures; 1-5 PPM of Na_2O in Sodium, Regulated by Uranium Gettering	
Unalloyed V	-0.23
V-10Ti-1Cb	+0.16
V-10Ti-3Cb	+0.26, +0.30[a]
V-10Ti-3Ta	+0.20, +0.37
V-5Ti-20Cb	+0.07, +0.27
9-Day Exposures; Approximately 15 PPM of Oxygen in Sodium, Regulated by Zirconium Gettering	
V-10Ti	-2.7, -3.2
V-20Ti	-3.3, -3.7

(a) Double listings indicate two exposures, each specimen in a different metallurgical condition (cold rolled, stress relieved, recrystallized, etc).

However, as is the case for the columbium-base materials, there is distinctly less corrosion of vanadium-base materials when the oxygen level of the sodium is reduced to near zero.

SODIUM AND NaK — TANTALUM- AND TANTALUM-BASE ALLOYS

2.8 TANTALUM AND TANTALUM-BASE ALLOYS

As might be expected from consideration of thermodynamic constants and solubility information,* the corrosion behavior of tantalum in contact with

* Solubility data for tantalum in sodium are presented in Table 2.5. Tantalum forms a more stable oxide than sodium according to free-energy data; for example, at 1000 K (1338 F) for the reaction $2Ta + 5\,Na_2O \rightarrow Ta_2O_5 + 10Na$, the free-energy change is $\Delta F^o = -56{,}050$ cal/mole, which suggests that tantalum will readily reduce Na_2O.

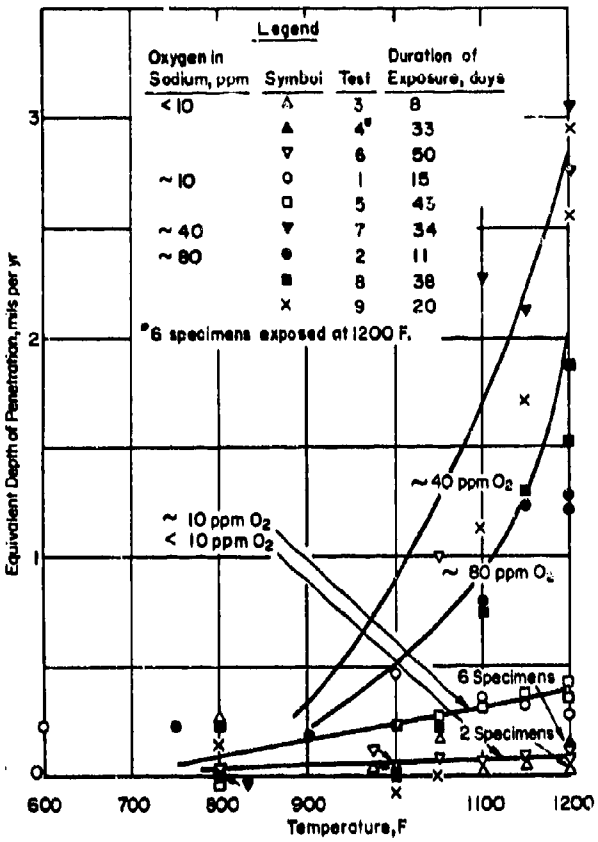

FIGURE 2.21. EFFECTS OF TEMPERATURE AND OXYGEN CONTENT OF THE SODIUM ON ITS ATTACK ON TANTALUM[73]

sodium is sensitive to the temperature level and the oxygen content of the sodium. Illustrative data are presented in Figure 2.21. These data were obtained by exposing tantalum (containing about 200 ppm of oxygen) inserts to sodium circulating in a polythermal pumping loop constructed of Type 316 stainless steel.[73] Cold trapping and gettering by zirconium foil were utilized to maintain the oxygen levels indicated. Other observed compatibility characteristics included the following:

(1) There was no evidence of cold-zone mass-transfer deposits of significant magnitude.

(2) Intergranular penetration was not a significant mode of attack, although it occurred in specimens fabricated of arc-cast tubing exposed to sodium containing 80 ppm of oxygen.

(3) Oxygen migrated from tantalum containing approximately 200 ppm oxygen to high-purity sodium. Final oxygen levels in the tantalum were usually less than 50 ppm. This behavior could not have been predicted from available thermodynamic information* except for the case of very pure sodium, containing oxygen in the 1 ppm range, for example.

(4) Exposure to low-oxygen sodium did not have a deleterious effect on the creep characteristics of tantalum at 1200 F.

The results shown in Figure 2.21 are similar to those obtained in another tantalum-sodium investigation[6] where weight losses for tantalum

(1) Began at about 1075 F and increased to an equivalent of about 8 mils/year at 1220 F when the tantalum was exposed to cold-trapped sodium

(2) Began at about 970 F and increased to an equivalent of about 0.5 mil/year at 1220 F.

There is a general dearth of information relative to the performance of tantalum and tantalum alloys in sodium at temperatures above 1200 F. One exception is the indication of good corrosion resistance exhibited by a tantalum insert exposed to 2200 F sodium in a Cb-1Zr refluxing capsule experiment operated for 5000 hours. Another involves a series of Ta-10W refluxing capsules exposed with sodium boiling at 2310 F for 160 hours. Insert specimens with longitudal test welds were utilized. The material exhibited generally poor corrosion behavior, characterized by severe intergranular penetration, particularly in weld zones.[70]

* Solubility data for tantalum in sodium are presented in Table 2.5. Tantalum forms a more stable oxide than sodium according to free-energy data; for example, at 1000 K (1338 F) for the reaction $2Ta + 5Na_2O \rightarrow Ta_2O_5 + 10Na$, the free-energy change is $\Delta F^\circ = -56,050$ cal/mole, which suggests that tantalum will readily reduce Na_2O.

2.9. MOLYBDENUM

Information relative to the corrosion behavior of molybdenum in sodium or NaK is quite limited and virtually no parametric data are available. Good corrosion resistance is indicated by the fact that inserts of molybdenum in a thermal-convection loop exhibited no attack, pitting, or intergranular corrosion after exposure to 1400 F NaK-78 for periods up to 3000 hours. Also, there was no evidence of corrosion of a molybdenum insert exposed to 2200 F sodium in a Cb-1Zr refluxing capsule experiment operated for 5000 hours (see Table 2.22).[70]

An analysis of the possible reaction products between molybdenum and sodium oxide has led to the conclusion that sodium molybdate is the probable reaction product.* At 1340 F, calculated free energies of formation (ΔF°) are as follows:**

$$4Na_2O + Mo \rightarrow Na_2MoO_4 + 6Na; \quad \Delta F^\circ = -2 \text{ kcal/g (mole)} \qquad (1)$$

$$2Na_2O + MoO_2 \rightarrow Na_2MoO_4 + 2Na; \quad \Delta F^\circ = -36 \text{ kcal/g (mole)} \qquad (2)$$

$$2Na + 2MoO_2 \rightarrow Na_2MoO_4 + Mo; \quad \Delta F^\circ = -69 \text{ kcal/g (mole)} \qquad (3)$$

$$Na_2O + MoO_3 \rightarrow Na_2MoO4; \quad \Delta F^\circ = -80 \text{ kcal/g (mole)} \qquad (4)$$

$$2Na + 4/3MoO3 \rightarrow Na_2MoO_4 + 1/3Mo; \quad \Delta F^\circ = -106 \text{ kcal/g (mole)}. \qquad (5)$$

These findings were developed in conjunction with a study investigating characteristics of molybdenum rubbing surfaces, both dry and in contact with liquid sodium. The data obtained indicated that the liquid-sodium case was characterized by the presence of a Na_2MoO_4 film, which reduced friction, and that the film was continuously replenished by reaction with oxygen in the sodium.

* From thermodynamic considerations (free-energy data), metallic molybdenum does not appear to be oxidized by Na_2O to the simple oxides (MoO_2, MoO_3, etc.).

** The free-energy data presented in Reference No. 74 have been revised, and the values shown are the new values.

2.10. TUNGSTEN

Tungsten, like molybdenum, is generally regarded to be resistant to attack by sodium, although there is even less evidence on which to predicate a judgment. Chemically, tungsten is similar to molybdenum, and the thermodynamics are favorable for the formation of Na_2WO_4 as the product of the reaction between tungsten and sodium oxide.* For example, at 1340 F, the free-energy values** are:[74]

$$4Na_2O + W = Na_2WO_4 + 6Na; \quad \Delta F^\circ = -31 \text{ kcal/g (mole)} \qquad (1)$$

$$Na_2O + WO_3 = Na_2WO_4; \quad \Delta F^\circ = -87 \text{ kcal/g (mole)} \qquad (2)$$

$$2Na + 4/3WO_3 = Na_2WO_4 + 1/3W; \quad \Delta F^\circ = -106 \text{ kcal/g (mole)}. \qquad (3)$$

The sodium tungstate film (Na_2WO_4) was found[74] to have frictional characteristics comparable to those of the corresponding molybdate film (Na_2MoO_4), previously mentioned.

2.11 URANIUM, THORIUM, AND THEIR ALLOYS

When exposed to sodium containing oxygen, both uranium and thorium will react with the Na_2O impurity to form stable oxides at exposed surfaces.*** The uranium oxide is not adherent, and consequently not protective. However, the thorium oxide would appear to be fairly adherent.

* Tungsten does not appear to be oxidized by Na_2O to the simple oxides (WO_2, WO_3, etc).

** The free-energy data presented in Reference No. 74 have been revised, and the values given are the new values.

*** For example, at 1000 K (1340 F), from the thermodynamics of the following reactions,

$$U + 2Na_2O = UO_2 + 4Na; \quad \Delta F^\circ = -87{,}100 \text{ cal/mole} \qquad (1)$$

$$3U + 8Na_2O = U_3O_8 + 16Na; \quad \Delta F^\circ = -167{,}500 \text{ cal/mole} \qquad (2)$$

$$Th + 2Na_2O = ThO_2 + 4Na; \quad \Delta F^\circ = -115{,}650 \text{ cal/mole}, \qquad (3)$$

both uranium and thorium would be expected to reduce Na_2O.

The available exposure data[75] for uranium show somewhat erratic values, but high specimen weight losses, indicating that sloughing off of the oxide layers is the rule rather than the exception. Illustrative data for dynamic-corrosion situations are presented in Table 2.25. In the case of the samples from the tilting-furnace experiments, there was evidence of deposition of constituents of the Type 347 stainless steel containers on the uranium samples. It is not clear whether this accounted in part for the weight gains recorded for the 1200 and 1250 F peak-temperature exposures.[76]

A few experiments analogous to those referred to in Table 2.25 have been conducted with preirradiated uranium samples. In these cases, the progress of corrosion was tracked by monitoring the buildup of radioactivity throughout the containment system. Generally, no differences were observed between the corrosion behavior of irradiated and unirradiated samples.

Static exposure data for thorium and uranium samples are given in Table 2.26. There is some indication that thorium is more resistant than uranium to the oxygen impurity in sodium. The likelihood of a difference in protectiveness of the oxide films is brought out in the following discussion[75] relating to the adherence of oxide films to base metals:

> "The adherence . . . . is governed by, among other factors, the ratio V_{ox}/V_m:
>
> $$E = \frac{V_{ox}}{V_m} = \frac{\text{volume per metal atom in oxide}}{\text{volume per atom in metal}}$$
>
> Maximum adherence would be expected in systems where E = 1. For both UO_2 and ThO_2, the ratio is given by
>
> $$E = \frac{\text{molecular weight oxide}}{\text{atomic weight metal}} \times \frac{\text{density metal}}{\text{density oxide}}$$
>
> For ThO_2, E is about 1.3; for UO_2, about 2. On this criterion, the oxide of thorium should be more adherent than that of uranium and should, in fact, compare favorably with such well-known protective oxides as Al_2O_3 (E = 1.3 to 1.5)."

TABLE 2.25. SELECTED CORROSION DATA FOR URANIUM EXPOSED TO SODIUM OR NaK IN DYNAMIC SYSTEMS[4,76]

Temperature, F	Flow Velocity, fps	Weight Change,[a] mg/(cm²)(month)
	Corrosion in Pumping Loops Cold Trapped at 356 F; NaK-78; 500 Hours[4]	
940	1.02	- 65
940	1.67	- 90
1075	1.67	-139
1075	3.21	-222
	Corrosion in Pumping Loop With An Oxygen Level (in Sodium) Mostly Between 10 and 80 PPM but as High as 610 PPM; Sodium; 781 Hours, Accumulated by 8-Hour-Working-Day Increments	
752 to 932	8	-616
	Corrorion in Tilting-Furnace Capsules With an Oxygen Level (in Sodium) Between 200 and 250 PPM; Sodium; 100 Hours[76]	
1250 (High) 1050 (Low)	-	+ 34
1200 (High) 980 (Low)	-	+ 47
1000 (High) 752 (Low)	-	- 21
1000 (High) 752 (Low)	-	- 9

(a) A weight loss of 47 mg/(cm²)(month) is approximately equivalent to uniform dissolution of 1 mil/month.

TABLE 2.26. SELECTED CORROSION DATA FOR THORIUM, URANIUM, AND THEIR ALLOYS IN SODIUM AND NaK IN STATIC SYSTEMS[75]

Material	Temperature, F	Time, hours	Oxygen Level in Liquid Metal	Weight Change, mg/(cm²)(month) In Sodium	In NaK
Thorium	1382	720	200 to 250 ppm	+ 2	2
Th-3 wt % U	1382	720	Ditto	+ 1	2
Th-4 wt % U	1382	720	"	-40, +3	-12
Thorium	1132	144		+ 4.5	
Uranium	392	144	Reduced by gettering with uranium		- 0.08
Uranium	1132	144	Ditto		+ 3.1
Uranium	761	160	"		+ 7
Uranium	745	160	"		+ 1.4
Uranium	932	166	Reduced by gettering with beryllium or calcium	- 0.1	
U-10 wt % Pu	662	160	Reduced by double filtering		-216
U-10 wt % Pu	761	160	Ditto		-288
U-60 wt % Al	844	124	Reduced by gettering with beryllium or calcium	-30	
U-60 wt % Al	932	170	Ditto	+ 8	
U-60 wt % Al	1220	164	"	-720	
U-69 wt % Al	932	167	"	-220	

2.12 BRAZE ALLOYS

Braze alloys containing copper, silver, and precious metals are generally not useful for sodium-environment service since the individual metals are readily attacked. It has been found that the most useful brazes are nickel with alloying ingredients such as silicon and boron. Table 2.27 summarizes the results of static corrosion tests performed at Oak Ridge[77] for several nickel-base alloys in sodium. These static tests were conducted at a temperature of 1500 F for 100 hours. Several materials which appeared promising on the basis of these static tests (together with others thought to hold promise) were investigated more extensively in seesaw furnace experiments, in which sodium was circulated for 100 hours at a hot-zone temperature of 1500 F and a cold-zone temperature of 1100 F. Since the seesaw tests provided a more rigorous means of evaluating corrosion data, no brazing alloy which had poor corrosion resistance to sodium in the static test was seesaw tested. The results of these seesaw furnace experiments are shown in Table 2.28 and indicate several promising brazing alloys for short-time sodium service.

In recent experiments at Atomics International,[78] several nickel-base brazing alloys were tested in a liquid-sodium thermal-convection loop for periods up to 10,000 hours at temperatures of 1200 and 700 F. Table 2.29 indicates the alloys tested and pertinent test conditions. On the basis of gross weight changes and photomicrographic examinations of the exposed brazing-alloy specimens, the authors concluded that Ni-Cr-Si-B (CM53) and Ni-Si-B(CM52) were the most resistant to sodium attack. Ni-Cr-Si(CM60) was judged to be suitable for only short-term use (less than 1500 hours) or lower temperature (below 700 F) applications. Also CM59 and Nicobraz 135 were shown to have good resistance to sodium attack up to a 5000-hour exposure at 1200 F. However, CM1700N and CM1700CN did undergo deleterious attack at 700 F after the 5000-hour exposure. Between the latter two, CM1700N appeared to be superior.

SODIUM AND NaK GRAPHITE

2.13 GRAPHITE

Graphite has been employed as the moderating medium in liquid-metal-cooled thermal reactors such as the sodium reactor experiment and the Hallam Nuclear Power Facility. Unfortunately its corrosion resistance to sodium can hardly be considered as anything but poor. Thus, any graphite used in a sodium system, must be kept from direct contact with the sodium.[79,80]

Numerous investigations have been conducted in an attempt to explain the action of liquid sodium on graphite at elevated temperatures. Many of the earlier works have been reviewed by Carniglia.[61] The effects observed have included swelling or dilation, cracking or spalling, and corrosion and mass transfer at temperatures above 1200 F. High-density carbon-impregnated graphites, as well as the normal commercial grades, have not been immune to these deleterious effects, and exhibit the same poor corrosion resistance. Liquid sodium readily wets graphite, ultimately soaking into the pores and being rather uniformly distributed throughout the capillary space available. Coultas and Cygan[81] studied this capillarity or "sponge" effect, by immersing a graphite rod in a reservoir of sodium within an evacuated chamber. The results of this study, Figure 2.22, indicated that roughly 60 percent of the connected voids were filled by liquid at 842 F, and 100 percent at 1022 F. Carbon impregnation of the graphite did little to alleviate the situation. In similar experiments, Greening and Davis[82] observed that 68 percent of the connected voids were filled at 1202 F, and Collins[83] found 90 percent impregnation at 1355 F.

This uptake of sodium is accompanied by an anisotropic dilation or swelling of the graphite. Greening and Davis[82] measured this dilation as a function of temperature from 302 to 1202 F. Figure 2.23 shows their curves, which were corrected for normal thermal expansion. It is interesting to note that the addition of 1 percent potassium greatly aggravates the situation. Gill[84] conducted a series of static capsule experiments on the dilating effect of graphite by employing graphite samples ranging in density from 1.6 to 1.89. His results, Table 2.30 indicate linear dilations of the order of 1 percent, decreasing somewhat with increasing density in times up to 100 hours at 950 F. The greater degree of expansion perpendicular to the axis of extrusion stems from the anisotropy of the graphite. Table 2.31 shows the dilation of TSP graphite parallel to the extrusion axis as a function of exposure time and temperature. It is seen that the dilation does not vary markedly with exposure time (500 to 2000 hours) or temperature (950 to 1200 F). Gill further observed that in some cases, decrepitation and disintegration (loss of strength) occurred in the graphite owing to the dilation.

Some investigators attribute the dilation and disintegration of graphite to the formation of interlamellar compounds between the graphite and sodium.[79,84] It is well known that potassium, rubidium, and cesium form interlamellar compounds with graphite, although early experimental and theoretical work indicated that sodium could not participate in reactions of this type.[85] However, later work at Harwell[86] provided evidence for the existence of at least one interlamellar compound of sodium, namely, $C_{64}Na$.

TABLE 2.27. SUMMARY OF RESULTS OF 100-HOUR STATIC CORROSION TESTS AT 1500 F FOR NICKEL BASE BRAZING ALLOYS[77]

Good Corrosion Resistance	
General Electric No. 81	Ni-16Si-6Mn
Coast Metals No. 52	Ni-13Si
Ni-10P-10Cr	Ni-10P-13Cr
Nicrobraz	Ni-6Si-30Mn
Ni-25Ge	Ni-9P-11W
Ni-25Mo-25Ge	Ni-10Si-13Cr-19Fe-3Mo
Ni-25Ge-10Cr	Ni-5P-6Si
Ni-9Si-18Cr	Ni-8P-3Si
Ni-3P-9Si	
Ni-10Si-8Mn	

Poor Corrosion Resistance (> 5 Mils Attack or Other Deterioration)	
Ni-60Mn	Ni-9P-15Fe-5Cr
Ni-55Mn-10Cr	Ni-11P-9Si
Ni-32Sn	Ni-10P-4Mo
Ni-57Mn-3Cr	Ni-12P
Ni-23P	Ni-11P-8Mn
Mn-10P-2Cr	Ni-10P-4Mo
Ni-12P	Ni-10P-11Fe
Ni-11P-8Mn	

TABLE 2.28. BRAZING ALLOYS ON INCONEL T-JOINTS SEESAW TESTED IN SODIUM FOR 100 HOURS AT A HOT-ZONE TEMPERATURE OF 1500 F AND A COLD-ZONE TEMPERATURE OF 1000 F[77]

Brazing Alloy Composition (In Order of Decreasing Corrosion Resistance)	Weight Change (for Braze and Base Material), Gram	Percent	Metallographic Notes
Coast Metals No. 52	-0.0011	-0.073	No attack along surface of braze fillet
Coast Metals No. 53	-0.0009	-0.071	1-mil erratic attack along surface of braze fillet
Low-melting Nicrobraz	-0.0007	-0.051	Subsurface voids to a maximum depth of 1.5 mils along surface of braze fillet
Coast Metals No. 50	-0.0012	-0.077	1 to 5-mil very erratic attack along fillet
Ni-13Ge-11Cr-6Li	-0.0023	-0.139	Nonuniform attack along surface of braze fillet to a depth of 2.5 mils
Coast Metals Np	-0.0069	-0.622	2.5-mil uniform attack along surface of braze fillet
Nicrobraz	0.0	0.0	Very erratic stringer attack to a maximum depth of 4 mils along surface of braze fillet
Ni-25Ge-10Cr	-0.0019	-0.113	Intermittent surface attack to a maximum depth of 4 mils along braze fillet

TABLE 2.29. EXPERIMENTAL BRAZING ALLOY DATA FOR SODIUM THERMAL LOOP EXPERIMENTS[78]

Brazing Alloy Designation				Exposure Conditions	
Experiment	Trade Designation	Nominal Composition, wt %	Temperature, F	Temperature, F	Time, hours
A	CM52	4.50Si - 0.06C-2.90B, Ni bal	1900	700 and 1200	10,000
B	CM52 Special	4.50Si - 20.00Co-3.30B, Ni bal	1900	1200	5,000
C	CM53	4.50Si - 3.00Fe - 7.00Cr-2.90B, Ni bal	1900	700 and 1200	10,000
D	CM60	10.00Si - 3.00Fe-20.00Cr, Ni bal	2150	700 and 1200	10,000
E	CM59	4.33Si - 3.30B - 0.69Ti-1.40Fe - 0.11C, Ni bal	2000	1200	5,000
F	Nicrobraz 135	3.00Si - 1.00B-0.06C, Ni bal	2000	1200	5,000
G	CM1700 CN	63.00Cu - 10.00Co-22.00Mn - 5.00Ni	1700	700	5,000
H	CM1700 N	67.50Cu - 9.00Ni-23.00Mn	1700	700	5,000

SODIUM AND NaK GRAPHITE

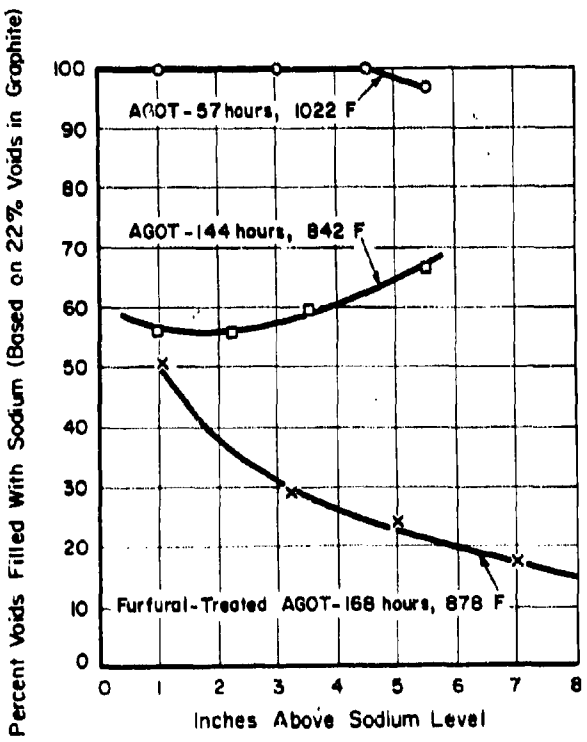

FIGURE 2.22 SODIUM ABSORPTION BY GRAPHITE CAPILLARY EFFECT[81]

SODIUM AND NaK GRAPHITE

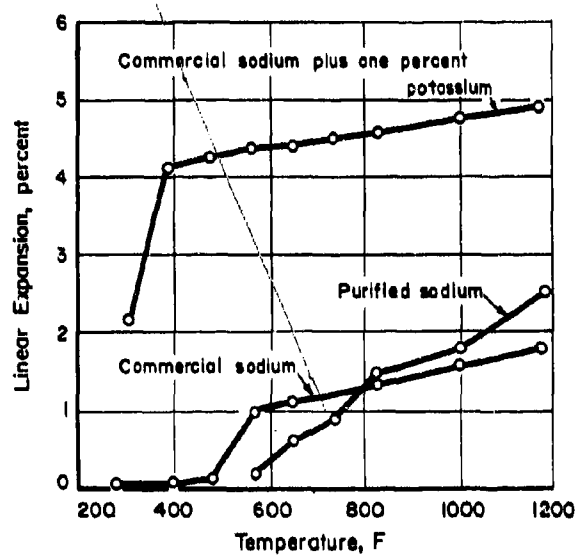

FIGURE 2.23. DILATION OF TSP GRADE GRAPHITE DUE TO ABSORPTION OF SODIUM[82]

TABLE 2.30. DILATION OF GRAPHITE IN 950 F SODIUM AFTER 100 HOURS[84]

Graphite Type	Density, g/cm^3	Dilation Parallel to Extrusion Axis, percent	Dilation Perpendicular to Extrusion Axis, percent
SA25	1.60	1.40	1.46
TSP	1.70	0.82	1.00
CCN	1.89	0.60	0.84

TABLE 2.31. DILATION OF TSP GRAPHITE PARALLEL TO EXTRUSION AXIS[84]

Temperature, F	Dilation, Percent, After Indicated Exposure Time			
	200 Hours	5000 Hours	1000 Hours	2000 Hours
950	-	0.75	0.69	0.65
1000	-	(a)	0.70	0.60
1050	-	1.04	0.82	0.62
1100	-	0.99	0.70	0.73
1150	0.92	1.19	-	0.74
1200	-	0.90	(a)	(a)

(a) No measurement made.

The structure of this material was determined by means of X-ray diffraction and is shown in Figure 2.24. In this interesting compound, the sodium-metal atoms are located between the plane sheets of carbon atoms which comprise the graphite structure. The sodium has penetrated into every

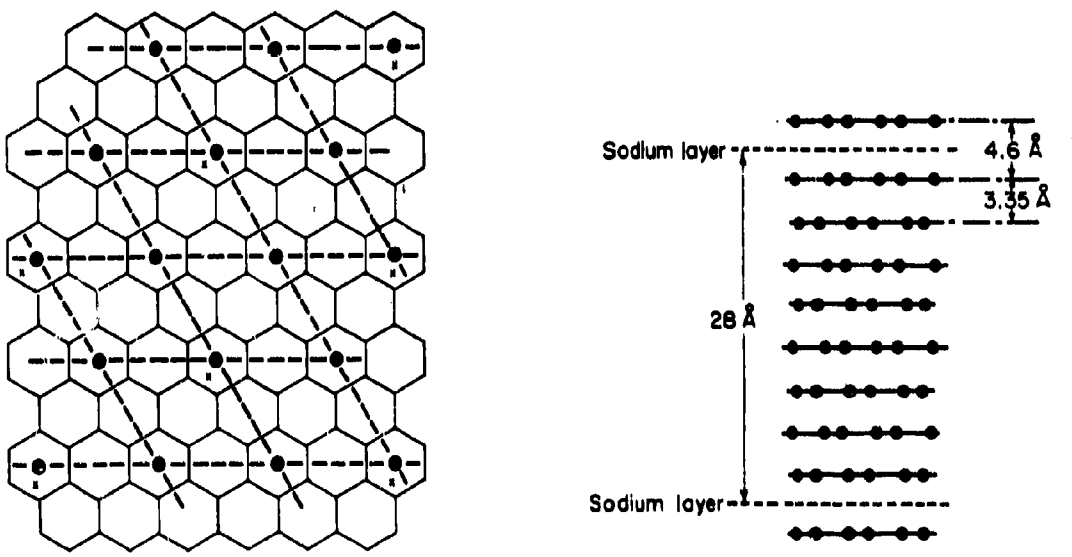

FIGURE 2.24. TOP AND SIDE VIEWS OF THE SODIUM-GRAPHITE COMPOUND $Na_{64}C$ AS DEDUCED FROM X-RAY DIFFRACTION MEASUREMENTS BY R. C. ASHER[86]

eighth interplanar gap and exists in a ratio of 64 carbon atoms to 1 sodium atom. At the sodium-carbon gap position, the interplanar spacing has increased from 3.35 A to about 4.6 A in the compound. It is postulated[79] that the sodium atom is too large to be comfortably accommodated in the graphite structure and tends to distort the graphite. Hence, this distortion and the resulting stresses are what cause the material to disintegrate.

Radiation may also contribute appreciably to the dilation and swelling of graphite in liquid sodium and appears to have contributed to the severe distortion following moderator sheath failures in the Hallam reactor.[87] Atomics International found that graphite absorbed sodium up to 20 percent in volume upon exposure to reactor neutron fluxes.

2.14 CERMETS AND CERAMIC MATERIALS

The resistance of cermet and ceramic materials to sodium and NaK has been investigated to some extent, inasmuch as these materials are potentially useful for specialty applications such as bearing surfaces in practical flow systems. In the case of cermets, emphasis has been placed on evaluation of the commercially available cemented carbide materials, and many of these have been found to be stable in high-temperature exposures, as demonstrated by the information in Table 2.32. However, as indicated in Table 2.33 subtle changes in surface quality can occur even for materials which resist gross attack very well. In applications where surface integrity is essential, these microscopic surface changes may limit reliability and long life.

Ceramics exposed to sodium or NaK resist attack, usually in accordance with their stability predicted on the basis of thermodynamic data, their purity, and their freedom from porosity. For the most part, the exposure data presented in Table 2.34 substantiate these generalizations. Exceptions of some interest include Sm_2O_3 in particular, and Si_3N_4 which appeared to possess resistance to attack although quite porous.

A set of pertinent data for lower-temperature exposures is presented in Table 2.35.

TABLE 2.32. CORROSION RESISTANCE OF CERMETS TO SODIUM AND NaK[88,89]

Exposure to 1500 F Static Sodium or to Sodium in Tilting-Furnace Equipment Where T_{High} = 1500 F and T_{Low} = 1100 F; Each Involves a 100-Hour Exposure[88]	Exposure to NaK-50 for 168 Hours in Tilting Furnace Equipment Where T_{High} = 1600 F and T_{Low} = 1200 F[89]
Cermets Showing No Observable Attack and Very Slight Weight Losses	
WC-6 wt% Co (Carboloy 44A)[a]	WC-4 wt% Co (K-8)
WC-9 wt% Co (Carboloy 779)[a]	WC-12 wt% Co (K-94)
WC-13 wt% Co (Carboloy 55A)[a]	WC-12 wt% Ni
WC-20 wt% TaC-6 wt% Co (Carboloy 907)[a]	TiC-20 wt% Co (K-138)
TiC-10 wt% CbC-10 wt% Ni (K-150A)[b]	TiC-20 wt% Ni (K-151)
TiC-10 wt% CbC-20 wt% Ni (K-151A)[b]	TiC-20 wt% Fe
TiC-6 wt% CbC-30 wt% Ni (K-152B)[b]	TiC-15 wt% CbC-5 wt% Co (K-139A)
TiC-6 wt% CbC-5 wt% Mo-25 wt% Ni (K-162B)[b]	TiC-15 wt% CbC-20 wt% Co (K-138A)
Cr_2C_3-20 wt% WC-15 wt% Ni (Carboloy 608)[a]	TiC-10 wt % CbC-10 wt% Ni (K-150A)
	TiC-10 wt% CbC-20 wt% Ni (K-151A)
	TiC-6 wt% CbC-30 wt% Ni (K-152B)
	TiC-6 wt% CbC-40 wt% Ni (K-153B)
	TiC-6 wt% CbC-5 wt% Mo-25 wt% Ni (K-162B)
	Cr_3C_2-20 wt% WC-15 wt% Ni (Carboloy 608)
	Mo_2C-4 wt% Ni
Cermets Showing Significant Degrees of Attack	
SiC-Si[b]	Mo_2C-12 wt% Co
	$MoSi_2$-12 wt% Co
	$MoSi_2$-12 wt% Ni

(a) Static test.

(b) Tilting-furnace test. In this test, a sample of test material is confined to one end of a sealed tube partially loaded with liquid metal. The tube is rocked in such a way that the fluid flows back and forth over the sample, which is maintained at a temperature higher than that at the opposite end. Thus, as the fluid moves, it undergoes a temperature cycle.

TABLE 2.33. SURFACE-ROUGHNESS DATA FOR SELECTED MATERIALS EXPOSED TO NaK-50 FOR 158 HOURS IN 1600 F PEAK-TEMPERATURE TILTING-FURNACE EXPERIMENTS[89]

Material	Average Surface Roughness (Profilometer), microinches, rms	
	Before Exposure	After Exposure
WC	1-1/2, 1	2-1/2, 3
TiC	1, 1/2	3-1/2, 1
WC-12 wt% Co (K-94)	3, 4	6, 6
WC-12 wt% Ni	5, 5	12, 12
TiC-15 wt% CbC-5 wt% Co (K-139A)	5, 5	6, 7
TiC-15 wt% CbC-5 wt% Co (K-138A)	6, 5	7, 6
TiC-6 wt% CbC-5 wt% Mo-25 wt% Ni (K-162B)	7, 7	6, 6
TiC-6 wt% CbC-30 wt% Ni (K-152B)	4	9
TiC-6 wt% CbC-40 wt% Ni (K-153B)	5, 4	20, 10

TABLE 2.34. CORROSION RESISTANCE OF CERAMICS TO SODIUM AND NaK[88,89]

Exposure to 1500 F Static Sodium for 100 Hours[88]	Exposure to NaK-50 for 168 Hours in Tilting-Furnace Equipment Where T_{High} = 1600 F and T_{Low} = 1200 F[89]
Ceramics Showing No Observable Attack And Very Slight Weight Losses	
Cr_3C (98.7)[a]	CbC (<1)[a]
TiC (97.4)	TiC (<1)
ZrC (100)	WC (<3)
Al_2O_3 (single crystal) (100)	BeO (<1)
BeO (96)	
MgO (single crystal) (100)	
Mg_2AlO_4 (single crystal) (100)	
Sm_2O_3 (79)	
~49.5 Sm_2O_3-27 Gd_2O_3-balance: other rare-earth oxides (90)	
ZrB_2	
Ceramics Showing Relatively Little Attack But Enough to Distinguish Them From Materials in the Category Indicated Above	
B_4C (80-90)	TiN (<3)
SiC	TiB_2 (2)
ThO_2 (75-80)	
Si_3N_4 (67.7)	
$MoSi_2$	
Ceramics Showing Significant Degrees of Attack	
ZrO_2 (Ca-stabilized)	B_4C (0.5)
BN (60-98)	B_4C-20 wt% ZrB_2 (0.4)
	Mo_2C (8)
TiN	SiC-Si (0.3)
	ZrC (<1)
	Ta_2O_5 (2)
	ThO_2 (<2)
	UO_2 (2)
	ZrB_2 (0.7)
	CaF_2 (1)
	$MoSi_2$ (<1)
	MoS_2 (19)
	CeS (19)

(a) In the left column the numbers in parenthesis refer to percent of theoretical density; in the right column, the corresponding numbers refer to apparent porosity in percent.

TABLE 2.35. RESISTANCE OF SELECTED CERAMICS AND CERMETS TO ATTACK BY AGED AND FILTERED SODIUM[90]

Mole Compositions, Except as Indicated	Corrosion Rate, mg/(cm^2)(month) 932 F	1382 F	Absorption, percent	Density, g/cc
		Ceramics		
Artificial periclase crystal	-0.4	- 0.25		
BeO	0.14			
Stabilized ZrO	2.7			
1BeO : 1Al_2O_3	0.0003		0.18	
1MgO :4ZrO_2	-0.091	-14.6	0.01	
1MgO : 8BeO : 1Al_2O_3	-0.44	- 1.6	0.03	
76BeO : 4Al_2O_3: 20ZrO_2 (+2 wt% CaO)	-0.64	0.54	0.01	
3MgO : 90BeO : 1ZrO_2	-0.68	- 0.96	0.03	
Hot-pressed synthetic mica	Disintegrated			2.74
TiN	Spalled			2.39
$CaZrO_3$	28.7			4.28
CdO	Missing			5.33
ZnO	Missing			2.33
Be_2C (swelled due to hydration after test)	4.5			
$MoSi_2$	Missing			6.10
		Cermets		
K-138 (Co-bonded TiC	-0.275			
K-138A (Co-bonded CbC)	-0.225			
K-L7 (Co-bonded WC)	-0.15	- 0.1		
K-152 (Ni-bonded TiC)	-0.15	- 1.77		
K-152B (Ni-bonded CbC)	-0.05	- 1.6		
100 percent TiC	-0.025	- 0.22		

3. POTASSIUM

3.1 COLUMBIUM ALLOYS

3.1.1 Compatibility - General

Pure columbium has excellent resistance to attack at elevated temperatures by high-purity potassium liquid and vapor. However, its corrosion resistance is reduced as the amount of oxygen impurity in the columbium, the potassium, or the atmosphere is increased. Alloying columbium with a small percentage of some strong oxygen getter like zirconium or hafnium decreases its sensitivity to oxygen contamination. The solid-solution addition of a refractory metal like tungsten or molybdenum to a "gettered" columbium alloy improves its high-temperature strength without hurting its resistance to corrosion by potassium.

The solubility of columbium in potassium has been found[91,92,93c] to be rather limited (<30 ppm) and to vary only slowly with temperature up to about 2400 F (see Table 3.1). The weight changes, surface roughening, mass transfer, and grain-boundary attack which have been observed in assorted corrosion tests on columbium and its alloys are generally attributable to impurity effects and to dissimilar materials in the systems.

Theories of corrosion of columbium alloys by potassium generally start with oxygen either in solution in the metal or in the potassium, or else in the form of an adsorbed gas or an oxide film on the solid-metal walls.[94] In ungettered alloys and in gettered alloys with high oxygen contamination, this oxygen combines with the potassium and constituents of the columbium alloy to form stable complex oxides, which may go into solution in the potassium. In two-phase systems, the distilled potassium can pick up oxygen from the walls in the condensing region and give it up to the walls in liquid zones. This leaves the metal surface rough or etched, particularly in the condensing region. In some cases, interstitials concentrated at grain boundaries are leached out, leaving evidences of grain-boundary penetration. The extent of degradation depends on time, temperature, and whether or not a continuing source of oxygen (e. g., from the test environment) is present.

Corrosion experiments on columbium alloys tend to substantiate such theories. For example, several laboratories[91,94,95] have identified $KCbO_3$, CbO_2, and Cb in the corrosion-product layers on the walls after heating potassium in a columbium capsule at 1500 F or above, with

TABLE 3.1. SOLUBILITY OF TRANSITION METALS IN POTASIUM[93c]

(Solution equilibrated, centrifuged, and collected in tungsten-lined cup.)

Solute Element	Equilibration Temperature, F	Oxygen in Starting K,[a] ppm	Solubility,[b] ppm
Cb	2065	23	10
	2235	23	19[c]
	2275	10	11[d]
Ta	2065	23	17
	2235	23	15
	2275	10	139[c]
	2425	23	11[c]
Fe	1700	10	452
	1830	10	500
Ni	1700	10	3[d]
	1830	10	4
Ti	1830	10	82[d]
Zr	1830	10	110[d]

(a) By the vacuum mercury-amalgamation method.
(b) Values obtained with 10-ppm oxygen potassium were for equilibrated and centrifuged longer, and are considered more reliable than those obtained with 23 ppm oxygen.
(c) Average of two determinations.
(d) Average of three determinations.

purposely high oxygen contamination present. Refluxing capsule tests have shown oxygen to be depleted from the condensing-zone walls and concentrated in the liquid-zone walls. Gettered columbium alloys have been exposed for thousands of hours in boiling-potassium capsules and loops under clean conditions at temperatures of 2000 F and above with only minor corrosive attack.

3.1.2. Cb-1Zr in Monometallic Systems

Workers at NASA-Lewis observed solution, intergranular attack, and mass-transfer deposits in Cb-1Zr refluxing capsules containing purified potassium at 1800 and 2200 F (Table 3.2).[96] These results are not typical of the behavior of other gettered columbium alloys, nor are they duplicated by Cb-1Zr performance in low-oxygen potassium systems at other sites. The investigators suspect that the corrosion was the result of inward diffusion of residual oxygen during a brief period early in the exposures when the pressure in the vacuum chamber increased from $\sim 10^{-8}$ to $\sim 10^{-3}$ torr.

Cb-1Zr capsules with Cb-1Zr tab inserts, tested by General Electric for 5,000 hours with 2000 F refluxing potassium, showed only a small amount of general corrosion in the form of stains, slight increase in hardness in the vapor region, some polishing above the liquid zone, and insignificant dimensional and weight changes.[97,98a] A similar capsule tested for 10,000 hours showed, in addition, some fine black deposits and gold discoloration on the walls between the primary condensing zone and the liquid zone.[97] These capsules had been fabricated by rolling 80-mil sheet and TIG welding the axial seam and end caps, then homogenizing the welds for 1 hour at 2200 F. Posttest metallography of the 5000-hour capsule welds showed large grains containing a fine precipitate, but no corrosive attack. However, an earlier Cb-1Zr capsule, which had been operated with unstable boiling for 1000 hours at 2000 F, suffered grain-boundary attack (maximum, over 10 mils deep) in a few selected grain boundaries in the weldments submerged in liquid potassium.[98a] It was conjectured that this nonreproducible attack was associated with vapor-nucleation sites.

Similar attack in the heat-affected zone of an incomplete-penetration weld of a Cb-1Zr thermocouple well in a natural-convection boiling-potassium Cb-1Zr loop was observed at Oak Ridge after 2800 hours of loop operation at 2050 F.[89] The porous, irregular surface at the root of the weld appeared to be an ideal vapor-bubble nucleation site, and the observed attack (<1 mil) was assumed to have resulted from the violent agitation of liquid potassium in this region. This was the only corrosion detected metallographically in this loop, though a maximum condenser-wall loss of 0.1 mg/cm^2 (corresponding to a removal rate of only 12 μ-inch/year) was detected by weight changes of sleeve inserts. Also, a very slight quantity ($\sim$ 1 milligram) of mass-transfer crystals was recovered from the stripping solution used to clean the insert specimens from the subcooler region. Overall, however, the corrosion of the Cb-1Zr in this 2800-hour, 1200 F liquid, 2050 F boiling-potassium loop was negligible.

Table 3.3 includes the conditions and results of boiling-potassium capsule and loop tests operated at Oak Ridge with Cb-1Zr.[93e,100] The corrosion tabs underwent weight losses or gains, depending on their locations. In all cases, oxygen in the metal was transferred from the condensing vapor regions to the coolest liquid regions. The weight changes were approximately equivalent to the changes in oxygen content. Thus, the weight changes appear to reflect migration of oxygen rather than metal transfer.

In the forced-circulation loop of Table 3.3, erosion by wet potassium vapor was studied in a turbine simulator, consisting of Cb-1Zr nozzles and blades. There were no signs of corrosion anywhere in the loop after 3000 hours of operation, except for approximately 1 mil of erosion at a wet-vapor (83 percent quality) impingement area and up to 1 mil of localized crystalline deposits nearby.

Pratt & Whitney's 3000-hour thermal-convection loops showed comparably good behavior for Cb-1Zr in boiling potassium.[101] As indicated in Table 3.4 dissolution occurred to a limited extent in the cooler portions of the Cb-1Zr loops, the worst effect being a loss of less than 0.5 mil/yr. Weight changes in the higher-temperature boiler sections were insignificant. No evidence of corrosion could be found metallographically, and no serious migration of interstitials occurred.

The endurance limit in reversed bending of stress-relieved (1 hour at 2200 F) 30-mil Cb-1Zr sheet submerged in liquid potassium at 800 F was measured at Battelle-Columbus[102] as 27,000 psi. In these tests, the neutral axis was parallel to the rolling direction and runouts were 10^7 cycles. No comparable data are available for vacuum or inert-gas environments.

3.1.3 Columbium Alloys Other Than Cb-1Zr

NASA-Lewis used capsules machined from bar stock of the test material as specimens for boiling-refluxing potassium compatibility studies.[96] In addition to Cb-1Zr, other columbium alloys tested, under conditions indicated in Table 3.2 are:

TABLE 3.2. CORROSION OF REFRACTORY ALLOYS BY REFLUXING POTASSIUM[96]

Alloy	Temperature, F	Time, Hour	Corrosive Attack			Other Comments
			Type	Depth, Inches	Location	
SCb-291	1800	1000	Intergranular	1.5	Weld	
	2200	1000	Solution	2.0	Condensing section	General attack
			Intergranular	16	Liquid section	General attack
B-33	1800	2000	None	-	-	-
	2200	1000	Solution	1.0	Condensing section	-
			Solution	3.0	Liquid-vapor interface	-
	2300	380	Intergranular	1.0	High stress area in condensing section	Very slight solution attack at liquid-vapor interface
Cb-1Zr	1800	2000	Intergranular	7.0	Liquid-vapor interface	-
			Intergranular	0.8	Liquid section	General attack
	2200	123	Solution	-	Condensing section	General attack
			Intergranular	4.5	Liquid-vapor interface	1.5 mils deposit
D-43	2200	2000	None	-	-	Film at liquid-vapor interface
	2300	2000	None	-	-	Amber film over entire inner surface
Cb-752	2200	4000	None	-	-	Cb and ZrO_2 film at liquid-vapor interface
D-14	2000	4000	None	-	-	Cb and ZrO_2 film at liquid-vapor interface
AS-55	2200	4000	None	-	-	Heavy etching, about 0.2 mil
B-66	2200	4000	Solution	0.2	Condensing section	Cb and ZrO_2 film at liquid-vapor interface
C-129	2200	4000	None	-	-	Film at liquid-vapor interface
FS-85	2200	4000	None	-	-	Cb or Ta film at liquid-vapor interface
	2300	2000	None	-	-	Film at liquid-vapor interface
	2400	2000	None	-	-	Film at liquid-vapor interface

TABLE 3.3. SUMMARY OF OAK RIDGE BOILING POTASSIUM - REFRACTORY METAL COMPATIBILITY TESTS[98e,100]

(Initial oxygen in potassium: 70 to 200 ppm by getter-vacuum-fusion; 20 to 50 ppm by mercury amalgamation.)

Number of Tests	Material		Temperature, F		Time Per Test, hours	Condensing Rate, g/(min)(cm^2)	Weight Change,[a] mg/cm^2	Results	
	Specimen	Container	Maximum	Minimum				Chemical	Metallographic
					Refluxing Capsules				
1	TZM	TZM	2300		5000	0.27	+7 to -0.4	Increase in concentration of Ti and Mo in K	No attack
3	D-43	D-43	2200-2550		850 to 5000	0.27 to 0.57	+1.7 to -0.002	Oxygen transfer from top to bottom of capsule; some decarburization at bottom; No Cb, Zr, or W in K after test	No attack, ZrO_2 layer on surface of end-plug weld
4	Cb-1Zr	Cb-1Zr	2000-2200		600 to 5000	0.17 to 0.28	+0.08 to -0.1	Oxygen transfer from top to bottom of capsule	No attack
					Natural-Circulation Loops				
1	Cb-1Zr	Cb-1Zr	2100	1200	2800		+0.13 to +0.01	No significant change in specimens from condenser of subcooler	No attack
1	Cb-1Zr	Cb-1Zr	2200	1250	1200	0.19	+0.7 to -0.2	Increase in oxygen concentration of specimens in subcooler	No attack
1	D-43	D-43	2200	1530	3000	0.35	+0.6 to +0.2	Increase in oxygen of specimen in subcooler	No attack
1	T-111	T-111	2800	1900	3000	0.53	+2.5 to -0.4	Examinations incomplete	
1	TZM	D-43	2280	1830	3000	0.32	Slight gains	Examinations incomplete	
					Forced-Circulation Loop				
1	Cb-1Zr	Cb-1Zr	2000	670	3000	270 g/min		Increase in oxygen concentration in boiler and condenser regions; no increase in concentration of Cb or Zr in K	~1 mil of erosion damage, second-stage blade

(a) A weight loss of 22 mg/cm^2 is equivalent to about 1 mil of uniform surface removal.

TABLE 3.4. CORROSION OF SPECIMENS IN COLUMBIUM-ALLOY THERMAL-CONVECTION LOOPS OPERATED 3000 HOURS WITH BOILING POTASSIUM[101]

				Boiler				Condenser and Subcooler			
Loop	Estimated Potassium Flow Rate, g/hr	Loop Material	Insert Material	Temperature, F	Number of Specimens	Weight Change, mg/cm^2	Equivalent Maximum Dimensional Change, μin./yr	Temperature, F	Number of Specimens	Weight Change, mg/cm^2	Equivalent Maximum Dimensional Change, μin./yr
1			Cb-1Zr	1960	2	-0.09, -0.10	-12	1600	6	-3.3 to -3.6	-430
	4540	Cb-1Zr	PWC-533	-	-	-	-	1600	4	+0.01 to +0.06	+ 7.2
2	5450	PWC-533	PWC-533	2050	4	0	0	1800 to 1600	6	-1.7 to -2.2	-330
3	4100	Cb-1Zr	PWC-11	2000	10	+0.1 to +0.2	+24	1300	4	-0.6 to -0.7	- 84
4	1000	Cb-1Zr	Cb-1Zr	1850	6	-0.02 to +0.01	- 2.4	1300	5	-0.19 to -0.03	- 22.8
	Ditto	Ditto	Cb-1Zr	-	-	-	-	1250	5	+0.08 to -0.08	± 9.6
	"	"	TZM	1850	3	+0.01 to +0.05	+ 6	1850 to 1300	8	-0.07 to -0.02	- 8.4
	"	"	316SS	-	-	-	-	1250	4	-0.16 to -0.03	- 19.2

POTASSIUM COLUMBIUM ALLOYS

B-33(Cb-4V)
SCb-291(Cb-10Ta-10W)
D-14(Cb-5Zr)
AS-55(Cb-5W-1Zr-0.2Y-0.06C)
B-66(Cb-5Mo-5V-1Zr)
D-43 or X-110 (Cb-10W-1Zr-0.1C)
FS-85(Cb-27Ta-10W-1Zr)
Cb-752(Cb-10W-2.5Zr)
C-129(Cb-10W-10Hf).

It is apparent from Table 3.2 that the ungettered alloys, B-33 and SCb-291, were more severely attacked than the others, which contain either zirconium or hafnium. The gettered alloys showed only slight effects from exposure to refluxing potassium. The most noticeable effect was a dark film or ring at the liquid-vapor interface. X-ray patterns on the more prominent blemishes revealed the presence of ZrO_2 and columbium crystals, in conformity with the concept that mainly oxygen is responsible for any corrosion found in these systems. On the basis of this study, Schauermann concluded that the following materials look promising as potassium containers (in order of decreasing corrosion resistance): C-129, D-14, Cb-752, D-43, AS-55, B-66, and FS-85. The ungettered alloys, B-33 and SCb-291, were considered unsatisfactory.

The encouraging resistance to boiling potassium exhibited by the D-43 and AS-55 alloys was confirmed in capsule and loop experiments by General Electric[97,98a,98b,103] and Oak Ridge.[93a,100] Capsules with up to 2550 F refluxing potassium inside and vacua of 10^{-7} to 10^{-9} torr outside were exposed for periods up to 10,000 hours. One 5000-hour AS-55 capsule showed dark stains at the liquid-vapor interface and elsewhere, which did not appear in a duplicate capsule that had been charged with potassium by an improved transfer technique. This implies that atmospheric contaminants introduced during charging were responsible for the staining in the first capsule. No attack of grain boundaries in either the weldments or recrystallized-sheet tubing walls was observed in either alloy. Some of the AS-55 capsules showed sparse, isolated, white nonmetallic deposits, believed to be Y_2O_3. There was some coalescence of carbides, but no loss in creep-rupture strength at 2000 F. Neither alloy suffered mass transfer of carbon. However, oxygen was leached from both the AS-55 and D-43 alloys in the condensing zones when the starting material was high in oxygen (400 ppm or more). In fact, the weight changes observed in D-43 inserts in the Oak Ridge experiments (Table 3.4) are believed to reflect oxygen migration rather than metallic-element transfer.

To assess the mass-transfer situation in a polythermal, circulating potassium heat-exchange system, General Electric ran two all-liquid thermal-convection loops for 2000 hours at T_{max} = 2000 F and T_{min} = 1850 F.[98b] One loop was constructed of AS-55 alloy and the other was Cb-10W-1Zr (D-43 alloy without the carbon). The latter contained a short hot-zone section of AS-55 tubing to see whether interstitials would transfer between the two alloys. Posttest metallographic and dimensional examinations revealed no signs of corrosion or mass transfer. Chemical analyses showed no measurable transfer of carbon, nitrogen, or hydrogen in either loop. However, oxygen was gettered by the AS-55 insert in the hot zone of the Cb-10W-1Zr loop, and the surface stain found on this insert was thought to be a yttrium compound. Room-temperature tensile strengths of the alloys were not altered appreciably by the exposures, but the 2000 F tensile strengths were reduced by about 20 percent (from 30,000 to 24,000 psi), with no significant migration of interstitials or alloying elements. Furthermore, as indicated in Figure 3.1, the 3000-hour exposure had no measurable effect on the yield strength of PWC-533 tabs located at various places in the loop.

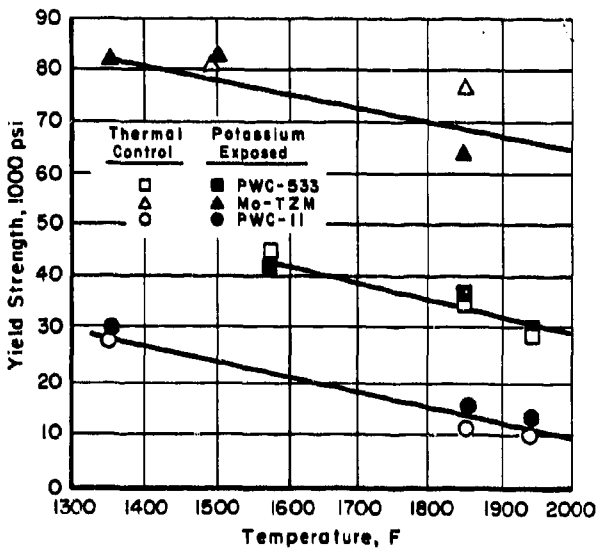

FIGURE 3.1. EFFECT OF FLOWING POTASSIUM ON YIELD STRENGTH OF SPECIMENS EXPOSED FOR 3000 HOURS AT 1350 TO 1950 F[101]

Initial oxygen in potassium: 10 to 40 ppm, by mercury emalgamation.

3.1.4 Columbium Alloys in Heterometallic Systems

3.1.4.1 Cb-1Zr - Hastelloy X

Table 3.5 shows Rocketdyne's results of capsule tests,[104a] using relatively impure potassium. The general conclusions from these results are:

TABLE 3.5. CORROSION OF COLUMBIUM AND [illegible] ALLOY TABS EXPOSED TO "AS-RECEIVED" POTASSIUM IN ISOTHERMAL CAPSULES[Refs]

Temperature, F	Time, Hour	Capsule Material	Tab Materials	Tab Weight Change, mg/(cm²)(day)	Metallographic Observations on Tab
1450	356	Hastelloy X	Cb, weld	-0.44	No reaction layer
		Hastelloy X	Cb-1Zr, weld	-0.39	Ditto
		Inconel X	Cb, weld	-2.32	"
		Inconel X	Cb-1Zr, weld	-1.90	"
1800	63	Hastelloy X	Cb, weld	-1.88	-
	63	Ditto	Cb-1Zr, weld	-2.89	-
	63	"	Cb-1Zr, wrought	-1.13	-
	100	"	Cb, wrought	-0.32	0.3-mil reaction layer
	100	"	Cb, weld	-0.78	0.3-mil reaction layer; 1 to 3 mils' penetration
	348	"	Cb, wrought	-0.26	1-mil reaction layer
	348	"	Cb, weld	-0.29	1-mil reaction layer; 0 to 5 mils' penetration
1900	50	Hastelloy X	Cb, wrought	-2.80	0.5 to 1-mil reaction layer
	50	Ditto	Cb-1Zr, wrought	-1.29	0.5 to 1-mil reaction layer
	63	"	Cb, wrought	-7.23	1.5-mils reaction layer
	63	"	Cb, weld	-5.30	-
	63	"	Cb-1Zr, weld	-2.90	3 to 5-mil reaction layer; 5 to 8 mils' penetration
	159	"	Cb, weld	-3.58	-
	159	"	Cb-1Zr, weld	-2.89	-
2000	24	Hastelloy X	Cb, wrought	-0.83	-
	24	Hastelloy X	Cb, weld	-1.43	-
	300	Cb-1Zr	Cb, wrought	-0.03	No reaction layer
	300	Cb-1Zr	Cb-1Zr, wrought	+0.06	No reaction layer
2100	100	Cb-1Zr	Cb, wrought	-0.04	-
	100	Ditto	Cb, weld	-0.04	Finely dispersed second phase throughout, except in grain boundaries
	100	"	Cb-1Zr, wrought	+0.09	-
	100	"	Cb-1Zr, weld	+0.07	Finely dispersed second phase throughout, except in grain boundaries
2200	140	Cb-1Zr	Cb, wrought	-0.07	-

(1) Columbium and Cb-1Zr tabs undergo pronounced weight losses when exposed to 1450 to 2000 F potassium in Hastelloy X capsules. Wrought material is superior to welded, and Cb-1Zr is superior to unalloyed columbium.

(2) At 1800 and 1900 F, columbium and Cb-1Zr welds suffer severe intergranular penetration when exposed to potassium in Hastelloy X capsules, and both welded and wrought materials show CbN and/or CbC reaction layers.

(3) Weight changes of columbium and Cb-1Zr specimens tested in Cb-1Zr capsules at temperatures up to 2200 F are small in comparison with those in Hastelloy X capsules. The columbium specimens lose weight, and the Cb-1Zr specimens gain. These changes are orders of magnitude greater than those observed by Pratt & Whitney and General Electric workers, presumably because the Rocketdyne capsule systems contained substantially more oxygen impurity.

3.1.4.2 Cb-1Zr - Austenitic Stainless Steel

General Electric tested two Type 321 stainless-steel and two Type 316 stainless-steel isothermal capsules each containing two Cb-1Zr test specimens, for 1000 hours at 1400 F in air.[93d,105] The Cb-1Zr specimens in the Type 316 stainless-steel capsules came out tarnished and showed weight gains, whereas those in the Type 321 stainless-steel capsules did not. Chemical analyses showed that the Cb-1Zr specimens in the Type 316 stainless-steel capsules picked up substantial quantities of carbon and nitrogen, whereas those in the Type 321 stainless-steel capsules did not (Table 3.6). The resistance to migration of the carbon and nitrogen from the Type 321 stainless steel is attributed to its titanium, which forms highly stable carbides and nitrides. The oxygen and hydrogen contents were not affected significantly in either case. The increased strength and decreased ductility resulting from the carbon and nitrogen pickup in the Cb-1Zr specimens in the Type 316 stainless-steel capsules are apparent in Table 3.6. Such "embrittlement" is not serious, since 15 percent elongation of Cb-1Zr at room temperature represents adequate ductility.

This behavior was corroborated by United Nuclear,[93b,106] in thermal-convection loop experiments. The loops were made of Type 316 stainless steel and contained strings of Cb-1Zr and Type 316 stainless-steel tabs, and in one case, two Type 321 stainless-steel tabs. Maximum and minimum temperatures were 1600 and 1200 F, respectively, and the potassium used was filtered and gettered to 25 ppm oxygen, 35 ppm carbon, and 5 ppm nitrogen. In such systems:

(1) Carbon and nitrogen are depleted from Type 316 stainless steel (but not from Type 321 stainless steel) in high-temperature regions and transported to lower-temperature regions without serious deterioration of structural properties of the stainless steel.

(2) The Cb-1Zr tabs are saturated at low carbon and nitrogen levels and remain ductile for at least 5000 hours (longest test). A thin (<1 mil) carbonitride surface layer inhibits carbon and nitrogen diffusion into the matrix, slowing the formation of embrittling carbides and nitrides.

(3) Carbon additions to the potassium result in carburization of the Type 316 stainless steel throughout the loop, but no increased pickup of carbon by the Cb-1Zr. Similiarly, the use of nitrogen instead of argon for the atmosphere above the potassium does not increase the total nitrogen pickup by the Cb-1Zr.

In the above systems, the Type 316 stainless steel:Cb-1Zr surface area ratio was between 20:1 and 100:1. When the ratio is reversed (Cb-1Zr >> Type 316 stainless steel), the large refractory-alloy surfaces would be expected to getter interstitials from the limited stainless surfaces. This is illustrated by the four Type 316 stainless steel tabs in the 1250 F region of Pratt & Whitney's Cb-1Zr Loop 4 (Table 3.4). These specimens all underwent minute weight losses during the 3000-hour test, presumably by leaching of interstitials, and the Cb-1Zr tabs immediately downstream showed corresponding slight weight gains. There was no measurable migration of Type 316 stainless-steel constituents to the Cb-1Zr anywhere else in the loop.

3.1.4.3 Cb-1Zr - TZM (Mo-0.5Ti-0.08Zr)

Since the SNAP-50/SPUR power-conversion system may employ a TZM turbine wheel in a Cb-1Zr casing, the compatibility of this combination of alloys with wet potassium vapor is of special interest. On the basis of examinations of the TZM inserts from Pratt & Whitney's Cb-1Zr Loop 4 (Table 3.4),[101] it was concluded that TZM is compatible with wet potassium vapor at 1850 F. However, the yield-strength results for potassium-exposed TZM shown in Figure 3.1 suggest a possible reduction in high-temperature strength as a result of the exposure.

General Electric ran two Cb-1Zr, 2000 F refluxing-potassium, capsule tests with TZM tubular inserts in the condensing region.[107] One was exposed for 2500 hours and the other for 5000 hours. Preliminary results indicate excellent compatibility

TABLE 3.6. EFFECT OF 1000-HOUR EXPOSURE TO 1400 F POTASSIUM ON 0.040-INCH THICK Cb-1Zr SPECIMENS CONTAINED IN TYPES 316 SS AND 321 SS CAPSULES[93d,105]

Capsule Material and Specimen	Chemical Analyses of Cb-1Zr Alloy Specimens, ppm				Room-Temperature Tensile Properties of Cb-1Zr Alloy Specimens		
	C	N	O	H	0.2% Offset Yield Strength, psi	Ultimate Tensile Strength, psi	Elongation, percent
Unexposed-1	10	14	75	6	23,300	40,000	37
Unexposed-2	50	50	200	24	-	-	-
Type 321 SS-3	50	21	147	13	29,600	49,300	30
Type 321 SS-4	35	16	114	14	25,300	42,800	36
Type 316 SS-1	210	206	258	23	46,700	56,000	20
Type 316 SS-2	280	336	156	7	40,300	57,000	15

for this system. The only changes observed were some staining of the walls in the vapor region, minute weight losses (1.3 mg/cm^2, maximum) of the inserts in the condensing zone of the 5000-hour capsule, and some surface decarburization and recrystallization of the TZM.

3.1.4.4 Cb-1Zr - PWC-11 (Cb-1Zr-0.1C)

As indicated in Table 3.4, fourteen PWC-11 tabs were inserted at various locations in Cb-1Zr Loop 3[101] and exposed for 3000 hours to flowing potassium between the 1300 F subcooled liquid state and the 2000 F vapor state. Since the only difference between the Cb-1Zr loop material and the PWC-11 inserts was the carbon in the latter, carbon migration and its side effects were of particular interest.

Posttest examinations revealed the following:

(1) Tabs in the boiler gained weight; those in the condenser and subcooler lost weight (Table 3.4).

(2) All tabs showed some increase in carbon at the surfaces, the greatest gain being in tabs in the 1975 F liquid in the boiler zone (from pretest value of 900 to 1000 ppm to posttest value of 1300 to 1900 ppm).

(3) There were no significant changes in the nitrogen, oxygen, or zirconium concentrations in the PWC-11 tabs.

(4) The strength of the PWC-11 was not altered by the exposure, as can be seen in Figure 3.1.

3.1.4.5 Cb-1Zr - PWC-533 (Cb-5Mo-3Ti-3Zr-0.1C)

Pratt & Whitney workers exposed welded samples of PWC-533 alloy to 2000 F potassium for 1600 hours in Cb-1Zr capsules with no measurable weight changes, corrosive attack, or material transfer. This outstanding performance was duplicated by the PWC-533 tabs in the 1600 F condensing zone of a boiling-potassium Cb-1Zr thermal-convection loop (Loop 1, Table 3.4).[101]

3.2 MOLYBDENUM ALLOYS

3.2.1 Compatibility - General

Molybdenum and various molybdenum alloys have been tested in liquid and vapor potassium with results varying from a loss of 7 mg/(cm^2)(day) at 1800 F[104a] to no measurable attack after 2500 hours at 2000 F.[93a] The controlling factor in this seemingly inconsistent behavior is the oxygen content of the potassium.

The apparent equilibrium solubility of molybdenum in potassium increases roughly linearly with increasing oxygen content in the potassium, as illustrated in Figure 3.2.[108] Pure molybdenum is essentially insoluble in pure potassium as suggested by the fact that it drops below 1 ppm in 2000 F potassium which has been purified to 70 ppm oxygen or less.

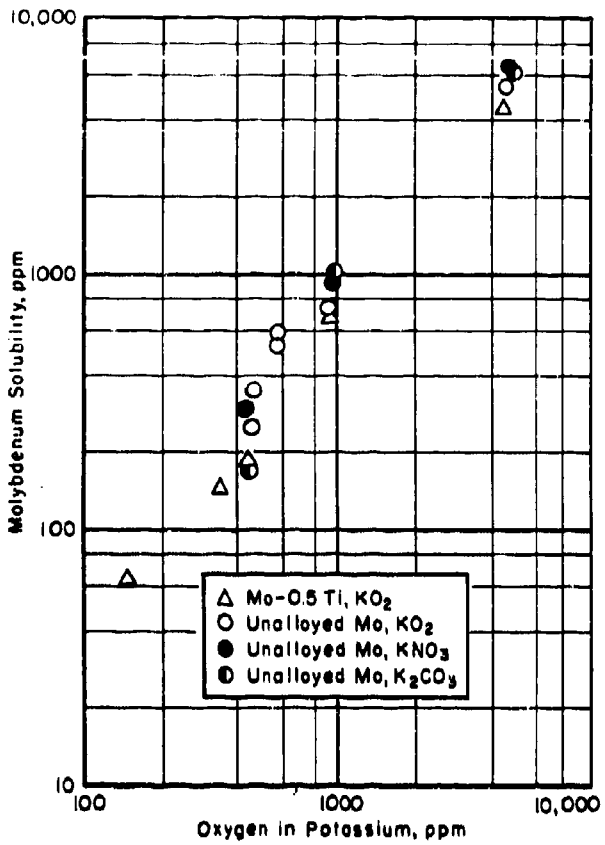

FIGURE 3.2. APPARENT EQUILIBRIUM SOLUBILITY OF MOLYBDENUM IN POTASSIUM AS A FUNCTION OF OXYGEN CONTENT[108]

It is evident that the molybdenum detected in these solubility tests is in the form of products of chemical reactions which require the presence of oxygen in some form. Though the solubility of molecular oxygen in molybdenum is low (45 to 65 ppm at 2000 to 3000 F), surface oxides can form quite readily. When these oxides (MoO_2 or MoO_3) come in contact with molten potassium or with potassium oxides at temperatures above about 500 F, free energies favor the formation of stable complex oxides, such as K_2MoO_4.[109] The latter compounds or their dissociation products go into solution in the potassium, and their molybdenum atoms are detected spectrographically as "dissolved" molybdenum. As implied in Figure 3.2, these Mo-O-K interactions continue as long as oxygen is being added. Presumably, the apparent molybdenum solubility would level off if enough oxygen were added to saturate the potassium with complex oxides - a limit which has not been reached in Figure 3.2 (>6000 ppm oxygen at 2000 F).

In summary, molybdenum has excellent resistance to attack by high-purity potassium at temperatures to 2500 F. However, its resistance is reduced as the oxygen content of the potassium is increased. Alloying the molybdenum with small amounts of oxygen getters like titanium and zirconium raises its recrystallization temperature and improves its mechanical properties, but has little effect on its sensitivity to oxygen contamination. Thus, molybdenum and alloys like Mo-0.5Ti, TZM (Mo-0.5Ti-0.08Zr), or TZC (Mo-1.2Ti-0.25Zr-0.15C) are practical long-time containers for high-temperature molten potassium and potassium vapor only when the oxygen in the system can be kept low (< 50 ppm, by amalgamation).

3.2.2 Corrosion and Mass-Transfer Tests

As shown in Table 3.3, sleeves of TZM (Mo-0.5Ti-0.08Zr-0.03C) exposed to 2300 F boiling-refluxing potassium inside a TZM capsule underwent weight gains and losses indicative of material transfer from the top of the condensing zone to the regions below. While these weight changes were greater than those of columbium-base alloy specimens under similar conditions, the maximum equivalent corrosion rate was actually insignificant (0.035 mil/yr of uniform surface removal). Post-test analyses showed no interstitial migration in the TZM and some pickup of titanium and molybdenum in the potassium. These manifestations are consistent with the previously described concept that dissolutive attack of molybdenum by potassium stems from Mo-O-K (and Ti-O-K) interactions. The tests covered in Table 3.3 were conducted under vacuum in the range 10^{-7} to 10^{-9} torr, and initial oxygen in the potassium was less than 50 ppm (by the amalgamation method). With such restricted availability of oxygen, it is not surprising that the absolute rate of corrosion of the TZM inserts was negligible.

Though the examinations were not complete at the time of this writing, the TZM inserts in the D-43 columbium-alloy loop shown in Table 3.3 showed a consistent pattern of very slight weight gains, which may be indicative of dissimilar-metal mass transfer.

During the course of creep experiments in a potassium-vapor environment to check the suitability of TZM alloy for the potassium-vapor turbine in the SNAP-50/SPUR power plant, mass-transfer crystals (99+ wt% molybdenum) were found on the specimen surfaces.[110] A special study was made with TZM capsules under boiling-refluxing conditions to determine how various system parameters influenced the mass transfer.[111] This study, utilizing peak potassium temperatures between 1500 and 2040 F and oxygen contents of 48 to 500 ppm (determined by mercury amalgamation), led to the following salient conclusions:

(1) The amount of mass transfer is more sensitive to the amount of oxygen in the potassium than to any other variable in the study.

(2) The amount of mass transfer is relatively insensitive to temperature gradients; transferred material tends to deposit preferentially on the hottest surfaces, signifying that chemical reactions and diffusion processes, rather than solution-precipitation effects, are responsible.

(3) The chemical reactions leading to crystal deposition reach an equilibrium or saturation condition in a relatively short time, as demonstrated by the fact that deposits were no heavier after 480 hours than they were after 50 hours.

As pointed out in the section on Columbium Alloys, TZM inserts showed excellent compatibility with Cb-1Zr in boiling-refluxing potassium after 5000 hours at 2000 F.[93a] Similar capsule experiments gave insignificant weight changes for Mo-0.5Ti inserts in 1800 F refluxing potassium after 500 hours.[93b] Consequently, several investigations were run to examine the ability of TZM and Mo-0.5Ti simulated turbine blades and nozzles to withstand erosion by high-velocity potassium vapor.

At AiResearch, 2000 F potassium vapor with a calculated quality of 80 to 100 percent was expanded in a Cb-1Zr loop through a series of nozzles, and impinged on Mo-0.5Ti stationary test coupons at each nozzle exit.[112] The potassium had been gettered with zirconium sheet for 14 hours at 1400 F prior to the test. Examinations of the Mo-0.5Ti test couples and nozzles after the 307-hour test showed the following:

(1) Nozzle 1, which was Mo-0.5Ti exposed to the highest-quality vapor, did not change in diameter.

(2) Subsequent nozzles, which were Cb-1Zr exposed to lower quality vapor, increased in diameter by 0.3 to 0.4 mil.

(3) Mo-0.5Ti test coupons did not change thickness measurably, but lost 0.2 to 0.8 milligram (of ~2.7 grams), and their mirror finish developed a satiny texture in the impingement areas.

(4) Metallography to 200X revealed no surface irregularities in the satiny zones.

In similar experiments at Oak Ridge, TZM-alloy nozzle and turbine-blade specimens in Type 316 stainless steel loops showed severe cratering and relatively high weight losses after 504 to 2067 hours' exposure to 1280 F potassium vapor at 83 percent quality.[93f,100] Reaction products removed from the TZM components showed unusually high concentrations of carbon and oxygen. However, a repeat experiment, with the addition of a full-flow zirconium hot trap to provide oxygen-free potassium to the TZM test nozzles and blades, yielded virtually no cratering or weight losses of the TZM. This signifies that the severe attack and mass transfer in the original tests were caused by oxygen contamination in the original potassium. An analogous capsule experiment, using alternate Type 316 stainless steel and TZM sleeves inside a Type 316 stainless steel capsule containing highly purified 1600 F refluxing potassium (20 ppm oxygen by amalgamation) revealed no corrosion or dissimilar-metal mass transfer in any of the components. This verifies the compatibility of Type 316 stainless steel with TZM in low-oxygen potassium systems.

3.2.3 Effects of Exposure on Mechanical Properties

Creep-rupture tests were run for up to 1539 hours on vacuum-arc-cast, hot-rolled, stress-relieved Mo-0.5Ti[98f,113] and TZM[110] alloys. For most of the work, hollow specimens were tested in an evacuated chamber. Sealed inside the test specimens were small charges of potassium, so that the inside walls would be exposed to potassium vapor at the test temperatures (1800 and 2000 F) during the creep experiments. The potassium used contained less than 80 ppm oxygen, as measured by mercury amalgamation. Similar control specimens were tested without potassium.

For both alloys, the design curves, shown in Figures 3.3 and 3.4 were the same for the potassium-exposed specimens as for the controls. Thus, it was concluded that the creep-rupture behavior, at least up to 1000 hours at 1800 and 2000 F, of these alloys is not affected significantly by potassium vapor. However, the discovery of mass-transfer deposits inside the potassium-exposed specimens led to a study[111] which demonstrated that the mass-transfer rate is sensitive to the amount of oxygen in the potassium. Thus, in systems where significant oxygen contamination is present, mass transfer would be expected to accelerate the creep after enough time for corrosion to weaken the material. Where oxygen contamination can be successfully excluded, exposure of Mo-0.5Ti or TZM alloy to 2000 F potassium should have no adverse effect on creep behavior.

Using tension-tension axial loading on hollow cylindrical specimens, a fatigue-test program was carried out on vacuum-arc-cast, hot-rolled, stress-relieved Mo-0.5Ti alloy.[114] The load ratio (alternating stress to mean stress) was 0.95, and the frequency was 60 cps. As in the creep tests, small charges of potassium (<80 ppm oxygen by mercury amalgamation) were sealed inside the specimen cavities so that the inner walls would be

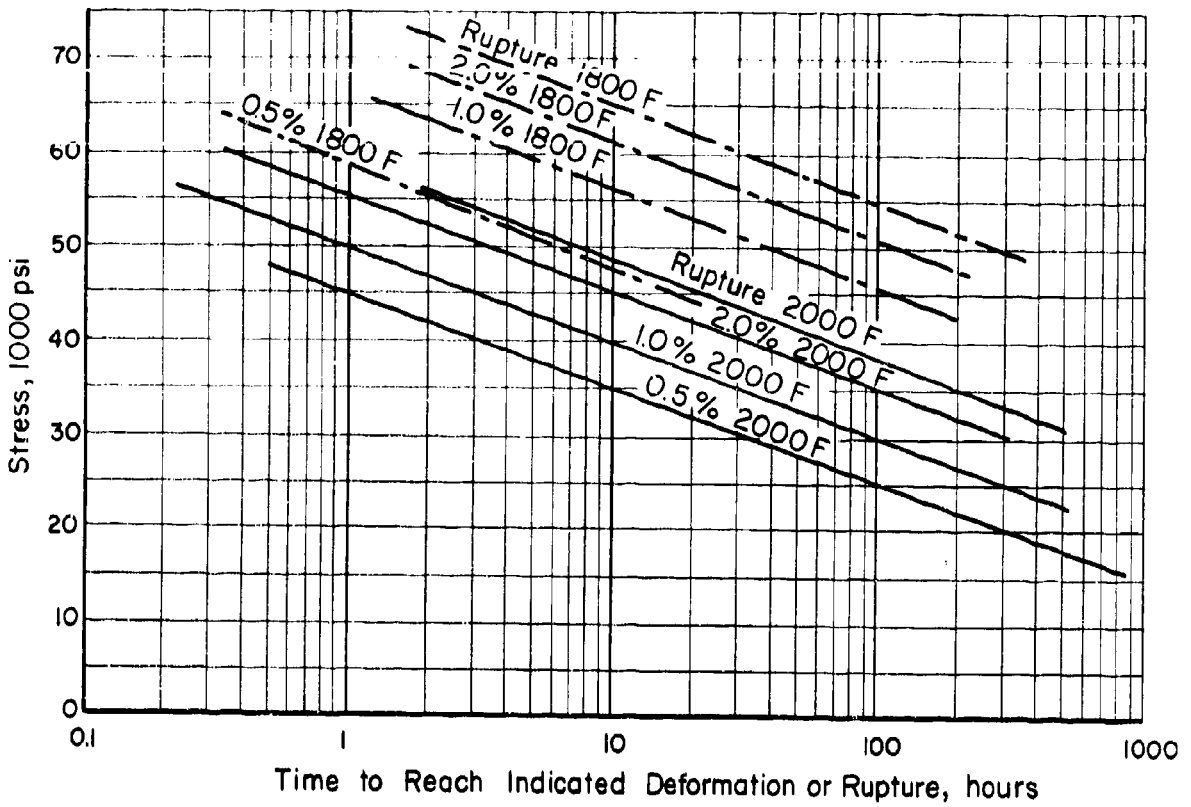

FIGURE 3.3. DESIGN CURVES FOR STRESS-RELIEVED Mo-0.5Ti ALLOY IN POTASSIUM VAPOR OR VACUUM(98f)

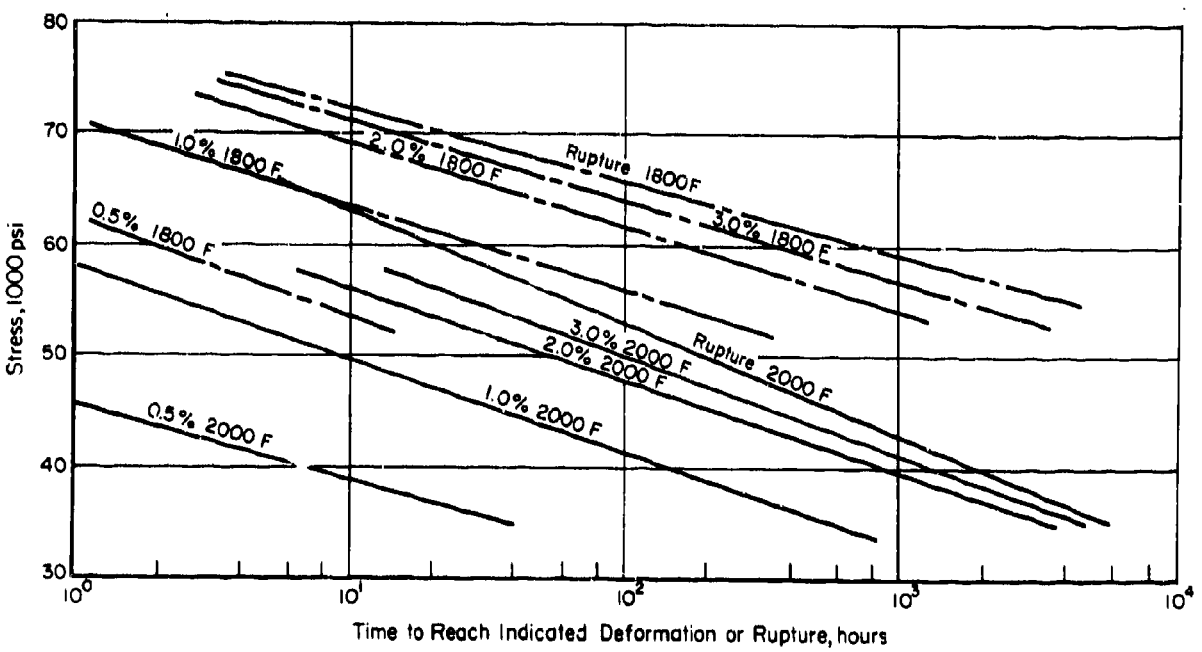

FIGURE 3.4. DESIGN CURVES FOR STRESS-RELIEVED TZM ALLOY IN POTASSIUM VAPOR OR VACUUM(110)

exposed to saturated potassium vapor at the test temperatures (1500 and 2000 F). Similar specimens were tested without potassium, as controls.

The results, shown in Figure 3.5, indicate that the endurance limit is reduced significantly by the presence of potassium vapor. This phenomenon seems to be associated more with surface effects than with gross corrosion, because it occurs with short- as well as long-lifetime specimens. The study was not comprehensive enough to pinpoint the actual cause of the lowered fatigue life of of the potassium-exposed Mo-0.5Ti.

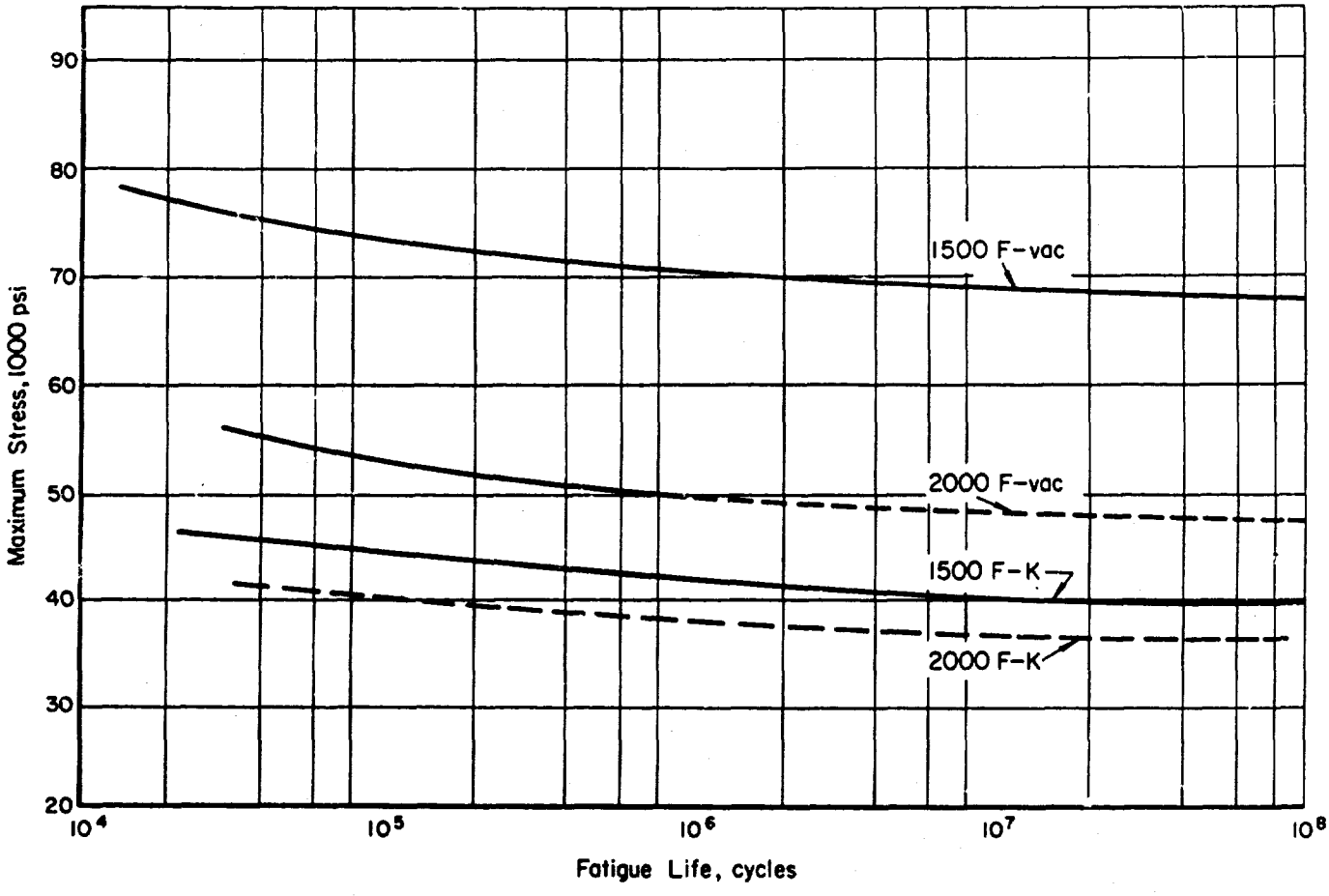

FIGURE 3.5. RESULTS OF AXIAL-LOAD FATIGUE TESTS ON Mo-0.5Ti IN HELIUM-VACUUM ATMOSPHERE, OR POTASSIUM-VACUUM ATMOSPHERE AT 1500 F AND 2000 F[114]

3.3 TANTALUM ALLOYS

Pure tantalum has excellent resistance to attack at elevated temperatures by high-purity potassium liquid and vapor. However, its corrosion resistance is drastically reduced by small amounts of oxygen impurity in the tantalum or the potassium. This effect is apparently even more pronounced in tantalum than it is in columbium. Similar to columbium, alloying tantalum with a small percentage of some strong oxygen getter like zirconium or hafnium decreases its sensitivity to oxygen contamination.

On the basis of data in Table 3.1 using 3-hour equilibrations, tantalum appears somewhat more soluble in potassium at 2275 F than niobium. However, to date there has been no systematic study of the effects of interstitials on the measured solubility.

Table 3.7 summarizes the results of tantalum-alloy capsule tests with refluxing potassium at 1800 to 2400 F. Several facts are immediately apparent:

TABLE 3.7. CORROSION OF TANTALUM-ALLOY CAPSULES EXPOSED TO HIGH-PURITY REFLUXING POTASSIUM[a] INSIDE AND HIGH VACUUM[b] OUTSIDE[96]

Alloy	Temperature, F	Time, Hour	Corrosive Attack and Observations	Oxygen in Capsule Walls, ppm		
				Pretest	Posttest	
					Top	Bottom
Ta-10W	1800	110	12 mils intergranular through cap seal weld	-	-	-
Ta-10W	2200	8	16 mils intergranular through cap seal weld	8	55[e]	34
T-222[c]	1800	4000	No attack	-	-	-
T-222	2200	4000	No attack; $K_2Ta_4O_{11}$ film at interface; some WO_3	-	-	-
T-222	2400	4000	No attack; $K_2Ta_4O_{11}$ film at interface; some WO_3	48	57	1780
T-111[d]	2200	4000	No attack; film at liquid-vapor interface	-	-	-
T-111	2300	2000	No attack; film at liquid-vapor interface	25	48	74

(a) Oxygen content: <20 ppm, by vacuum distillation and mercury amalgamation methods.
(b) 10^{-7} to 10^{-8} torr.
(c) Composition: Ta-9.6W-2.4Hf-0.01C.
(d) Composition: Ta-8W-2Hf.
(e) Sample taken from cap weld area.

(1) The ungettered alloy Ta-10W picked up a small amount of oxygen and suffered severe intergranular penetration, particularly in the large-grained heat-affected zone of the end-cap weld, which began to leak potassium into the vacuum chamber in a relatively short time.

(2) Neither the T-222 (Ta-9.6W-2.4Hf-0.01C) nor the T-111 (Ta-8W-2Hf) capsules showed any metallographic evidence of corrosive attack after exposures to refluxing potassium up to 4000 hours at temperatures up to 2400 F.

(3) Films were found at the liquid-vapor interface of the T-222 and T-111 capsules which had been exposed at 2200 F and above. X-ray patterns from the T-222 capsules showed $K_2Ta_4O_{11}$ and WO_3, but no positive identification of HfO_2.

(4) The T-222 and T-111 capsule walls picked up oxygen preferentially at the bottom during the exposures. Since each capsule started with only 1-1/4 centimeters of low-oxygen (<20 ppm) potassium, the contamination must have come from the vacuum-chamber atmosphere. The pickup to 1780 ppm oxygen (Table 3.7) is thought by the experimenter to have occurred mostly during short-time operation within the test temperature range, early in the test, at pressures up to $\sim 10^{-5}$ torr.

Although the examinations were incomplete at the time of this writing, indications are that the T-111 natural-convection loop at Oak Ridge (Table 3.3) will give results comparable to the T-111 capsule results in Table 3.7. The 0.4 mg/cm^2 in 3000 hours maximum weight loss of tabs in the condensing zone is equivalent to a uniform surface removal of 1 mil in 20 years. The weight gains in lower-temperature tabs are probably due to surface films.

3.4 ZIRCONIUM, TITANIUM, AND HAFNIUM

Zirconium, titanium, and hafnium are chemically active transition metals which interact readily with impurities such as oxygen, hydrogen, nitrogen, and carbon in potassium. Because the products of such interactions are usually deleterious to their mechanical properties, these metals (or alloys in which they are the major constituents) are generally unsatisfactory as container materials for high-temperature potassium. However, sinch they are more highly active than other transition metals, they are very useful as getters to remove impurities from potassium contained in some other construction material. These impurities might otherwise react with the container and lower its ductility and/or corrosion resistance.

Zirconium, titanium, and hafnium may be used as getters in potassium systems in one of two ways: (1) as minor alloying constituents of the containment materials themselves, and (2) as active packing (in the form of foil, mesh, or chips) in a full-flow or bypass-flow hot trap. The effectiveness of gettering by alloying is demonstrated by the superior corrosion resistance to high-temperature potassium of B-66 (Cb-5V-5Mo-1Zr) over B-33 (Cb-4V), FS-85 (Cb-27Ta-10W-1Zr) over SCb-291 (Cb-10Ta-10W, and C-129 (Cb-10W-10Hf) over SCb-291 (Cb-10W-10Ta), as shown in Table 3.2. Similarly, as shown in Table 3.7, replacement of a few percent of the tungsten in Ta-10W by hafnium completely eliminated the intergranular attack.

Workers at Oak Ridge studied the distribution of oxygen between zirconium and liquid potassium at 1500 F.[115] Where no oxide scale was visible, the final weight fraction of oxygen in the zirconium varied from 3 to 30 times that in the potassium, and increased with time at a given zirconium specimen thickness as shown in Figure 3.6. The data in Figure 3.6 were successfully applied to the analysis of potassium for oxygen in the 100 to 3000-ppm range. This was accomplished by simply measuring the amount of oxygen in a zirconium tab before and after a 100-hour exposure to the potassium at 1500 F, and calculating how much was in the potassium originally.

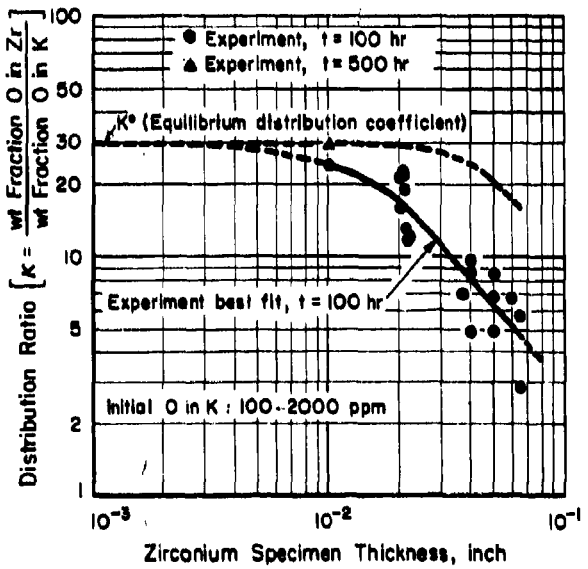

FIGURE 3.6. DISTRIBUTION RATIO FOR OXYGEN BETWEEN ZIRCONIUM AND POTASSIUM AT 1500 F[115]

3.5 NICKEL-, AND IRON-, AND COBALT-BASE ALLOYS

3.5.1 Compatibility - General

Aside from corrosion considerations, the dropoff in high-temperature strength of nickel-, iron-, and cobalt-base alloys limits their use as containers for potassium to systems where temperatures are below about 1900 F at best. However, many commercially available nickel-, iron-, and cobalt-base alloys are endowed with attractive oxidation resistance, fabricability, and strength below 1900 F; so that their suitability for potassium heat-exchange systems would depend largely on their compatibility with the potassium.

On the basis of the solubility data shown in Table 3.1 and Figure 3.7,[92,93c,116] it appears that the use of nickel- and cobalt-rich alloys should not be seriously limited by solubility criteria in potassium heat-exchange systems. Iron-rich alloys, on the other hand, would be expected to suffer significant mass transfer from solution-precipitation phenomena in polythermal systems. It was found experimentally that the apparent solubility of iron is increased by the presence of oxygen in the potassium. Thus, the successful use of iron-base alloys would be contingent largely upon maintaining a low oxygen level in the potassium. Indeed, in low-oxygen loops containing potassium in austenitic stainless steel, the mass-transfer kinetics are such that nickel and chromium are leached preferentially, leaving a ferritic surface layer on the hot-zone walls and deposits rich in nickel and chromium on the cold-zone walls.

In general, it has been found that the resistance of cobalt-base alloys to attack by potassium is about the same as that of iron-base alloys. Nickel-base alloys, however, appear to be inferior.

Migration of carbon (and other interstitials) from hot to cooler regions has been observed in polythermal potassium loops fabricated of iron-, nickel-, or cobalt-base alloys. The extent of such migration is dependent on temperature patterns, time, and the nature of the interstitial-element sources and sinks present. The seriousness of this problem hinges upon the amount of property deterioration (embrittlement or loss of strength) suffered by the alloy in question as a result of carburization, decarburization, or other interstitial-element transfer.

Dissolutive attack of iron-, nickel-, or cobalt-base alloys in clean potassium heat-transfer loops has been found to be relatively mild. Similarly, with the exception of a few highly contaminated loop experiments, long-term tests have not been troubled with plugging by the sparse mass-transfer crystals formed. However, such crystals have been known to find their way into small-

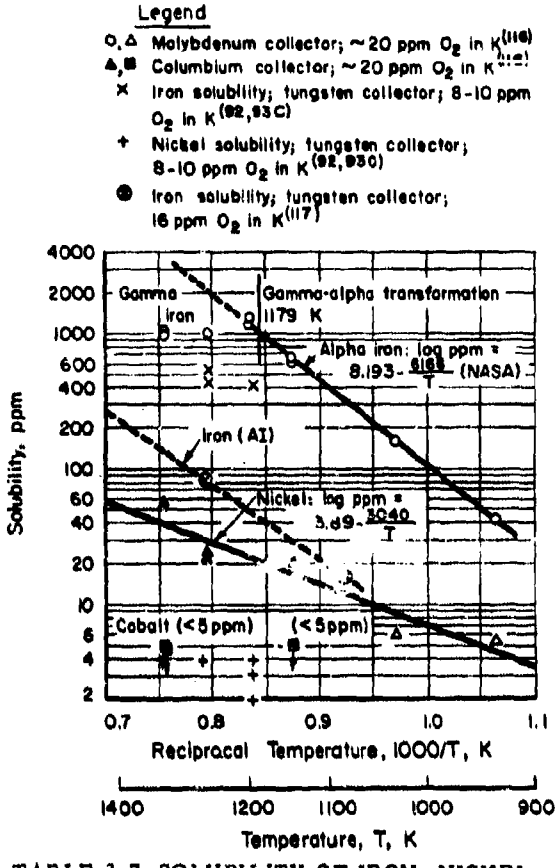

TABLE 3.7 SOLUBILITY OF IRON, NICKEL, AND COBALT IN POTASSIUM

clearance liquid-metal-lubricated bearings and cause galling - a problem which can likely be circumvented by placing filters ahead of the bearings.

3.5.2 Nickel-Base Alloys

3.5.2.1 Inconel (78Ni-15Cr-7Fe)

Inconel does not resist attack by 1600 F boiling potassium as well as Haynes Alloy No. 25 or Type 316 stainless steel. Refluxing capsules with 1600 F boiling potassium, after operation for 1000 hours at Oak Ridge, showed measurable weight losses from the condensing zone and weight gains in the subcooled liquid region.[118a] This mass-transfer pattern was repeated in the 1500-hour Inconel natural-convection loop depicted in Table 3.8 (Loop 3).[119] The boiler and condenser regions of this loop developed extensive intergranular cracks up to 20 mils deep. In addition, there was decarburization and grain growth in the 1600 F regions of the boiler and condenser, and mass-transfer deposits (enriched in iron and carbon and depleted in chromium) on the 1250 F subcooler walls.

Since boiling in this loop was not stable, it is not certain how much of the grain-boundary damage is due to thermal fatigue and how much to solution attack. Workers at NASA-Lewis experienced complete penetration of the 14-mil Inconel wall at the liquid-vapor interface of an early 1650 F boiling potassium loop after 490 hours, suggesting solution attack of grain-boundary material - particularly when the potassium purity is not closely controlled.[118b] Posttest metallographic examination of a subsequent 500-hour loop corroborates this. The Inconel wall was thinned several mils at the liquid-vapor interface, and showed severe intergranular penetration about 5 mils deep.

3.5.2.2 Hastelloy X (45Ni-24Fe-22Cr-9Mo)

A limited amount of experimentation has been conducted with Hastelloy X as a container for molten potassium. Its corrosion resistance is generally inferior to that of stainless steels and Haynes Alloy No. 25. Its suitability for potassium containment would thus be limited to low-temperature, long-life applications, or to short-service applications at higher temperatures.

The most serious drawback to the use of Hastelloy X in polythermal potassium systems is the mass-transfer problem. A forced-circulation all-Hastelloy X loop test with 1800 F - 1350 F potassium flowing at 10 fps was terminated by complete plugging of the electromagnetic pump cell after only 530 hours of operation.[104b] The metallic plug and a heavy layer of deposited crystals throughout the cold leg of the loop analyzed predominantly nickel. The hot leg was severely roughened, and showed 4 mils of intergranular attack. Data were not obtained to indicate the role of oxygen impurity in these corrosion and mass-transfer effects.

Hastelloy X corrosion tabs were exposed for 500 hours in two Cb-1Zr capsules containing boiling-refluxing potassium at 1800 - 1700 F and at 1650 - 1350 F, respectively.[104b] The tabs in the higher-temperature test underwent solution-type attack and intergranular penetration. The lower-temperature specimens gained weight, suggesting a transfer of material from the Cb-1Zr capsule walls to the Hastelloy X specimens, similar to that found in a comparable experiment at another site.[104a] Again, there was no indication of what would happen if these experiments were repeated using ultrapure potassium.

3.5.3 Steels

3.5.3.1 Stainless Steel

Experiments with Type 316 stainless steel refluxing capsules and thermal-convection loops containing potassium boiling at 1500 to 1600 F showed consistent patterns of slight weight losses from the walls in the hot-liquid and hot-vapor regions and slight gains in the cold-liquid regions.[118a,119] Typical data from two such loops are included in Table 3.8 (Loops 1 and 2). Highlights of the conclusions from these experiments are:

POTASSIUM NICKEL-, IRON-, AND COBALT-BASE ALLOYS

TABLE 3.8. OAK RIDGE POTASSIUM LOOP TEST RESULTS[119]

Loop Material	Test Time, Hour	Temperature, F: Boiler (max)	Temperature, F: Condenser	Temperature, F: Subcooler (min)	Condensing Rate, g/min	Insert Weight Change[a], mg/in.^{2}: Condenser	Insert Weight Change[a], mg/in.^{2}: Subcooler	General Metallographic Results	General Chemical Results
1. Type 316 SS	3000	1600	1600	1250	180	- 4 (nonuniform)	+30 (maximum)	(b)	(c)
2. Type 316 SS	3000	1670	1600	1250	180	- 8 (uniform)	+90 (maximum)	(d)	(e)
3. Inconel	1500	1600	1600	1250	180	- 8 (uniform)	+50 (maximum)	(f)	(c)
4. Haynes Alloy No. 25	3000	1600	1600	1250	180	-10 (uniform)	+40 (maximum)	(g)	(e)
5. Haynes Alloy No. 25	3000	1800	1740	1470	300	-14	+70	(h)	(e)

(a) A weight loss of ~130 mg/in.^{2} is equivalent to 1 mil of uniform surface removal.
(b) Subsurface voids at liquid level in boiler 2 mils deep. Surface roughening in condenser approximately 0.5 mil deep.
(c) Transfer of carbon from condenser to subcooler. No preferential removal of iron, nickel, or chromium from condenser.
(d) Surface roughening to 0.002 inch in boiler. Subsurface voids in condenser 10 to 12 mils deep. Severe cracking in condenser at liquid level. Mass-transfer deposit in subcooler 8 mils deep.
(e) Transfer of carbon from condenser to subcooler.
(f) Intergranualr attack to 20 mils in boiler, 15 mils in condenser. Mass-transfer deposit in subcooler 5 mils deep.
(g) Surface roughening in boiler to approximately 0.5 mil. Numerous cracks in boiler at liquid level. Severe cracking in condenser, especially in weld zones. Scattered mass transfer in subcooler 0.5 mil thick.
(h) Surface roughness to <0.5 mil in depth in boiler and condenser. Mass-transfer deposit 7 mils deep in subcooler. Cracks to 28 mils in depth at liquid level in condenser.

(1) Unstable boiling can subject the loop tubing to thermal fatigue as a result of alternate surges of potassium vapor and liquid at the liquid-vapor interface in the condenser and boiler. For example, severe cracking occurred in the condenser of Loop 2 (Table 3.8 which operated unstably for 3000 hours, but not in Loop 1, which operated stably.

(2) Dissolutioning occurs in hot zones and precipitation of solids occurs in cold zones of Type 316 stainless steel loops operating with 1670 F boiling, 1250 F subcooled potassium. However, these effects are slight. For instance, the 8 mg/in.^{2} condenser weight loss in Loop 2 (Table 3.8) is equivalent to a uniform reduction in wall thickness of only 0.06 mil during the 3000-hour test.

(3) In polythermal potassium loops, material leached from hot-zone Type 316 stainless steel walls and deposited in the cold zones appears to be enriched in nickel and chromium and depleted in iron. Thus, the crystalline deposits from the cool walls of Loop 2 (Table 3.8) were found to contain iron, nickel, and chromium in the approximate weight ratios of 50:20:30, as compared with the pretest Type 316 stainless steel composition of 70:12:18.

(4) In a Type 316 stainless steel boiling-condensing potassium loop, carbon is transferred from the condensing region and subsequently deposited and and diffused into the subcooler walls. In Loop 2 (Table 3.8), for instance, a 3-mil surface layer from the 1600 F condensing region dropped from a pretest carbon analysis of 0.08 wt % to a posttest value of 0.036 wt %, while the 1250 to 1400 F liquid-submerged condenser and subcooler surfaces increased in carbon content to ~0.5 wt %. X-ray analysis of crystals from the latter region yielded patterns matching $Cr_{23}C_6$, among other things.

(5) Under some combinations of thermal history and carbon pickup in potassium systems, Type 316 stainless steel can be embrittled by the formation of a nearly continuous grain-boundary carbide phase. This occurred in a specimen in Loop 2 (Table 3.8) exposed to liquid potassium at 1290 F which showed a posttest room-temperature elongation at fracture of 15.5 percent compared with 51.5 percent for a control specimen. All other tensile specimens (both carburized and decarburized) from this loop showed significant drops in [illegible] strength, but only slight changes [illegible]gation and ultimate strength.

POTASSIUM NICKEL-, IRON-, AND COBALT-BASE ALLOYS

Potassium does not appear to be as corrosive to Type 316 stainless steel as sodium. This is based on progressive weight losses of removable Type 316 stainless steel specimens from the hot zones of identical loops containing sodium and potassium, as shown in Figure 3.8.[98c] The corrosion rate of the stainless steel decreased with time in both sodium and potassium, apparently due to selective leaching of constituents from the steel. A ferritic layer formed on the exposed surfaces in both cases. At 5000 hours, the corrosion rate in 1575 F potassium was 20 mg/(cm^2) (month), equivalent to a uniform surface removal rate of 0.12 mils/year. The corresponding rate in sodium was three times this value.

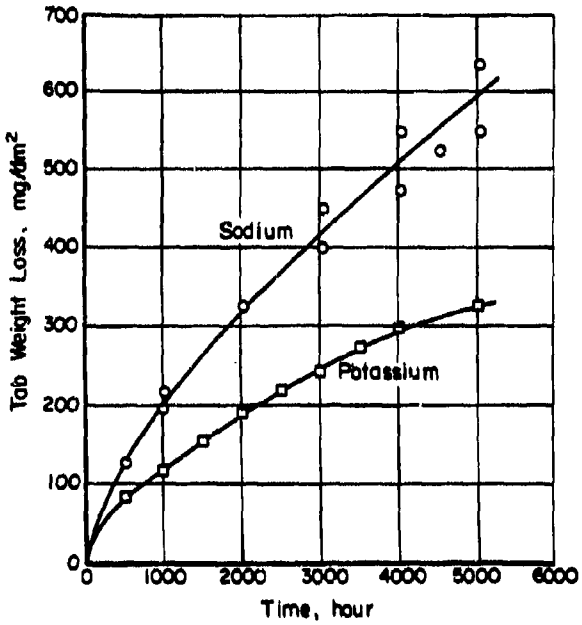

FIGURE 3.8. SODIUM-POTASSIUM CORROSION COMPARISON. TAB WEIGHT LOSS VERSUS TIME FOR TYPE 316 STAINLESS STEEL TABS SUSPENDED IN SODIUM AND POTASSIUM FLOWING IN IDENTICAL STAINLESS STEEL THERMAL-CONVECTION LOOPS AT 1575 F (475 F Δ T)[98c]

When a Type 316 stainless steel rotating component, such as the impeller of a centrifugal pump, is operated in molten potassium under cavitating conditions, it is more susceptible to cavitation damage than if it were operating in water. This was demonstrated by controlled experiments in which an investment cast Type 316 stainless steel impeller showed no damage after running for 300 hours in 100 F water under cavitating conditions, but was pitted and tunnelled to a maximum depth of 50 mils after 350 hours in 1400 F cavitating potassium.[120] Detailed metallographic and chemical studies of the damaged impeller led to the conclusion that such pitting is caused primarily by mechanical implosion forces, with essentially no contribution by chemical interactions involving potassium.

Erosion by 3000-fps wet potassium vapor impinging on Type 316 stainless steel is apparently not as damaging as the cavitation described above. In a 750-hour test of Type 316 stainless steel simulated turbine nozzles and blades in a Type 316 stainless steel loop, the only damage found was a smooth shallow depression where the 1280 F vapor (83 percent quality) impinged on the second-stage blade.[93f]

3.5.3.2 Carbon Steels

Static, isothermal capsule exposures of SAE 4340 steel specimens to 1000 F potassium liquid and vapor for 500 hours produced only small weight losses.[104b] Metallographic examinations of normalized and tempered (RC 33) SAE 4340 steel specimens following creep experiments in 800 and 1000 F potassium vapor revealed decarburization of the surfaces on the order of 1 mil deep after about 1000 hours' exposure.[98d,121] This decarburization did not accelerate the creep noticeably. However, over longer periods of time, progressive decarburization of the SAE 4340 steel by the potassium would be expected to lower its creep resistance.

This effect was observed in creep experiments on the air-hardening tool steel H-11 in 800 and 1000 F liquid potassium.[122] Little influence of the exposures on creep rate was noted in short-time tests, but long exposures resulted in accelerated creep. Metallography of the specimens following long-time tests revealed pitting corrosion, decarburization, and a surface coating.[123] The accelerated creep is attributed to time-dependent losses in strength caused by heating near the tempering temperature, progressive decarburization, and mild corrosion.

3.5.4 Haynes No. 25 (or L-605) Alloy (50Co-20Cr-15W-10Ni-3Fe-1Si-1Mn)

Capsule and loop experiments indicate that Haynes Alloy No. 25, while not completely inert to potassium up to 1900 F, has good resistance to corrosive attack. Test conditions for two Haynes Alloy No. 25 thermal-convection boiling-potassium loops run for 3000 hours at Oak Ridge[119] are included in Table 3.8. Highlights of the results are:

POTASSIUM NICKEL-, IRON-, AND COBALT-BASE ALLOYS

(1) Cracks observed in the condenser walls of both loops, and in the boiler at the liquid level in the 1600 F loop, were attributed to thermal fatigue resulting from alternate surges of potassium vapor and liquid because of unstable boiling. Design of loops for stable boiling should minimize this problem.

(2) Dissolutive attack of the walls was evidenced by surface roughening (0.5 mil or less) in the boiler and weight loss in the condenser. The latter was equivalent to a uniform surface removal of about 0.1 mil in the 3000-hour period.

(3) Mass transfer was manifested by crystalline deposits on the subcooler walls - noticeably heavier in the higher temperature loop. Compared with Haynes Alloy No. 25, these crystals were enriched in chromium, nickel, iron, and manganese, and depleted in cobalt and tungsten.

(4) In both loops, carbon was depleted from the hottest portions of the boiler and condenser walls and deposited in the subcooler and preheater. For example, surface carbon, originally 0.09 wt %, dropped to 0.04 wt % in the 1800 F condenser and increased to 0.38 wt % in the 1480 F subcooler after the 3000-hour exposure. These changes in carbon content increased the strength about 10 percent and decreased the ductility about 10 percent as compared with the properties of control specimens which were heat treated in vacuum or inert atmosphere. A 0.5-mil deposit in the subcooler showed $Cr_{23}C_6$ and Cr_7C_3.

(5) The higher temperature loop exhibited less severe aging embrittlement and fatigue cracking than the lower temperature loop.

These results were generally corroborated by findings from an extensive General Electric program involving 1250 to 1850 F potassium in Haynes Alloy No. 25 static capsules, refluxing capsules, and a thermal-convection (single-phase) loop.[104c,124] There are two major differences between these tests and the Oak Ridge work: (1) General Electric had no boiling instabilities, and (2) their capsules and loop contained zirconium or Cb-1Zr inserts as getters. Consequently, the General Electric loop did not develop fatigue cracks, in spite of operating over 1000 hours and then being given ten 2-hour thermal cycles between 1850 and 400 F and two cycles to room temperature.

The objective of including getters was to prevent carburization (and possible embrittlement) of the cooler zones of the Haynes Alloy No. 25. It was found that essentially all of the carbon and nitrogen were removed from the Haynes Alloy No. 25 walls throughout the system and taken up by the getters (Table 3.9), with no significant effects on the strength or ductility of the Haynes Alloy No. 25. Thus, it is feasible to use a Cb-1Zr or zirconium hot trap in a potassium loop made of Haynes Alloy No. 25.

Aging embrittlement of Haynes Alloy No. 25 from prolonged heating in the 1250 to 1750 F temperature range, with or without exposure to potassium, is considered to be a very serious limitation of this alloy in practical heat-transfer systems. The poor room-temperature ductility of the aged material enhances the probability of cracking during standby periods.

As a turbine nozzle or blade material, Haynes Alloy No. 25 has good resistance to erosion by 1280 F wet potassium vapor. This was demonstrated by a 1679-hour test of Haynes Alloy No. 25 simulated turbine nozzles and blades in a Type 316 stainless steel loop, where the only damage observed was a smooth shallow depression at the impingement area of the wettest (83 percent quality) vapor.[93f]

3.6 BEARING MATERIALS

Several studies have been undertaken to evaluate materials for rubbing-surface applications in space power systems where potassium is the working fluid.[93g,104b,109,125] In general, screening tests using weight changes and metallographic examinations as rating criteria have not been very discriminating, because none of the candidate materials underwent gross corrosion under the test conditions (temperatures to 1600 F and test periods to 1000 hours). More significant perhaps, is the ability of a pair of mating materials to resist wear and frictional overheating when lubricated by hot potassium.

At Battelle, it was found that the presence of reaction products of the type $Na_xM_yO_z$ in the form of surface films can provide effective lubrication and protection against gross surface damage of certain pairs of materials rubbing together in sodium.[126] An investigation was carried out to see under what conditions analogous beneficial compounds form in potassium systems.[109] The study employed differential thermal analysis to tell (1) whether a particular material reacts with

TABLE 3.9. OXYGEN, NITROGEN, AND CARBON TRANSFER TO ZIRCONIUM, Cb-1Zr, AND Mo-0.5Ti ALLOYS IN A HAYNES ALLOY NO. 25[a] CONVECTION LOOP CONTAINING 1485-1850 F POTASSIUM[b] FOR 1309 HOURS[124]

Material	O_2,[c] wt%		Estimated O_2 Increase, 10^{-4} lb	N_2,[c] wt%		Estimated N_2 Increase, 10^{-4} lb	C,[c] wt%		Estimated C Increase 10^{-4} lb
	Initial	Final		Initial	Final		Initial	Final	
Zr[d]	0.065		2.46	0.030		0.58	0.006		1.31
Top		0.35			0.079			0.18	
Bottom		0.43			0.134			0.17	
Cb-1Zr[e]	0.050		0.09	0.030		0.03	0.025		0.34
Top		0.058			0.040			0.13	
Bottom		0.101			0.043			0.15	
Mo-0.5Ti[f]	0.010		0.006	0.001		0.003	0.035		0.22
Top		0.011			0.002			0.25	
Bottom		0.021			0.004			0.23	

(a) Internal surface area about 133 in.^{2} (including specimen); loop volume about 21.4 in.^{3}
(b) About 0.48 pound at 1850 F; slagged, filtered, distilled to <100 ppm oxygen, and hot trapped during loop operation.
(c) Average of two analyses.
(d) Two pieces, 3 inch x 7/8 inch x 1/16 inch, total surface area about 10.5 in.^{2}
(e) 3-1/8 inch x 1-1/2 inch x 0.020 inch, total surface area about 9.5 in.^{2}
(f) 3-1/8 inch x 1-1/2 inch x 0.006 inch, total surface area about 9.5 in.^{2}

POTASSIUM BEARING MATERIALS

potassium at temperatures to 1400 F, (2) if so, at what temperature the reaction occurs, and (3) whether the reaction is exothermic or endothermic and how strong it is.

The materials tested and the results are shown in Table 3.10. It was found that oxides of the form MO_2, MO_3, or M_2O_5 were generally too reactive to form stable, adherent films in the presence of potassium. The MO types apparently did not react at all, and of the two M_2O_3 types examined (Y_2O_3 and Al_2O_3), Y_2O_3 did not react and Al_2O_3 formed what appeared to be suitable potassium aluminate surface films.

The friction and wear resistance of selected pairs of materials were measured, using a potassium-lubricated ball-on-plate sliding friction tester at temperatures from 400 to 1400 F.[109] The materials tested and their sliding behavior are summarized in Table 3.11. Most of the materials were coated with a stable reaction-product film when removed from the apparatus after exposure to potassium, and this film protected the surfaces from galling and reduced the kinetic friction. Of the two commercial cermets, Materials B and C, the one with the lower percentage of metal binder (Material B) was more resistant to galling. The performance of the chromium-bonded alumina cermet could undoubtedly have been improved by increasing the proportion of alumina in its composition, since it had mostly metal phase in sliding contact during the tests. More alumina in contact would have provided improved resistance to galling and surface damage.

At General Electric, a program is in progress to evaluate candidate materials for potassium-lubricated journal bearings. At the time of this writing, the results of corrosion, dimensional stability, thermal expansion, and hot-hardness tests on 14 candidate materials had been reported.[93g,125] Additional properties being investigated include compressive strength, modulus of elasticity in compression, wetting characteristics with potassium, and friction and wear of selected couples in potassium and high vacuum. The candidate materials are listed in Table 3.12.

Table 3.13 shows the effect of exposing samples of these materials to high-purity potassium (<15 ppm O_2, by mercury amalgamation) liquid and vapor for 1000 hours in Cb-1Zr capsules. Posttest metallography showed no deleterious effects on any of the materials, except what appears to be intergranular attack of the Zircoa 1027 and

TABLE 3.10. SUMMARY OF REACTION DATA FOR DENSE OXIDE BODIES EXPOSED TO POTASSIUM IN DTA EXPERIMENTS[109]

Specimen	Heating Rate, F/min	Reaction Temp, F	Extent of Reaction Exotherm, F	Analytical Results and Comments
			Single Oxides	
MoO_2	40	850, 1175	20	Several exotherms, 20 F maximum, some during second run; body partially decomposed; reaction formed K_2MoO_4 and Mo on the surface; K_2MoO_4, Mo, and MoO_2 detected beneath surface
TiO_2	20	740, 1075	15, 2	Products contained K_2TiO_3 and an unknown; body fragmented
Nb_2O_5	20	755, 820, 840, 935	40, 20, 10, 10	Several exotherms on first heating; body fragmented; products included Nb
Ta_2O_5	20	730-1050	35	Body fragmented
ZrO_2[a]	20	200-850	7	Body undamaged but discolored; analyses showed no change in composition except for increase in potassium from <10 ppm to 2000 ppm; a potassium zirconate probably formed
Al_2O_3[b]	20	320-890	1	Body undamaged; reaction products, if any, unidentified by X-ray diffraction
Al_2O_3[c]	20	300-1100	<1	Body undamaged; surface coated with a water-soluble aluminum compound, presumably a potassium aluminate
Al_2O_3[b]	20	780	<1	Body undamaged after DTA plus 200-hour exposure to 1350 F potassium; surface coated with a water-soluble aluminum compound, presumably a potassium aluminate
Al_2O_3[d]	20	-	-	Body undamaged; no reaction detectable by DTA; surfaces coated with a water-soluble aluminum compound
Al_2O_3[e]	20	880-1100	2	Body undamaged; aluminum-potassium compound detected on surfaces
BeO	20	-	-	Body undamaged; no evidence of a reaction
MgO	20	800	<1	Body undamaged; no evidence of a reaction
SiO_2	20	400-1200	2	Body fragmented
ThO_2	20	1000-1600	25	Body severely cracked; potassium compound on surfaces, and overall potassium content increased from <10 ppm to about 10,000 ppm
Y_2O_3	20	500	2	Body undamaged; no evidence of a potassium compound formation
			Mixed Oxides	
85 wt% Nb_2O_5 - 15 wt% TiO_2	20	715	200	Body fragmented

TABLE 3.10. (Continued)

Specimen	Heating Rate, F/min	Reaction Temp, F	Extent of Reaction Exotherm, F	Analytical Results and Comments
Mixed Oxides (Continued)				
88 wt% ZrO_2-12 wt% Y_2O_3	20	1400	1	Body undamaged; slight evidence of a potassium-zirconium reaction
$CaO \cdot ZrO_2$	20	-	-	Body undamaged; no evidence of a reaction
$MgO \cdot Al_2O_3$	20	1200	<1	Body undamaged; evidence of a potassium-aluminate formation on surfaces
99.7 wt% Al_2O_3-0.3 wt% MgO	20	900	<1	Body undamaged; very slight evidence of a potassium-aluminum oxide reaction
$3Al_2O_3 \cdot 2SiO_2$	20	410	1	Body crumbled; strong evidence of potassium aluminate and potassium silicate formations
99.5 wt% Al_2O_3-0.5 wt% SiO_2	20	660	<1	Surface cracks in body; strong evidence of potassium aluminate, and slight evidence of potassium silicate formations
Molybdenum Fiber-Reinforced Oxide Bodies (Blended Before Bonding)				
MoO_2 (11 vol% Mo)	40	610 to 1170	20 to 15	Reaction of relatively extensive duration; body severely decomposed
MoO_3 (7 vol% Mo)	40	585	25	Reaction mild during cooling and second heating; body swelled and decomposed; K_2MoO_4, Mo, and MoO_2 formed
MoO_3 (7 vol% Mo)	40	475	290	Body swelled and decomposed
WO_2 (8 vol% Mo)	40	600	100	Reaction apparently complete during first heating; body decomposed
WO_2 (8 vol% Mo)	40	520 to 1010	220	Reaction of extensive duration; peak ΔT at 820 F; body decomposed
Tungsten Fiber-Reinforced Oxide Body (Blended Before Bonding)				
WO_3 (3 vol% W)	47	750 to 990	165	Relatively mild exotherms during second heating; body decomposed
Pressure-Bonded Composite Bodies (75 Vol% Mo Matrices)				
MoO_2 (blended)	40	670	16	Several small exotherms observed during four successive heatings; body swelled; products included K_2MoO_4, Mo, and an unknown
WO_3 (blended)	20	730	32	Body decomposed
K_2MoO_4 (infiltrated)	20	-	-	No thermal activity observed; body swelled, cracked, lost weight
K_2MoO_4 (blended)	20	-	-	No thermal activity observed; body swelled, cracked, lost weight

TABLE 3.10. (Continued)

Specimen	Heating Rate, F/min	Reaction Temp, F	Extent of Reaction Exotherm, F	Analytical Results and Comments
Pressure-Bonded Composite Bodies (75 Vol% Mo Matrices) (Continued)				
K_2WO_4 (Infiltrated)	20	-	-	No thermal activity observed; body swelled, lost weight
K_2WO_4 (blended)	20	-	-	No thermal activity observed; body swelled, cracked, lost weight
Commercial Al_2O_3 Cermets[f]				
$23Al_2O_3$ - 77Cr	20	700	<1	Body undamaged; evidence of potassium aluminate formation on and beneath surfaces
$19Al_2O_3$ - 59Cr - 20Mo-$2TiO_2$	20	1150	1	Body undamaged; evidence of potassium aluminate formation on and beneath surfaces
$15Al_2O_3$ - 25Cr - 60W	20	850	1	Body undamaged; evidence of potassium aluminate formation on and beneath surfaces
$40Al_2O_3$ - 60Mo	20	900	2	Body undamaged; evidence of potassium-aluminum and potassium-molybdenum compound formations on surfaces
Specially Fabricated Al_2O_3 Cermet[g]				
$34Al_2O_3$ - 53Cr - 13Mo	20	200-900	1	Body undamaged; reaction indicated on second heating in 300 to 500 F range; considerable evidence of potassium aluminate formation on surfaces

(a) Stabilized with approximately 10 weight percent CaO.
(b) 99.8 weight percent Al_2O_3 - 0.15 weight percent MgO, large particles (~50 micron).
(c) 99.7 weight percent Al_2O_3 - 0.1 weight percent K, small particles (~1 micron).
(d) Sapphire.
(e) 99.6 weight percent Al_2O_3 - 0.3 weight percent Na.
(f) Compositions are given in approximate weight percents.
(g) Two specimens were exposed - one in liquid potassium, the other in potassium vapor. The reaction data apply to the liquid-exposed specimen, but approximately equal amounts of the potassium aluminate compound were detected on each after exposure.

TABLE 3.11. RESULTS OF SLIDING EXPERIMENTS IN VACUUM AND POTASSIUM ENVIRONMENTS[109]

Specimen[a]		Sliding Behavior at 1000 to 1400 F	
Ball	Flat	In Vacuum	In Potassium
A	A	Severe galling and scoring	Severe galling and scoring
A	B	Severe galling and scoring	Severe galling and scoring
B	B	High friction; chipping of carbide	Good boundary lubrication in potassium vapor
B	C	Good resistance to galling	Good boundary lubrication in potassium vapor
B	D	Some scoring of alumina at 1400 F	Good boundary lubrication in potassium vapor
D	D	Some galling and material transfer at 1400 F	Good boundary lubrication in potassium vapor
C	C	Galling and scoring of chromium phase 1200 to 1400 F	Good boundary lubrication in potassium vapor

(a) Specimen material:
A = Unalloyed, wrought molybdenum
B = 54TiC-6NbC-33.3Ni-6.7Mo
C = 77Cr-23Al_2O_3
D = Polycrystalline α-aluminum oxide of over 99 percent of theoretical density.

TABLE 3.12. CANDIDATE BEARING MATERIALS[93g]

Material Class	Candidate Material	Nominal Composition, percent
A. Nonrefractory Metals and Alloys	Star J	17W-32Cr-2.5Ni-3Fe-2.5C-bal Co
B. Refractory Metals and Alloys	Mo-TZM (arc cast; stress relieved)	0.5Ti-0.08Zr-0.02C-bal Mo
	Tungsten (arc cast; stress relieved)	99.96W (minimum)
C. Fe-Ni-Co Bonded Carbides	Carboloy 907	74WC-20TaC-6Co
	Carboloy 999	97WC-3Co
	K601	84.5W-10Ta-5.5C
D. Refractory Compounds - Oxides, Carbides, Borides	Lucalox	99.8Al_2O_3 (minimum) - 0.1MgO-0.02 SiO_2-0.02CaO-0.02Fe_2O_3
	Zircoa 1027	95.5ZrO_2-bal proprietary
	Titanium carbide	94TiC-4.25WC-0.9Ni-0.1Fe-0.68Co
	Titanium diboride	98TiB_2-0.39Fe-0.30C
E. Refractory-Metal Bonded Carbides	TiC+5W	90TiC-4.79WC-5W-0.36Fe
	TiC+10Mo	85.4TiC-10.5Mo-3.99WC-0.13Fe
	TiC+10Cb	83.6TiC-9.54Cb-5.85WC-0.73Co-0.33Fe
	Grade 7178	-

TABLE 3.13. DIMENSIONAL AND WEIGHT CHANGES OF SPECIMENS EXPOSED TO POTASSIUM FOR 1000 HOURS AT 1600 F IN Cb-1Zr CAPSULES[125]

Material[a]	Maximum Dimensional Change,[b] percent	Maximum Weight Change,[c] mg	Initial Weight,[d] g	Remarks
Carboloy 999	-0.151	-10.9 (L)	31.6	Weight loss caused by migration of carbon to capsule walls
Carboloy 907	+0.290[e]	- 3.0 (L)	30.5	Weight loss caused by migration of carbon to capsule walls
Mo-TZM	-0.081	- 0.7 (L)	20.6	-
Tungsten	-0.044	- 0.4 (V)	39.5	-
Lucalox	+0.185	+ 6.4 (V)	8.2	Surface reaction and possible formation of $KAlO_2$
Zircoa 1027	+0.794	+23.3 (V)	11.9	Weight gain caused by reaction with K; color change from red-brown to blue-black
K-601	+0.083	-11.4 (L)[f]	32.9	-
TiC	-0.007	- 0.7 (L)	10.2	-
TiC-5W	+0.024	- 1.6 (V)	10.7	Considerable porosity
TiC-10Mo	+0.024	- 1.3 (V)[f]	11.2	-
TiC-10Cb	+0.002	- 1.4 (V)[f]	10.8	-
Grade 7178	+0.072	- 4.6 (L)[f]	29.7	-
Star J	+0.250	- 9.2 (L)	18.2	Growth due to aging reaction; weight change from loss of carbon
TiB_2	-0.028	+ 1.5 (L)	8.5	Considerable porosity

(a) See Table 3.12 for compositions.
(b) Nominal dimensions were 1/4 x 1/4 x 2 inches. In all cases except TiC and TiC-10Cb, maximum percent change occurred in a 1/4-inch direction.
(c) Specimens exposed to liquid (L) and vapor (V) were weighed, and greater change listed.
(d) To nearest 0.1 gram.
(e) Growth thought to be from surface reaction with contaminated atmosphere after testing.
(f) Specimen edges or corners chipped.

the general surface reaction on the Lucalox. Considerable carbide precipitation occurred in the Star J. No significant changes in metallic-impurity content of the potassium were found following the tests, except for some chromium and iron in the potassium that was used with the Lucalox specimens (presumably from impurities in the Lucalox).

In addition to the data shown in Table 3.13, information on the dimensional stability of these materials at 800, 1200, and 1600 F was obtained in high vacuum (10^{-9} torr). Zircoa 1027 and Star J were the only materials to exhibit significant dimensional changes after 1000 hours at 1600 F (+0.4 and +0.06 percent, respectively). Only Zircoa 1027 showed significant dimensional changes at the lower temperatures.

4. LITHIUM

4.1 GENERAL COMPATABILITY OF MATERIALS

Over the past few years, considerable information regarding the corrosion of metals by lithium has been developed. A significant portion of this information has been obtained on columbium-base alloys, with the preponderance on the Cb-1Zr alloy. The refractory metals exhibit good resistance to attack by high-purity lithium at temperatures up to about 2200 F. Above this temperature, data are sparse. The corrosion resistance of the columbium-base alloys to lithium is reduced by the addition of oxygen to the lithium, the columbium itself, or the atmosphere. Alloying of the columbium with a small amount of an oxygen getter, such as zirconium or hafnium, decreases the sensitivity to oxygen contamination. The solubilities of a number of materials in lithium, were determined by Pratt & Whitney,[127] and are shown in Figure 4.1. It appears that these solubilities are rather limited and increase slowly with temperature. The weight changes, surface roughening, mass transfer, and grain boundary attack which have been observed below 2200 F are generally attributable to impurity effects and to dissimilar materials in the system. Figure 4.2 indicates the corrosion resistance to lithium of a number of potentially useful container materials.[128]

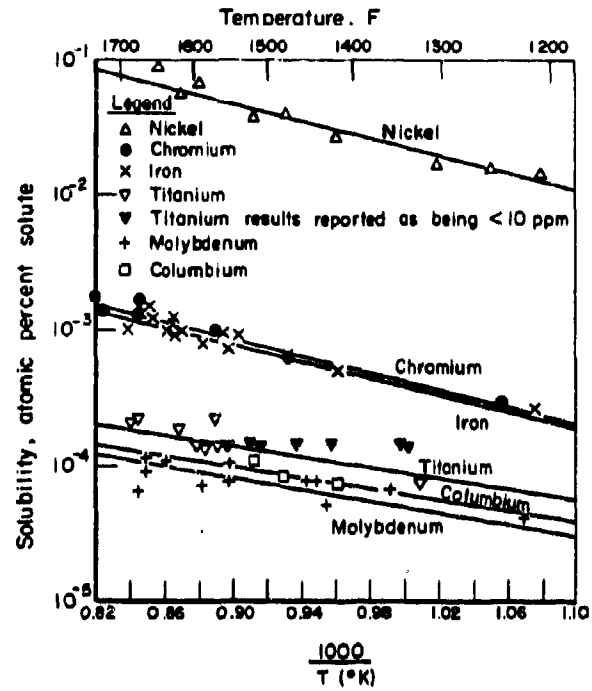

FIGURE 4.1. SOLUBILITY OF SOME METALS IN LITHIUM[128]

Nitrogen contamination 25 to 150 ppm

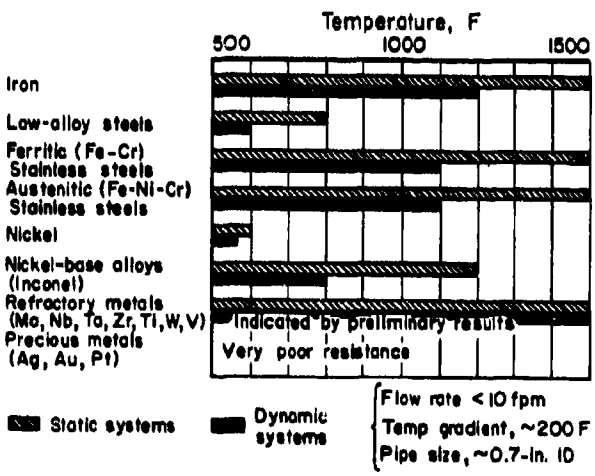

FIGURE 4.2. CORROSION RESISTANCE OF VARIOUS METALS AND ALLOYS TO LITHIUM[128]

4.2. COLUMBIUM ALLOYS

4.2.1 Compatibility - General

The corrosion of columbium alloys by lithium is generally predicated on the presence of oxygen either in solution in the lithium or the metal, or existing on the columbium walls in the form of an oxide film or perhaps as an adsorbed gas. In ungettered alloys and in some gettered alloys with high oxygen contamination, the oxygen readily combines with both the lithium and various constituents of the columbium alloys to form complex oxides, which are capable of dissolution in lithium. In some cases, interstitial impurities concentrated at the grain boundaries are preferentially leached out of the alloy, thus producing grain-boundary penetration.

4.2.2 Unalloyed Columbium

Because of its availability, good fabricability, and corrosion resistance to lithium as reported by Pratt & Whitney[129] (Table 4.1), columbium has been studied extensively. However, later work indicated that lithium penetration could occur under the proper conditions. Examination of a forced convection loop operated at 1600 F for 23 hours at Oak Ridge[128,130] revealed general attack in the welded regions and a random type of corrosion in other areas. These results led to an extensive evaluation of the effects of impurities on the corrosion resistance of columbium. Hoffman at Oak Ridge[131] demonstrated that the oxygen concentration in columbium was a principal variable governing the extent of penetration by lithium. Additions of oxygen, nitrogen, and carbon to columbium indicated, as shown in Table 4.2, that the attack is quite insensitive to the amounts of the latter two interstitials.

The effect[128] of lithium penetration on the mechanical properties of columbium is illustrated in Figure 4.3. These results indicate that, although the tensile strength of heat-treated columbium increases and the ductility remains essentially constant with increasing oxygen concentration, exposure to lithium results in a decrease in both tensile strength and elongation. The columbium also displays a significant loss of hardness upon exposure to lithium, as reflected in Figure 4.4. It is apparent that the area in the vicinity of the corrosion "front" exhibits a hardness peak. Although the corrosion product could not be identified positively, oxygen was found to be a constituent, and it was conjectured that this corrosion product consisted of a lithium-columbium-oxygen compound.

Other test variables investigated include temperature, time, grain size, heat treatment, deformation, and lithium purity. Although oxygen is the controlling variable in the corrosion process, other variables are also significant. With oxygen concentrations in the columbium of less than 500 ppm (Table 4.3), lithium penetration does not occur under certain test conditions. At oxygen concentrations above 500 ppm, temperature is the predominant variable.

Oak Ridge[128] observed that the rate of lithium penetration of columbium proceeds rapidly and reaches a maximum depth in less than a hour's exposure over a wide range of temperatures. The depth of attack is strongly dependent upon the same variables which affect oxygen-removal rates, such as grain size and initial oxygen concentration. No difference in the depth of attack is observed at 1500 F in specimens containing 1000 ppm oxygen for exposures from 1 to 500 hours. Chemical analysis showed that oxygen removal continued up to 100 hours. Comparison of hardness profiles[128] (Figure 4.5) across the above specimens shows a sharp gradient in specimens tested less than 100 hours.

Investigations at Pratt & Whitney[129] indicate that, although unalloyed columbium shows no thermal-gradient mass-transfer effects in forced-convection loops, its employment as a container material for high-temperature lithium is seriously limited by localized penetration corrosion. The reaction of lithium with unalloyed columbium, containing in excess of approximately 300 ppm oxygen, results in attack along grain boundaries and the {110} crystal planes. This is illustrated in Figure 4.6. Corrosion effects are noted in unalloyed columbium, unless the oxygen content of the columbium is reduced below 50 ppm.

4.2.3 Columbium-1 Zirconium Alloys

A substantial research effort has been expended in studying the behavior of the columbium-zirconium alloys in lithium. The majority of these investigations were conducted at Pratt & Whitney,[127,129,132,133] in forced-convection loops, and at Oak Ridge.[128,130,131,134,135] Almost all of the data presented here on the Cb-1Zr alloy were obtained from the above references.

Oak Ridge made systematic additions of oxygen to the Cb-1Zr alloy at 1830 F and subsequently exposed the material to lithium for 100 hours at 1500 F. Attack similar to that obtained with unalloyed columbium was observed, although heat treating at 2370 F eliminated this problem. It was concluded that an oxygen-to-zirconium atomic

TABLE 4.1. SUMMARY OF REFRACTORY METAL-LITHIUM FORCED-CONVECTION LOOP TESTS[129]

Material	Maximum Temperature, F	Thermal Gradient, F	Velocity, fps	Total Test Time, hour	Extent of Attack and Deposition
Titanium	1400-1500	200	13	1082	Light[a]
Zirconium	1500-1600	200	13	1070	Nil[b]
Columbium	1500-2000	200-400	10-50	8233	Nil[c]
Tantalum	1500-1800	200-400	3-13	2261	Nil[b]
Vanadium	1600	400	13	1194	Nil
Mo-0.5Ti	1500	200	13	694	Nil

(a) High nitrogen in pretest lithium.
(b) Carbide-nitride phase precipitate.
(c) Nitride deposits in early tests containing contaminated lithium.

TABLE 4.2. DEPTH OF ATTACK AS A FUNCTION OF OXYGEN, NITROGEN, and CARBON IN COLUMBIUM EXPOSED TO LITHIUM FOR 100 HOURS AT 1500 F[131]

Maximum Depth of Attack, mils	Initial Concentration, ppm		
	Oxygen	Nitrogen	Carbon
0	160	80	30
1	500	80	30
3	650	80	30
4	1000	80	30
10	1700	80	30
0	60	50	7
0	60	600	7
0	60	1350	7
0	40	60	500
0	40	60	1000

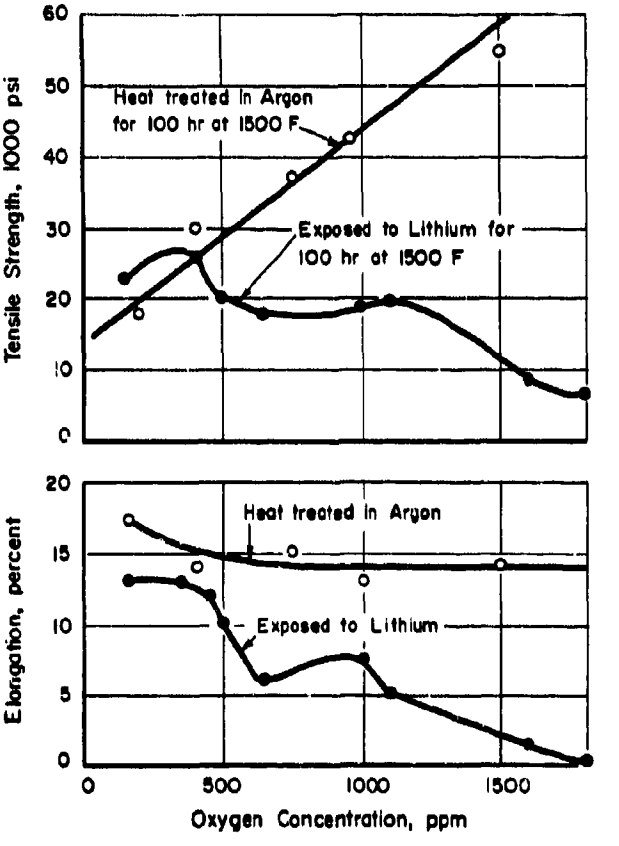

FIGURE 4.3. EFFECT OF INITIAL OXYGEN CONCENTRATION ON THE MECHANICAL PROPERTIES OF COLUMBIUM FOLLOWING HEAT TREATMENT IN ARGON AND EXPOSURE TO LITHIUM AT 1500 F[128]

Specimen thickness: 0.040 inch

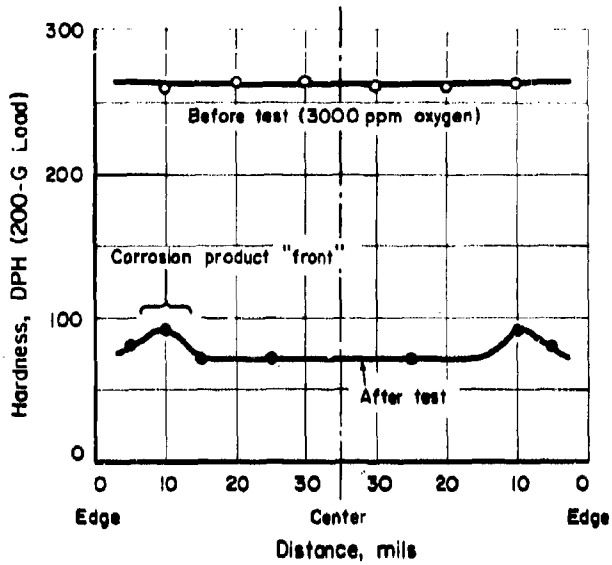

FIGURE 4.4. HARDNESS PROFILE ACROSS COLUMBIUM SPECIMEN BEFORE AND AFTER EXPOSURE TO LITHIUM FOR 100 HOURS AT 1500 F[128]

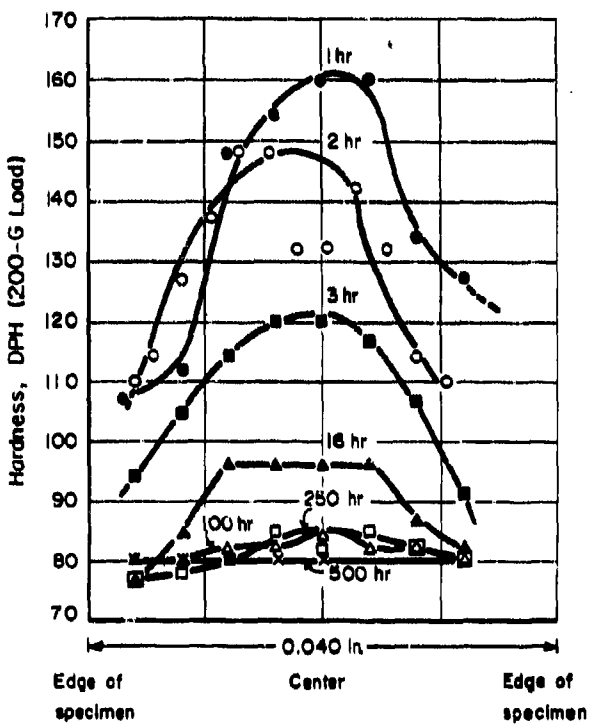

FIGURE 4.5. HARDNESS PROFILE ACROSS COLUMBIUM SPECIMENS FOLLOWING EXPOSURE TO LITHIUM FOR VARIOUS TIMES AT 1500 F[128]

FIGURE 4.6. PHOTOMICROGRAPH OF TYPICAL LITHIUM ATTACK ON UNALLOYED COLUMBIUM[129]

LCCS-1, 1600 F zone; tested 177 hours.

TABLE 4.3. LITHIUM PENETRATION OF COLUMBIUM CONTAINING <500 PPM OXYGEN[128]

Initial Oxygen Concentration, ppm	Test Variables			Depth of Attack, mils
	Temperature, F	Time, hours	Pretest Heat Treatment	
150	1500	100	Annealed 1 hour at 1832 F in vacuum	0
180	1500	100	Annealed 1 hour at 1832 F in vacuum	0
190	1500	100	Annealed 1 hour at 1832 F in vacuum	0
200	1500	100	Annealed 1 hour at 1832 F in vacuum	0
250	1500	100	Annealed 1 hour at 1832 F in vacuum	0
260	1800	100	Annealed 1 hour at 1832 F in vacuum	0
290	1800	100	Annealed 1 hour at 1832 F in vacuum	0
330	1800	100	Annealed 1 hour at 1832 F in vacuum	0
410	1500	24	Annealed 2 hour at 3272 F in vacuum	0
410	1500	100	Annealed 2 hour at 3272 F in vacuum	0
450	1800	100	Annealed 2 hour at 2372 F in vacuum	2
460	1500	100	Annealed 2 hour at 2912 F in vacuum	1
500	1500	100	Annealed 2 hour at 2912 F in vacuum	1
500	1500	500	Annealed 2 hour at 2912 F in vacuum	1
500	1800	100	Annealed 1 hour at 1832 F in vacuum	1.5

ratio of 2:1 is required for good corrosion resistance. The basis for this conclusion is presented in Table 4.4. The oxygen-to-zirconium atomic ratio of 2:1 corresponds to the stoichiometry of ZrO_2 and leads to the postulation that corrosion protection results from the formation of this oxide in columbium-zirconium alloys. In all cases, annealing at temperatures from 1830 to 2900 F is effective in stabilizing the oxygen in the Cb-1Zr alloy. Above 2900 F or in welding, the ZrO_2 redissolves and the alloy becomes susceptible to lithium attack. Pratt & Whitney[129] came to the same conclusions based on extensive work with the Cb-1Zr alloy. Table 4.5 lists the results of studies on the effects of zirconium additions. They determined that a zirconium content of between 0.8 to 1.2 with an oxygen-to-zirconium ratio of 2:1 is optimum.

4.2.4 Loop Tests of Cb-1Zr

A summary of the results of operations of three thermal-convection loops at Oak Ridge[134] is given in Table 4.6. Interlocking tab-type inserts were positioned around the loop to provide a complete weight-change profile of the dissolution and mass transfer of the alloy in lithium. All tests were conducted at a pressure of 10^{-8} to 10^{-9} torr. The results of the tests indicated that in monometallic systems, as in loop TCL-1R and TCL-3R, the principal interaction is the leaching of zirconium and interstitial oxygen, nitrogen, and carbon from the walls in the highest temperature region. In the dissimilar-metal loop (Cb-1Zr/TZM), a much greater weight loss was noted. A transfer of columbium from the Cb-1Zr to the TZM, and a transfer of molybdenum from the TZM to the Cb-1Zr was observed. Maximum transfer occurs, as

TABLE 4.4. DEPTH OF ATTACK BY LITHIUM OF COLUMBIUM-ZIRCONIUM ALLOYS AS A FUNCTION OF ZIRCONIUM CONCENTRATION, OXYGEN CONCENTRATION, AND HEAT TREATMENT[128]

Test Conditions: 100 Hours at 1500 F.

Zirconium Concentration, percent	Oxygen Concentration, percent	Depth of Attack, mils	
		After Oxidation at 1830 F[a]	After Heat Treatment at 2370 F[b]
0.05	0.09	15	15[c]
0.05	0.18	25	25[c]
0.05	0.23	30[d]	30[d]
0.4	0.09	15	0
0.4	0.18	20	15[c]
0.4	0.23	30[d]	30[c]
0.6	0.09	10	0
0.6	0.18	20	0
0.6	0.23	30[d]	25[c]
0.9	0.09	10	0
0.9	0.18	20	0
0.9	0.23	30[d]	0
1.3	0.09	5	0
1.3	0.18	10	0
1.3	0.23	25	0

(a) Specimen exposed to lithium after oxidation at 1830 F.
(b) Specimen heat treated in vacuum for 2 hours at 2370 F following oxidation and prior to exposure to lithium.
(c) Oxygen-to-zirconium atomic ratio was greater than 2.
(d) Complete penetration of 60-mil-thick specimen.

TABLE 4.5. EFFECT OF ZIRCONIUM ON LITHIUM ATTACK IN COLUMBIUM-ZIRCONIUM ALLOYS[129]

Zirconium Content, wt%	Maximum Temperature, F	Thermal Gradient, F	Number of Loop Tests	Total Time, hours	Maximum Depth of Corrosion Effect, mils	Remarks
0.001	1600	200	1	177	4.0	Unclad tubing
			2	447	7.5-10.0	Type 446 clad tubing
	1800	200	2	390	1.5-3.0	Unclad tubing
			3	382	5.0-8.5	Type 446 clad tubing
0.3	1600	200	3	750	Nil-2.5	Type 446 clad tubing
0.8-1.2	1800	200	2	500	Nil	Type 430 clad tubing
	2000	400	1	2000	Nil	Unclad tubing
	2200	400	1	1550	Nil	Unclad tubing
1.6	1800	200	1	250	Nil	Type 430 clad tubing
5.0	2000	400	1	343	Nil	Unclad tubing

(a) Corrosion data are for wrought sections.

TABLE 4.6. SUMMARY OF LITHIUM THERMAL-CONVECTION-LOOP TEST CONDITIONS AND RESULTS AFTER 3000 HOURS OF OPERATION[134]

	Loop Number		
	TCL-1R (Cb-1Zr)	TCL-2R (Cb-1Zr/TZM)	TCL-3R (D-43) (Cb-10W-1Zr-0.1C)
Maximum Hot-Leg Temperature, F	2170	2210	2190
Minimun Cold Leg Temperature, F	1970	1940	1885
Calculated Flow Rate, ft/min	10.6	7.5	7.5
Maximum Weight Loss, mg/cm^2	0.34	4.49	0.15
Maximum Weight Gain, mg/cm^2	0.78	2.69	0.21
Total Weight Loss, mg	99	810	37
Total Weight Gain, mg	87	626	17
Chemical Analyses, ppm			
	Before Test / After Test	Before[a] Test / After[a] Test	
Hot Leg			
Oxygen	81 / 10	20 / 32	
Nitrogen	50 / 11	7 / 11	
Carbon	80 / 50	30 / 50	
Zirconium[b]	1 / 1/2		
Cold Leg			
Oxygen	81 / 26	20 / 33	
Nitrogen	50 / 310	7 / 22	
Carbon	80 / 130	300 / 240	
Zirconium[b]	1 / 5		
Mass Transfer Deposits	ZrN	ZrN, Nb	None

(a) Surface analysis of Cb-1Zr.
(b) Analyses for TZM only.

would be expected, in the hottest protion of the loop. Exchange of carbon and oxygen was observed in both the hot and cold legs between the Cb-1Zr tube wall and the TZM alloy inserts. A weight-change profile[135] for the Cb-1Zr loop TCL-1R is shown in Figure 4.7. This loop was operated for 3000 hours at about 2200 F. Figure 4.8 illustrates the weight-change profile for the Cb-1Zr/TZM loop (TCL-2R), which was also operative for 3000 hours.

The following results were obtained by Pratt & Whitney[132] and summarize their loop operations between June, 1962, and June, 1965. All tests were conducted in an inert-atmosphere chamber. Helium with less than 1 ppm total impurities was used as a cover gas. The Cb-1Zr loops were wrapped in tantalum foil to further protect them against atmospheric contamination. Figure 4.9 illustrates schematically the loop design used extensively to evaluate a large number

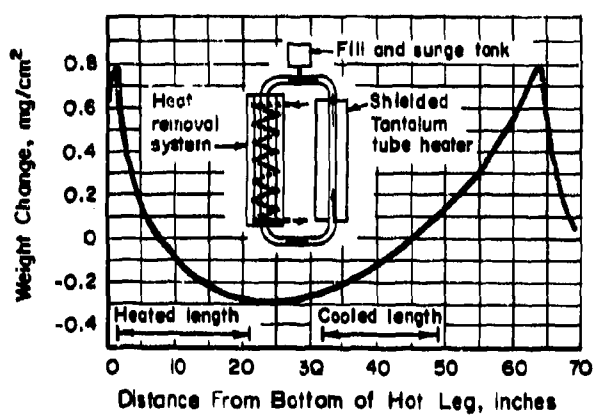

FIGURE 4.7. WEIGHT-CHANGE PROFILE FOR LITHIUM Cb-1Zr THERMAL-CONVECTION LOOP (TCL-1R)[135]

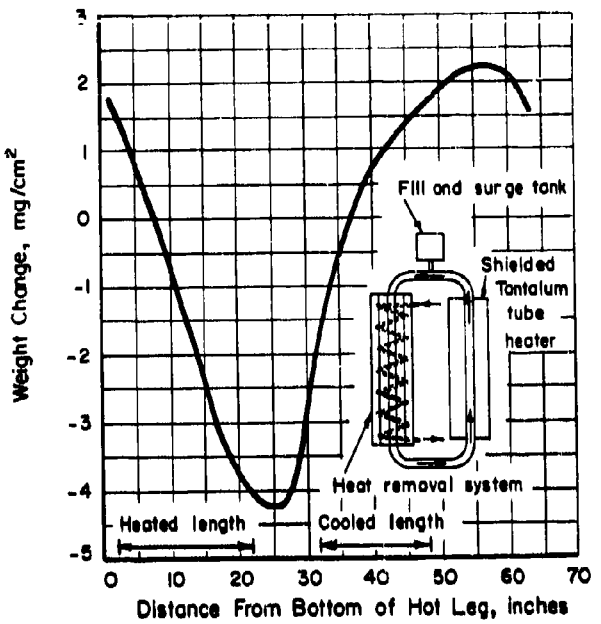

FIGURE 4.8. WEIGHT-CHANGE PROFILE FOR LITHIUM - TZM - CB-1Zr THERMAL-CONVECTION LOOP (TCL-2R)[135]

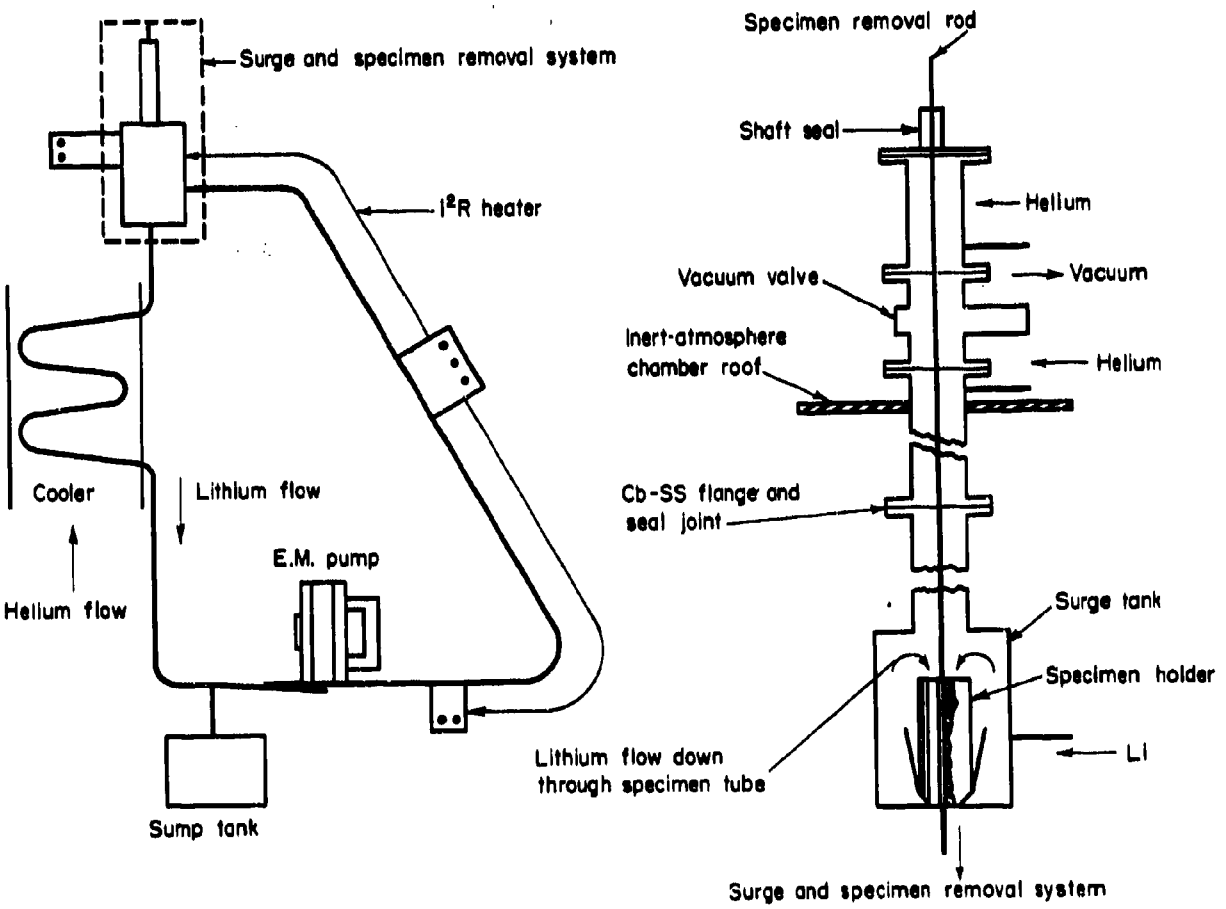

FIGURE 4.9. COLUMBIUM-LITHIUM ALLOY EVALUATION LOOP[133]

TABLE 4.7. TUBE BURST AND CHEMISTRY DATA FROM SPECIMENS EXPOSED TO LITHIUM IN THE Cb-1Zr ALLOY LCCDB-1 LOOP[132]

Specimen and Treatment	Test Conditions	Depth of Sample Analyzed, mils	Analysis, ppm C	N	O	Time to Rupture, hours	Percent Growth	Full-Wall Post-Mechanical-Test Analysis, ppm C	N	O
XM-1088 (Cb-1Zr-0.06C) 2900 F, 1 hour 2200 F, 2 hours	Control	OD-5	785	75	160	875		530	95	80
		5-10	700	60	300					
		10-15	665	75	220					
		15-20	640	95	190					
		20-ID	580	75	145					
	Argon, 2200 F, 1000 hours	OD-5	800	45	435	383		490	530	50
		5-10	585	35	250	389		570	840	50
		10-15	495	40	610					
		15-20	495	60	340					
		20-ID	530	160	230					
	Lithium, 2200 F, 1000 hours	OD-5	550	200	75	241	241	470	205	100
		5-10	510	220	75	285				
		10-15	485	220	85					
		15-20	625	300	165					
		20-ID	540	340	110					
	Lithium, 2200 F, 200 hours	OD-5	580	185		277				
		5-10	690	165						
		10-15	610	165	55					
		15-20	660	165	80					
		20-ID	560	185						
PWC-33 (Cb-3Zr-0.3C) XM-1063 Heat Code PMFT, 2200 F, 2 hours, cold swage from 0.312 OD to 0.304 OD	Control	OD-5	3080	85	100	697	42	3400	630	105
		5-10	3190	120	90	399	47			
		10-15	3160	135	145			3060	190	105
		15-20	3180	95	145					
		20-ID	3210	185	155					
	Lithium, 2200 F, 1000 hours	OD-5	2825		110	773	26	3500	760	220
		5-10	3160	770	105	847	34	3500	720	320
		10-15	3300	860	120					
		15-20	3290	900	125					
		20-25	2880	810	110					

TABLE 4.8. LITHIUM COMPATIBILITY OF OXYGENATED Cb-1Zr-0.1C ALLOY AFTER 50 HOURS OF EXPOSURE[133]

Test Temperature, F	Oxygen, ppm Pretest	Posttest	Carbon, ppm Pretest	Posttest	Metallographic Examination
2000[a]	500	230	400	400	Complete Intergranular attack
2000[b]	1000	480	700	700	No lithium penetration
2200[b]	2100	980	600	500	No lithium penetration

(a) Specimen exposed in the as-quenched condition.
(b) Specimens heat treated at 2200 F prior to test.

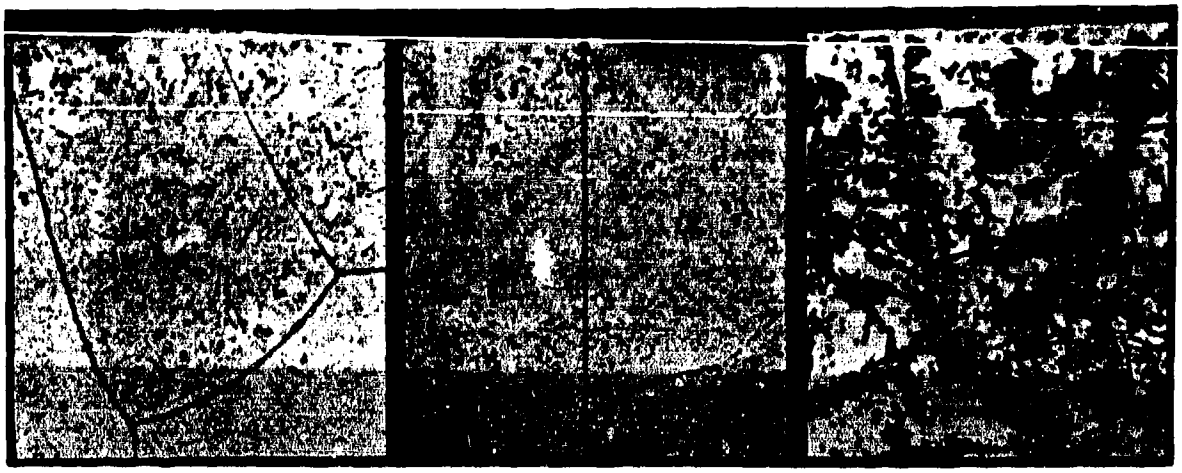

500X Lithium Interface

a. Pretest: Argon Soak, 1000 Hours

b. Posttest: Lithium Flow, 1000 Hours

c. Posttest: Lithium Flow, 200 Hours

FIGURE 4.10. EFFECT OF 1000 AND 200 HOUR, 2200 F ENVIRONMENTS ON Cb-1Zr-0.06C ALLOY[132]

Etchant: $10H_2O$, $5HNO_3$, 2HF.

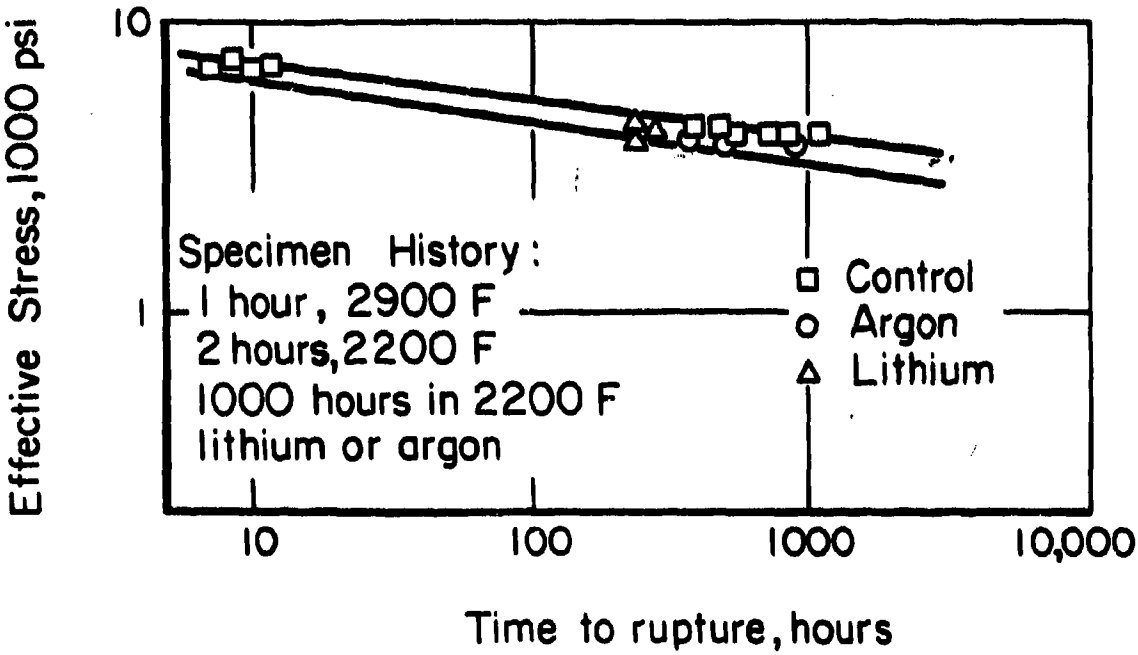

FIGURE 4.11. (Cb-1Zr-0.1C) ALLOY 2200 F STRESS-RUPTURE TESTS[133]

TABLE 4.9. SUSCEPTIBILITY OF OXYGEN-CONTAMINATED COLUMBIUM ALLOYS TO CORROSION BY LITHIUM[135]

Alloy	Attack by Lithium at 1500 to 1830 F		Critical Oxygen Level,[a] ppm
	As Contaminated at 1850 F	After Heat Treatment at 1850 F	
Cb-40V	Yes	Yes	500-1000
D-43	Yes	No	2400
B-66	Yes	No	2700
FS-85	Yes	Yes[b]	1900
Cb-752	Yes	No	3000

(a) Level above which heat-treated alloy is not resistant even after heat treatment.
(b) 2900 F heat treatment gave corrosion-resistant alloy.

TABLE 4.10. RESULTS OF SCREENING TESTS ON COLUMBIUM ALLOYS AFTER 250 HOURS IN FLOWING 1800 F LITHIUM[129]

Composition	Results
Cb-20Ti-5Zr	Good corrosion resistance
Cb-20Ti-5Co	Good corrosion resistance
Cb-20Ti-5Cr	Good corrosion resistance
Cb-20Ti-5Ni	Good corrosion resistance
Cb-10Ti	Good corrosion resistance
Cb-1Zr-1Ti-1Y	Good corrosion resistance
Cb-1Zr	Good corrosion resistance
Cb-5Zr	Good corrosion resistance
Cb-50Zr-5Ti	Good corrosion resistance
Cb-15Ti-5Al	Good corrosion resistance
Cb-5Mo	Slight Attack
Cb-33Ta	Slight Attack
Cb-10W	Slight Attack
Cb-2Al-2V	Good corrosion resistance
Cb-4Al-4V	Good corrosion resistance
Cb-6Al-6V	Good corrosion resistance
Cb-5Mo-2Ti-2Zr	Good corrosion resistance

TABLE 4.11. SCREENING TESTS IN FORCED CONVECTION LITHIUM LOOP FOR 250 HOURS[129]

Composition	Temperature, F	Results
Cb-20Ti-5Zr	2000	Excellent resistance
Cb-20Ti-5Co	2000	Excellent resistance
Cb-20Ti-5Cr	2000	Excellent resistance
Cb-20Ti-5Ni	2000	Excellent resistance
Cb-5Ti	2000	Excellent resistance
Cb-5Mo-2Ti-2Zr	1600	Excellent resistance
	2000	Excellent resistance

of different materials and to expose tubular specimens for mechanical-properties studies. With this type of experimental apparatus, Cb-1Zr was proven to have adequate corrosion resistance to 2200 F lithium. Pratt & Whitney[132] operated such loops up to 5000 hours in 2000 F lithium.

Attempts to both improve and strengthen the Cb-1Zr alloy, by alloy development, were made at Pratt & Whitney. In the loop shown in Figure 4.9, tubular specimens were exposed for 1000 hours, removed, and burst tested in 2200 F lithium. The results for two alloys, Cb-1Zr-0.06C and Cb-3Zr-0.3C, are summarized in Table 4.7. These results indicate that there is a slight reduction of rupture strength resulting from a 1000-hour, 2200 F thermal treatment in an inert-gas environment. There was no significant change in rupture strength due to interaction with lithium. The Cb-3Zr-0.3C alloy, after 1000 hours in 2200 F flowing lithium, experienced inside diameter and outside diameter depletion to 0.6 mil maximum, recrystallization of surfaces to depths of 6 to 8 mils and a very slight decrease in hardness at the surface (107 DPH versus 113 DPH in the center of the wall). The 200-hour Cb-1Zr-0.06C alloy exposed to lithium experienced surface and maximum grain-boundary second-phase depletion to 0.5 mil as seen in Figure 4.10. No attack or hardness gradients were apparent.

The phases present in the posttest materials were identified as (Cb-Zr)C with 47 mole percent zirconium in the specimen exposed for 200 hours and 62 mole percent zirconium in the 1000-hour specimen. The apparent difference in structure is due to sample preparation and etching, and is not a different phase.

A second-generation columbium alloy Cb-1Zr-0.1C was studied extensively at Pratt & Whitney. The carbon addition was made for the purpose of strengthening the basic Cb-1Zr alloy. In this alloy the carbon is precipitated as a mixed Cb-Zr carbide, which in its stabilized form is body-centered cubic. Specimens oxygenated at 2400 F and quenched from 3500 F show complete intergranular penetration by classical lithium attack. Stabilized specimens (2 hours at 2200 F after quenching) are not attacked. This behavior, as shown in Table 4.8, is similar to that observed in the Cb-1Zr alloy. The creep-rupture results are shown in Figure 4.11 and indicate that there is little or no reduction in rupture life due to lithium exposure.

The Cb-1Zr systems have been demonstrated by Pratt & Whitney and Oak Ridge to be highly resistant to attack by lithium up to 2000 F, when the Cb-1Zr is in the stabilized condition. Pratt & Whitney conducted an estimated 3000 tests which included capsule, stress-rupture, creep, dynamic loop, full-scale pressure vessels, and a 2000 F, 10,000-hour nonnuclear system test to establish this corrosion resistance of the Cb-1Zr alloy.

4.2.5 Miscellaneous Columbium Alloys

There has been a minor amount of work on a number of other columbium-base alloys. Oak Ridge[135] conducted a series of static tests on advanced columbium alloys, Cb-40V, D-43 (Cb-10W-1Zr-0.1C), B-66 (Cb-5Mo-5V-1Zr), FS-85 (Cb-27Ta-11W-1Zr), and Cb-752 (Cb-10W-2.5Zr). The tests were conducted for 100 hours at 1830 F, and the results are summarized in Table 4.9. The corrosion behavior exhibited is characteristic of Cb-1Zr. That is, alloys that were not heat treated following oxygen doping at 1830 F exhibit attack in the form of a Widmanstätten corrosion even at 930 F, with heavy intergranular attack at 1830 F. Heat treatment in the 2370 to 2900 F temperature range prior to exposure eliminates the attack by the lithium. The B-66 alloy was exposed in static corrosion tests to 2500 F lithium (in a TZM corrosion capsule) with no apparent attack in 100 hours. At Battelle,[136] exposure under the same conditions at 2800 F produced heavy grain-boundary penetration and surface attack.

Pratt & Whitney[129] conducted screening tests on a large number of columbium alloys in a Cb-1Zr thermal-convection loop at 1800 F. The alloys studied and the results are shown in Table 4.10. These results indicate that binary alloys with molybdenum, tantalum, and tungsten exhibit lithium corrosion behavior equivalent to that of unalloyed columbium. The other alloys showed somewhat improved corrosion resistance. Solution attack increased with increasing chromium content when concentrations exceeded 17.5 weight percent. The results of forced-convection-loop tests conducted on the more promising alloys are shown in Table 4.11. All of these materials showed good resistance to lithium attack. No further work was done with these alloys.

4.3 TANTALUM

There have been very few recent studies on the corrosion behavior of tantalum and tantalum alloys. Tantalum behaves in a manner similar to columbium. A stable oxide former such as hafnium is necessary to produce corrosion resistance.

Studies were conducted at Battelle[136] on Ta-12W and Ta-8W-2Hf (T-111) alloys. These

tests were performed in a dissimilar metal system utilizing TZM as the corrosion capsule. Both the Ta-12W and Ta-8W-2Hf alloys exhibit surface dissolution and grain-boundary penetration after 100 hours at 2500 F. Surface dissolution is severe after 1000 hours at 2500 F.

Pratt & Whitney[132] performed compatibility tests on T-111 alloy in flowing lithium for at least 1000 hours. The results of these tests showed no measurable corrosion rate during the test period. Also, there does not appear to be a deleterious effect on the stress-rupture properties of T-111 alloy due to lithium exposure. Figure 4.12 illustrates this latter effect.

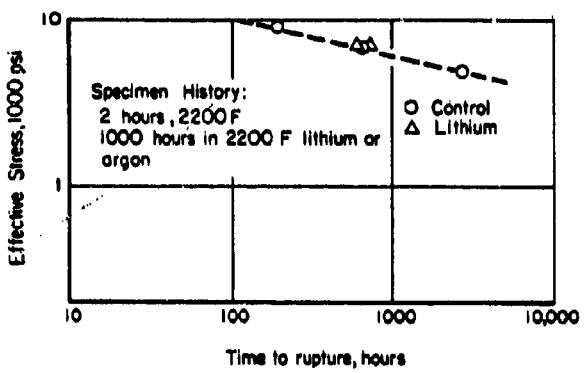

FIGURE 4.12. T-111 ALLOY 2400 F STRESS-RUPTURE TESTS[133]

4.4. MOLYBDENUM ALLOYS

Until recently, widespread interest in molybdenum compatibility with liquid lithium has been lacking. Battelle[136] conducted a number of 1000 to 3000-hour static corrosion experiments in lithium over the temperature range from 2500 to 3000 F. The alloys investigated were TZM (Mo-0.5Ti-0.08Zr) and (Mo-50Re), and neither alloy showed evidence of attack in this temperature range for exposures up to 1000 hours. The TZM alloy showed further resistance to corrosion by static lithium for periods of 3000 hours at 3000 F. Currently, studies are in progress at both Oak Ridge and Brookhaven on TZM and (Mo-0.5Ti) to shed further light on the corrosion behavior of molybdenum alloys in liquid lithium.

4.5 TUNGSTEN ALLOYS AND RHENIUM

As with molybdenum, only a limited number of studies, conducted principally by Pratt & Whitney[132] and Battelle,[136] have been reported concerning the compatibility of tungsten alloys with lithium. The Battelle studies, summarized in Table 4.12 indicate that all of the tungsten alloys investigated exhibit good resistance to attack by lithium at 2500 F. Also, after 1000 hours of exposure at 2800 F, W-15Mo and W-10Re showed only slight surface dissolution, while unalloyed tungsten, W-0.9Cb, and W-25Re exhibited some surface dissolution and grain-boundary penetration.

TABLE 4.12. LOWEST TEMPERATURE AT WHICH ATTACK BY LITHIUM WAS OBSERVED[a][136]

Material	Temperature, F	
	100 Hours	1000 Hours
W	3000[b]	2800[e]
W-0.9Cb	3000	2800[e]
W-15Mo	NA[c]	2800[b]
W-10Re	NA	2800[b]
W-25Re	NA	2800[e]
Re	3000[d]	2500[d]

(a) Specimen was exposed to lithium in TZM capsule at 2500, 2800, and 3000 F.
(b) Slight surface dissolution.
(c) No attack at 3000 F.
(d) Mass transfer from corrosion capsule.
(e) Surface dissolution and grain-boundary penetration.

Pratt & Whitney[132] conducted loop tests on the W-25Re alloy at 2200 F. Metallographic examinations of the tubing walls, although revealing sigma precipitation along the grain boundaries, showed no evidence of attack after 1000 hours of exposure to flowing lithium.

The Battelle investigation further showed that rhenium also was not attacked by lithium, but picked up molybdenum from the TZM capsule. In these rhenium tests, there was no apparent surface dissolution or other attack due to lithium. Metallographs showing the mass-transfer effect are presented in Figure 4.13.

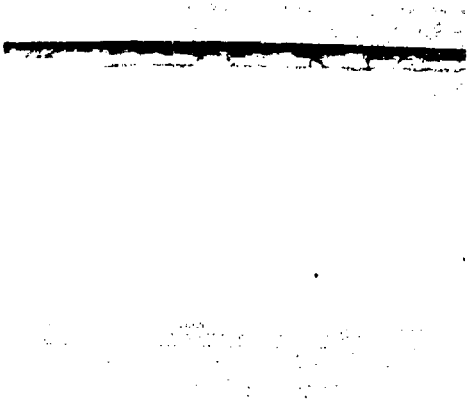

250X RM-39362

a. 100 Hours

Mo-Re sigma phase was present. This was due to mass transfer of molybdenum.

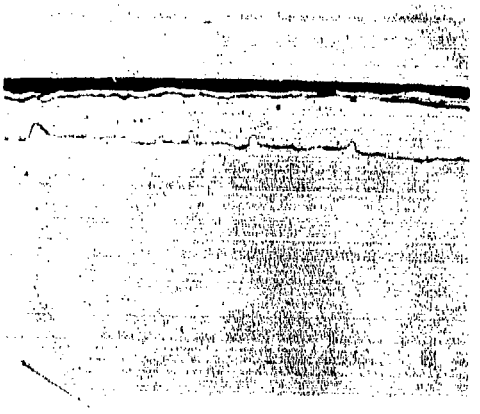

250X RM-41449

b. 1000 Hours

Note large zones of the surface. These two zones are due to molybdenum mass transfer.

FIGURE 4.13. MICROSTRUCTURES OF RHENIUM EXPOSED TO STATIC LITHIUM AT 3000 F[136]

The photographs were reduced approximately 20 percent in printing.

4.6 IRON-BASE ALLOYS

Pratt & Whitney[3] conducted extensive tests on commercially available ferrous alloys in forced-convection corrosion loops. These results, summarized in Table 4.13, indicate that pure iron and austenitic stainless steels are unsuitable in the 1300 to 1500 F temperature range. These materials exhibit severe solution corrosion, appreciable intergranular attack, and thermal-gradient mass transfer.

The temperature dependence of solution corrosion and mass transfer was evaluated in a series of Type 316 stainless steel loop tests. At a maximum circuit temperature of 1100 F and a 200 F thermal gradient, Type 316 stainless steel appears to be suitable for limited service. Only moderate attack and slight mass-transfer deposition were observed in 250- and 1000-hour tests. Data for these tests are summarized in Table 4.14.

4.7 NICKEL-BASE ALLOYS

Nickel-base alloys undergo severe solution attack and mass transfer, rendering them completely unsatisfactory for liquid-lithium service in the temperature range from 1200 to 1800 F. These results were corroborated by tests conducted at Pratt & Whitney,[129] as presented in Table 4.15. As can be seen, Waspalloy, Inconel, and Haynes Alloy No. 25 experience this type of behavior.

TABLE 4.13. RESULTS OF IRON AND STAINLESS STEEL FORCED-CONVECTION LOOP TESTS WITH 1500/1300 F LITHIUM[129]

Alloy	Time hours	Maximum Depth of Attack,[a] mils	Deposits: Maximum Thickness, mils	Deposits: Weight, grams	Number of Loops
Iron[b]	108-138	Nil 2.0-4.5 Δw	12.5-15.0	1.3-3.0	2
Iron	138-187	Nil-0.6 5.0-6.6 Δw	14.0-18.0	6.0-6.6	2
Type 316	52-155	1.0-4.5 IG 3.9-8.5 Δw	34.2-41.0	6.0-11.0	4
Type 304	105-138	1.0-5.0 IG 3.8-6.0 Δw	18.5-20.0	4.0-4.6	2
Type 310	64-96	3.0-4.0 IG 2.2-4.7 Δw	19.5-24.0	5.9-6.2	2
Type 321	69-200	Nil-2.0 IG 6.2-6.4 Δw	25.0-32.0	8.5-10.0	2
Type 347	82-160	0.5-0.6 IG 4.3-4.9 Δw	33.0-40.0	3.5-9.8	2

(a) IG = intergranular; Δw = apparent solution attack, decrease in wall thickness.
(b) Titanium getter in lithium flow stream.

TABLE 4.14. RESULTS OF TYPE 316 STAINLESS STEEL-LITHIUM FORCED-CONVECTION-LOOP TESTS[129]

Temperature Range, F	Time, Hours	Velocity, fps	Maximum Depth of Attack,[b] mils	Maximum Thickness, mils	Weight, grams	Number of Loops
1100/900	250	25.0	4.0 1.0-2.0 Δw	1.0	Nil	2
1100/900	1000	25.0	2.0 2.0-2.5 Δw	6.0	0.15	1
1200/1000	250	25.0	0-1.0 IG 3.0-4.0 Δw	15.0-21.0	1.5-1.8	2
1400/1200[b]	161-250	13.0-21.0	1.2-1.5 2.6-3.2 Δw	14.0-24.0	Not weighed	2
1400/1000[b]	177-250	10.0-13.0	1.5 IG 2.3-4.5 Δw	13.0-19.5	Not weighed	2
1400/1000	129-250	5.0-13.0	0.4-2.5 IG 1.4-2.9 Δw	11.0-27.0	Not weighed	2
1500/1300[b]	193	13.0	1.0 IG 6.0-6.5 Δw	49.0	Not weighed	1
1500/1300	52/155	13.0	1.0-4.5 IG 3.9-8.5 Δw	34.2-41.0	6.0-11.0	4
1600/1400[b]	15	13.0	9.2 IG 2.8-4.2 Δw	46.5	Not weighed	1

(a) IG = intergranular; Δw = apparent solution attack, decrease in wall thickness
(b) Titanium getter in flow stream.

TABLE 4.15. RESULTS OF LITHIUM CORROSION TESTS ON NICKEL-CONTAINING ALLOYS[129]

Material	Type of Test	Conditions: Temperature Range, F	Conditions: Time, hours	Results
Waspalloy	Forced-convection loop	1500/1300	3	Terminated because of severe mass transfer
Inconel[a]	Natural-convection loop	1600/1200	100	Terminated because of severe mass transfer
		1600/1500	72	
		1600/1400	5	
Haynes Alloy No. 25	Tab in natural-convection loop	1600/1350	245	-109 mg/cm^2 - 100 hour (Type 316 control: -16 mg/cm^2 - 100 hour)

(a) Two percent aluminum added to lithium.

CESIUM INTRODUCTION

5. CESIUM

5.1 INTRODUCTION

There are two primary applications for cesium in power systems: (1) as a working fluid in ion engines, and (2) to dissipate the current-limiting space charge in thermionic generators. Cesium could also be utilized in magnetohydrodynamic generators to seed an inert gas, like helium, and thus provide a high-temperature-conducting fluid stream for cutting lines of magnetic flux to generate a current. Most of the cesium corrosion studies conducted to date have been directed toward these applications.

CESIUM NICKEL-BASE ALLOYS

5.2 NICKEL-BASE ALLOYS

The sparse amount of corrosion testing completed on nickel-base alloys in cesium has been limited to relatively low temperatures and short periods of time. For example, it has been shown[137] that unalloyed nickel and René 41 are both unaffected by liquid cesium for up to 500 hours at 750 F. Likewise, Inconel X is not attacked severely by cesium liquid or vapor at 1600 F, although decarburization and leaching of precipitates were observed in static cesium capsules after 720 hours.[138] Ni-Span C[139] (Ni-40Fe-5.5Cr-2.5Ti) suffers no noticeable surface attack upon exposure to cesium vapor at 1200 F for 1000 hours, but it too loses subsurface precipitates. In addition, the cesium causes it to lose some ductility and yield strength. The effects of cesium on several nickel-base materials are summarized qualitatively in Table 5.1.

CESIUM IRON-BASE ALLOYS

5.3 IRON-BASE ALLOYS

Unalloyed iron[140] and many steels[137-140] are generally unaffected by cesium. The majority of the steels do, however, lose carbon to the cesium. There is evidence presented by IITRI[139] to suggest that the stainless steels experience liquid-metal embrittlement. This embrittlement is not catastrophic and is reversible in the sense that if the cesium is removed, the effect disappears. They also present stress-strain curves (Figure 5.1) which suggest that the yield strength is lowered if the material is wetted by cesium. Data presented in Table 5.2 indicate similar results for Type 430 stainless steel as well as a number of other materials. These results are presented as observations rather than conclusions because of the limited data available. However, they do suggest that cesium can serve as a surface-active agent and cause stress-corrosion cracking in some materials.

TABLE 5.1. CORROSION OF NICKEL-BASE MATERIALS IN CESIUM

Material	Temperature, F	Time, hours	Results	Remarks	Reference
Nickel	750	500	No apparent attack	Cesium vapor	137
	750	500	No apparent attack	Cesium liquid	
"A" Nickel	1380	1000	Surface grayed, no apparent attack	Cesium vapor	140
Rene 41	750	500	No attack	Cesium vapor	137
	750	500	No attack	Cesium liquid	
Inconel X	1600	720	Slight attack, cesium leached carbon from surface and regions adjacent to grain boundaries	Liquid cesium	138

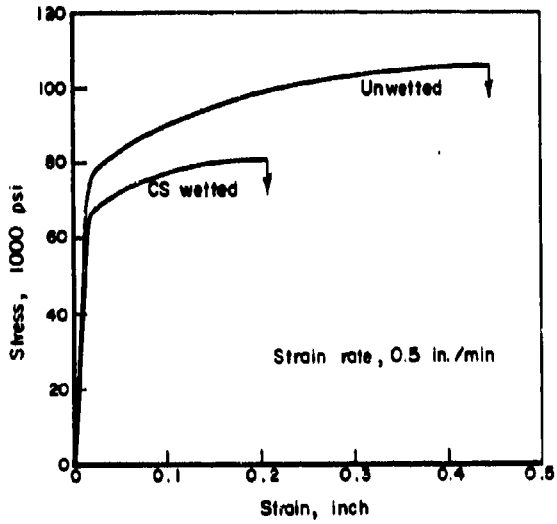

FIGURE 5.1. ROOM-TEMPERATURE STRESS-STRAIN CURVES FOR TYPE 302 STAINLESS STEEL[139]

TABLE 5.2. EFFECT OF CESIUM EXPOSURE ON THE TENSILE PROPERTIES OF VARIOUS MATERIALS AT 87 F[139]

(Strain rate, 0.5 in./min)

Material	Dry Control			Cesium Wetted[b]			1000-Hour Stressed, Cesium Wetted[b], Tested Dry		
	Yield Strength[a], psi	Ultimate Tensile Strength, psi	Elongation, percent	Yield Strength[a], psi	Ultimate Tensile Strength, psi	Elongation, percent	Yield Strength[a], psi	Ultimate Tensile Strength, psi	Elongation, percent
70/30 brass	17,000	49,000	55	18,500	47,500	59.2			
				17,200	48,000	57.1			
70/30 brass (sheet)	22,000	47,000	53				22,000	48,000	53
	23,000	48,000	56				22,500	49,000	56
Nickel	93,000	96,000	9.6	91,000	94,000	9.2	42,000	69,500	39
	43,000	69,000	36				42,000	71,000	39
	43,500	71,000	39						
Type 302 stainless	73,000	105,000	35	64,000	81,000	27			
				68,000	98,200	35			
Type 302 stainless, cold worked	140,000	193,000	7.6	173,000	181,000	7.9			
	144,000	182,000	7.8	160,000	173,000	6.3			
				143,000	158,000	6.8			
Type 302 stainless, cold worked and annealed	98,000	121,000	23	93,500	115,000	13			
	85,000	116,500	23	84,000	114,000	13			
				94,000	116,500	6			
Type 302 stainless (sheet)	45,000	83,000	57				44,000	85,000	63
	45,000	84,000	60				45,000	84,000	62
Type 430 stainless	96,000	108,500	11.6	88,000	108,500	10			
				81,400	107,500	12			
Type 430 stainless (sheet)	44,500	68,500	34				44,000	68,000	2[illegible]
	44,500	69,000	34				43,500	69,000	2[illegible]
Ni-Span C	142,000	150,000	5	140,000	147,000	5			
				139,000	146,400	5			
Ni-Span C (sheet)	135,000	139,500	5				140,000	148,000	[illegible]
	124,000	129,500	5				133,000	138,500	[illegible]

TABLE 5.2. (Continued)

Material	Dry Control			Cesium Wetted[b]			1000-Hour Stressed, Cesium Wetted[b], Tested Dry		
	Yield Strength[a], psi	Ultimate Tensile Strength, psi	Elongation, percent	Yield Strength[a], psi	Ultimate Tensile Strength, psi	Elongation, percent	Yield Strength[a], psi	Ultimate Tensile Strength, psi	Elongation, percent
Kovar	67,000	86,000	27.2	71,000	102,000	27			
				63,000	81,000	37			
Kovar	57,500	78,000	33				58,000	79,000	33
(sheet)	57,000	78,000	36				59,000	79,000	33
Titanium	63,000	74,000	20	60,000	70,000	22			
				59,600	71,000	20			
Titanium	91,000	97,000	19				93,000	102,000	18
(sheet)	91,000	99,000	22				89,000	99,500	23
Ti-30V	140,000	144,000	3	117,000	120,000	3			
	137,000	141,000	2	104,000	105,000	1.5			
Ti-30V	140,000	143,000	3				131,000	133,000	2
(sheet)	135,500	136,000	3				131,000	140,000	
Ti-6Al-4V	152,000	161,000	12	142,000	151,000	11.2			
				143,000	152,000	11.8			
Ti-6Al-4V	142,000	144,000	9				145,000	150,500	9
(sheet)	142,000	144,000	12.5				136,000	144,000	10
Ti-13V-11Cr-3Al	132,000	140,000	20	102,000	125,000	20			
	136,000	143,500	17.5	106,500	121,500	20			
Ti-13V-11Cr-3Al	142,000	147,000	8				141,000	144,000	11
(sheet)							140,000	143,000	10
Zircaloy-2	46,000	58,000	19	37,000	49,000	19			
	46,000	58,000	20	36,000	47,000	18.5			
Columbium	54,000	62,100	11	55,000	65,000	14			
				59,000	67,000	20			
Columbium	32,000	40,000	37				31,000	42,000	40
(sheet)	31,000	40,000	38				30,000	42,000	39

TABLE 5.2. (Continued)

Material	Dry Control			Cesium Wetted[b]			1000-Hour Stressed, Cesium Wetted[b], Tested Dry		
	Yield Strength[a], psi	Ultimate Tensile Strength, psi	Elongation, percent	Yield Strength[a], psi	Ultimate Tensile Strength, psi	Elongation, percent	Yield Strength[a], psi	Ultimate Tensile Strength, psi	Elongation, percent
Tantalum	87,000	88,000	8	85,000	86,000	8			
	78,000	81,000	6	80,000	81,000	9			
Tantalum (sheet)	38,000	39,000	52				36,000	46,000	52
	46,000	47,000	45				36,000	46,000	50
Molybdenum	96,000	99,000	35	94,000	97,500	16			
				88,000	91,200	35			
Molybdenum (sheet)	116,000	123,000	17				118,000	126,000	15
	119,000	124,000	14				117,000	125,500	15
Tungsten	225,000	225,000	nil	209,000	212,000	1.0			
	225,000	225,000	nil	208,000	211,000	0.9			
				205,000	213,000	0.8			
Tungsten (wire)	286,000	299,000	1.7	264,000	293,000	2			
	262,000	296,000	2	264,000	293,000	2.3			
	271,000	296,000	1.9	261,000	293,000	2.0			
	280,000	295,000	1.8	271,000	299,000	2.7			
Cu2Be Solution treated	30,000	66,000	56				30,000	67,000	56
							30,000	67,000	55
Solution treated and aged 300 C	86,000	119,500	23				80,000	115,000	27
							89,000	121,000	23
4340 steel (sheet)	191,000	200,000	7				188,000	202,000	8
	180,000	200,000	7				185,000	203,000	6
1040 steel (sheet)	142,000	158,000	3				151,000	169,000	7
	161,000	174,000	5						
2024 Al sheet, solution treated and aged	51,000	66,000	16				53,000	68,000	14
	52,500	67,000	18				54,000	68,000	13

TABLE 5.2. (Continued)

Material	Dry Control			Cesium Wetted[b]			1000-Hour Stressed, Cesium Wetted[b], Tested Dry		
	Yield Strength[a], psi	Ultimate Tensile Strength, psi	Elongation, percent	Yield Strength[a], psi	Ultimate Tensile Strength, psi	Elongation, percent	Yield Strength[a], psi	Ultimate Tensile Strength, psi	Elongation, percent
6061 Al sheet, solution treated and aged	41,500	45,000	9				41,000	44,500	10
	41,500	45,000	11				40,000	44,500	10
17-7 PH sheet, solution treated and aged	180,000	205,000	10				162,000	187,000	12
	145,000	200,000	16.5				192,000	204,000	7

(a) 0.2% offset.

(b) By wetting a specimen with cesium, it is meant that a thin layer or coating of cesium was maintained around the specimen throughout the course of the test.

Table 5.3 represents a summary of compatibility data pertaining to several iron-base alloys in cesium. These materials apparently do not experience significant attack by cesium during short exposures at temperatures up to 1600 F.

TABLE 5.3. CORROSION OF IRON-BASE MATERIALS IN CESIUM

Material	Temperature, F	Time, hours	Results	Remarks	Reference
Iron	1600	1000	No attack	Cesium vapor	140
17-4PH	750	500	No attack	Cesium vapor	137
	750	500	No attack	Cesium liquid	
AM-350	750	500	No attack	Cesium vapor	137
	750	500	No attack	Cesium liquid	
Type 416 SS	750	500	No attack	Cesium vapor	137
	750	500	No attack	Cesium liquid	
Type 304 SS	1600	1000	No attack	Cesium vapor	140
Type 310 SS	1600	720	Slight carbon transfer from stainless steel to cesium		138

5.4 REFRACTORY METALS (GENERAL)

By far the majority of the published information regarding cesium corrosion relates to refractory metals, which are generally resistant to attack by static cesium vapors at temperatures as high as 3000 F.[137,138,141] However, at 3400 F, tungsten-base materials do undergo surface dissolution and intergranualr attack.[141] Excessive oxygen, either in the cesium or in the refractory metals, is known to aggravate corrosion. Unfortunately, the lack of proven analytical techniques for oxygen in cesium and the scarcity of systematic corrosion data make it possible to state precisely what constitutes "excessive" oxygen.

All of the refractory metals exhibit a finite, although limited, solubility in liquid cesium. Very few quantitative solubility results are currently available. Measurements made by MSA Research,[142] on Cb-1Zr and Mo-0.5Ti alloys, are summarized in Table 5.4, and indicate that neither material is appreciably soluble in cesium.

Pratt & Whitney[143] conducted a number of tests in which various refractory metals were exposed to cesium vapor for 300 hours at 1600 F. Chemical analyses were performed, after exposures in both cesium vapor and vacuum, to determine what effect cesium might have on the carbon, nitrogen, oxygen, and hydrogen contents of the alloys. The test results, summarized in Table 5.5, indicate that exposure to cesium caused no significant changes in interstitial content of the materials studied.

5.5 COLUMBIUM-BASE ALLOYS

To date, most of the corrosion testing of refractory metals in cesium has been done on columbium-base alloys. The results[138,141,143] of simple static tests in cesium vapor are summarized in Table 5.6. For short exposure times, columbium and columbium-base alloys do not experience measurable attack up to temperatures as high as 2800 F.

TABLE 5.4. "SOLUBILITY" OF METAL SPECIES IN 2500 F CESIUM[142]

Alloy	Temperature, F	Equilibration Time	Sampling Crucible	Metal Analysis, ppm
Mo-0.5Ti	2500	5 minutes	Cb-1Zr	Mo - 10 Ti - <5
Mo-0.5Ti	2500	14 hours	Cb-1Zr	Mo - 25 Ti - 100
Mo-0.5Ti	2500	110 hours	Cb-1Zr	Mo - 10 Ti - 150
Cb-1Zr	2500	0.5 hours	Mo-0.5Ti	Cb - 10 Zr - <10
Cb-1Zr	2500	20 hours	Mo-0.5Ti	Cb - 20 Zr - >10
Cb-1Zr	2500	100 hours	Mo-0.5Ti	Cb - 30 Zr - 10

TABLE 5.5. CHEMICAL ANALYSIS OF REFRACTORY METALS TESTED IN CESIUM VAPOR AFTER 300 HOURS AT 1600 F[143]

	Analysis, ppm											
	Pretest				Posttest in Cesium				Posttest in Vacuum			
Alloy	C	N	O	H	C	N	O	H	C	N	O	H
Cb	120	260	820	2	150	220	550	2	65	190	830	15
Cb-1Zr	48	93	370	1	88	250	370	4	160	160	490	5
D-43	1000	48	360		1400	170	430	6	970	68	440	6
PWC-33	3600	130	170	4	3100	110	450	6	3100	99	175	5
Ta	66	190	95	6	76	91	160	1	80	115	46	3
Ta-10W	44	32	50	1	43	43	70	13	100	29	44	1
Ta-8W-2Hf	43	29	35	1	53	30	15	1	62	53	52	3
Mo	230	35	55	1	260	51	43	3	220	87	97	4
Mo-0.5Ti	180	56	50	1	210	90	59	4	190	42	51	10

CESIUM — COLUMBIUM-BASE ALLOYS

TABLE 5.6. CORROSION OF COLUMBIUM-BASE MATERIALS IN CESIUM (STATIC CAPSULE TESTS)

Material	Temperature, F	Time, hours	Results	Remarks	Reference
Columbium	1600	300	No attack	Cesium vapor	143
	1600	720	No attack	Cesium vapor	138
	2500	300	No attack	Cesium vapor	143
Cb-1Zr	1600	300	No attack	Cesium vapor	143
	1600	720	No attack	Cesium vapor	138
	2500	300	No attack	Cesium vapor	143
Cb-10W-1Zr-0.1C (D-43)	1600	300	No attack	Cesium vapor	143
	2500	300	No attack	Cesium vapor	143
Cb-3Zr-0.3C (PWC-33)	1600	300	No attack	Cesium vapor	143
	2500	300	No attack	Cesium vapor	143
Cb-5Mo-5V-1Zr (B-66)	2500	100	No attack	TZM corrosion capsules	141
		1000	Slight surface dissolution	TZM corrosion capsules	
	2800	100	No attack	TZM corrosion capsules	

In contrast to the static test results of Table 5.7, workers at Rocketdyne[138] found surface dissolution of columbium under refluxing cesium at 1800 F after 720 hours. At 2500 F, the dissolution was considerably more severe. Similar results were obtained with the Cb-1Zr alloy, though here the 1800 F capsule was attacked worse than the 2500 F capsule. These inconsistent results are attributable to contamination of the cesium by oxygen, and the severe attack would not be expected if clean cesium were employed.

To illustrate this, exposures of Cb-1Zr by MSA[142] to boiling low-oxygen cesium for 868 hours at 2100 F showed no significant dissolution of the alloy. Also, no deposited crystallites or hardness changes were noted. Similar results were obtained for Cb-25Ta-12W-0.5Zr alloy (FS-85) under identical conditions after 818 hours of exposure.

Studies[144] of mass transfer in cesium were conducted between (1) Cb-1Zr and TD-nickel, (2) Cb-1Zr and Mo-0.5Ti, and (3) Cb-1Zr and Haynes Alloy No. 25. In 500-hour isothermal liquid cesium tests on Cb-1Zr coupled with TD-nickel at 1800 F, a considerable amount of mass transfer was found. Appreciable quantities of columbium appeared as a thin coating on the TD-nickel. The columbium concentration in this thin layer was measured at approximately 24 weight percent. Nickel, on the other hand, was shown to be leached out of the TD-nickel and diffused into the Cb-1Zr tab to a depth of about 8 microns. The concentration of nickel within this narrow 8-micron band was 5 weight percent, which is the reported solid solubility. Similar results have been obtained after 100 hours in 1800 F cesium for a Cb-1Zr and Haynes Alloy No. 25 couple. Haynes Alloy No. 25 was attacked intergranularly, and the microstructure of the Cb-1Zr tab was grossly altered owing to absorption of the metallic components of the Haynes Alloy No. 25 alloy.

Cb-1Zr and Mo-0.5Ti couples were exposed to cesium at 2500 F for periods of 10,500 and 1000 hours.[144] Mass transfer of columbium and zirconium to the Mo-0.5Ti was suppressed by adding oxygen to the system in the form of Cs_2O. However, this addition did not inhibit decarburization of the Mo-0.5Ti by the Cb-1Zr.

CESIUM — MOLYBDENUM-BASE ALLOYS

5.6 MOLYBDENUM-BASE ALLOYS

The results of corrosion studies[137,138,141,143] involving molybdenum-base alloys, Table 5.7, indicate that unalloyed molybdenum, Mo-0.5Ti, TZM, and Mo-50Re resist attack by cesium vapor for

TABLE 5.7. CORROSION OF MOLYBDENUM AND MOLYBDENUM ALLOYS IN CESIUM

Material	Temperature, F	Time, hours	Results	Remarks	Reference
Mo	750	500	No attack	Cesium vapor	137
	1600	300	No attack		143
	1600	720	No attack		139
	2500	300	No attack		143
Mo-0.5Ti	1600	300	No attack		143
	2500	300	No attack		143
TZM	2500	100	No attack	Cesium vapor	141
		1000	No attack	Cesium vapor	141
	2800	100	No attack	Cesium vapor	141
		1000	No attack	Cesium vapor	141
	3100	100	No attack	Cesium vapor	141
		1000	No attack	Cesium vapor	141
	3400	100	No attack	Cesium vapor	141
		1000	No attack	Cesium vapor	141
Mo-50Re	2500	100	No attack	Cesium vapor	141
		1000	No attack	Cesium vapor	141
	2800	100	No attack	Cesium vapor	141
		1000	No attack	Cesium vapor	141
	3100	100	No attack	Cesium vapor	141
		1000	No attack	Cesium vapor	141
	3400	100	No attack	Cesium vapor	141
		1000	No attack	Cesium vapor	141

periods up to 1000 hours at temperatures up to 3400 F.

IITRI[139] observed a reduction in the ductility of molybdenum rod upon exposure to cesium, illustrated in Figure 5.2. The tests were performed in air at 85 F, molten cesium at 85 F, and cesium vapor at 400 F. The observed reduction in yield strength in cesium vapor at 400 F, relative to the control test in 85 F, is probably due to the difference in temperature between the two experiments. However, the elongation in cesium vapor (17.6 percent) is similar to that occurring in cesium liquid (16.0 percent), rather than in air (35.1 percent). This suggests that the presence of cesium vapor reduces the ductility of molybdenum.

Rocketdyne[138] reports that molybdenum undergoes general dissolution in 1800 F refluxing-cesium capsule tests, and that extremely severe general dissolution occurs at 2500 F in similar

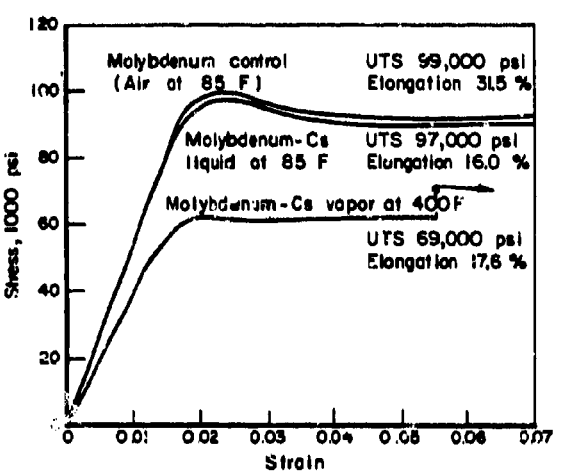

FIGURE 5.2. STRESS-STRAIN BEHAVIOR OF MOLYBDENUM IN CESIUM VAPOR AND LIQUID[139]

CESIUM MOLYBDENUM-BASE ALLOYS

tests. These results appear to be due to oxygen contamination. The authors[138] postulate a dissolution mechanism to explain this inadequate behavior in the following manner. Splashing and geysering, rather than condensing vapor, were the main methods of exposing the capsule walls to liquid cesium in the refluxing tests. Cesium liquid, saturated with molybdenum, repeatedly struck the cooler walls, precipitating out molybdenum. Condensing cesium vapor, running down the walls, dissolved some of the molybdenum crystal growth. The boiling zone in a 2500 F refluxing capsule underwent attack and dissolution greater than did the 1800 F condensing region. Tests conducted at 2100 F exhibited similar results, but much less severe. Approximately the same results were observed at MSA.[142] In all probability, the mechanism of attack postulated by the Rocketdyne workers[138] is valid, but this would not be expected to occur if pure cesium had been employed.

Dissimilar-metal tests were conducted at MSA[142] between zirconium and Mo-0.5Ti alloy for 725 hours at 2500 F. The hardness of the Mo-0.5Ti alloy was not significantly altered by exposure to pure cesium liquid and vapor at 2500 F with zirconium coupons present. Very little corrosion was experienced, and no mass transfer of metallic species was detected.

A TD nickel/(Mo-0.5Ti) couple in 1800 F cesium exhibited mass transfer in both directions.[142] Nickel transfer to the molybdenum was the lesser of the two effects. In a 500-hour exposure at 1800 F, mass transfer of molybdenum to the TD-nickel capsule through liquid cesium occurred at a rate of 1.7×10^{-4} g/(cm^2)(hour).

Mass transfer of metallic constituents across a Haynes 25/(Mo-0.5Ti) couple was not extensive.[142] After 100 hours at 1800 F, the molybdenum showed a slight increase in carbon (about 38 ppm) and an accompanying loss of about 20 ppm oxygen. Metal dissolution was small.

5.7 TANTALUM-BASE ALLOYS

Tantalum alloys[138,141,143] are satisfactory for short-time exposures in cesium up to 2500 F, as illustrated in Table 5.8. To date, very little experimental work has been conducted regarding tantalum compatibility with cesium. The results obtained in Rocketdyne's refluxing capsule tests at 1800 to 2500 F with oxygen-contaminated

TABLE 5.8. CORROSION OF TANTALUM-BASE MATERIALS IN CESIUM

Material	Temperature, F	Time, hours	Results	Remarks	Reference
Ta	1600	300	No attack		143
		720	No attack		138
	2500	300	No attack		143
Ta-10W	1600	300	No attack		143
	2500	300	No attack		143
Ta-12W	2500	100	No attack	TZM corrosion capsule	141
		1000	Surface dissolution		141
	2800	100	Carbide precipitate	Carbon leached from TZM capsules	141
	3100	100	Carbide precipitate	Carbon leached from TZM capsules	141
Ta-8W-2Hf (T-111)	1600	300	No attack		143
	2500	100	No attack		141
		300	No attack		143
		1000	No attack		141
	2800	100	Slight surface dissolution		141

TABLE 5.9. CORROSION OF TUNGSTEN-BASE MATERIALS IN CESIUM

Material	Temperature, F	Time, hours	Results	Remarks	Reference
Tungsten	750	500	No attack		137
	1600	720	No attack		138
	2500	100	No attack		141
		300	No attack		143
		1000	No attack		141
	2800	100	No attack		141
		1000	No attack		141
	3100	100	No attack		141
		1000	No attack		141
	3400	100	Slight surface dissolution	TZM corrosion capsules	141
		1000	Grain-boundary penetration	TZM corrosion capsules	141
W-0.9Cb	2500	100	No attack	TZM corrosion capsules	141
		1000	No attack	Ditto	141
	2800	100	No attack	"	141
		1000	No attack	"	141
	3100	100	No attack	"	141
		1000	No attack	"	141
	3400	100	No attack	"	141
		1000	Surface dissolution	"	141
W-15Mo	2500	100	No attack	TZM corrosion capsules	141
		1000	No attack	Ditto	141
	2800	100	No attack	"	141
		1000	No attack	"	141
	3100	100	No attack	"	141
		1000	No attack	"	141
	3400	100	No attack	"	141
		1000	Surface attack and grain boundary dissolution	"	141
W-3Re	2500	300	No attack		143
W-5Re	2500	300	No attack		143
W-10Re	2500	100	No attack	TZM corrosion capsules	141
		1000	No attack	Ditto	141
	2800	100	No attack	"	141
		1000	No attack	"	141
	3100	100	No attack	"	141
		1000	No attack	"	141
	3400	100	No attack	"	141
		1000	Grain-boundary attack and surface dissolution	"	141
W-25Re	2500	100	No attack	TZM corrosion capsules	141
		300	No attack	Ditto	143
		1000	No attack	"	141
	2800	100	No attack	"	141
		1000	No attack	"	141
	3100	100	No attack	"	141
		1000	No attack	"	141
	3400	100	No attack	"	141
		1000	Slight surface dissolution and grain-boundary penetration	"	141

cesium indicate that surface roughening and dissolution occur, although the attack did not appear to be severe. Refluxing tests on Ta-10W performed by MSA[142] indicate that mass transfer did not occur after 528 hours at 2100 F. It should be pointed out that tantalum is a very powerful carbon getter, as shown at Battelle.[141] Therefore, systems employing tantalum alloys should be free of carbon contamination to avoid embrittlement.

CESIUM TUNGSTEN-BASE ALLOYS

5.8 TUNGSTEN-BASE ALLOYS

All of the work to date[137,138,141] indicates that tungsten and tungsten-base alloys (Table 5.9) are not attacked by cesium up to 3100 F. However, experiments at Battelle[141] suggest that all of the tungsten-base materials studied were subject to surface dissolution and grain-boundary attack after 1000 hours in 3400 F cesium vapor. Unfortunately, little additional information is currently available regarding tungsten compatibility at elevated temperatures.

CESIUM MISCELLANEOUS MATERIALS

5.9 MISCELLANEOUS MATERIALS

The corrosion resistance of several materials is summarized in Table 5.10. Except for the rhenium results, these data are too sparse to lead to any significant conclusions. Recent work at Battelle[141] suggests that rhenium in TZM capsules promotes massive mass transfer of molybdenum from the TZM. However, there was no apparent attack of rhenium by the cesium. The mass transfer between Haynes Alloy No. 25 and Cb-1Zr and Mo-0.5Ti was discussed in the refractory-metal section.

TABLE 5.10. CORROSION OF MISCELLANEOUS MATERIALS IN CESIUM

Material	Temperature, F	Time, hours	Results	Remarks	Reference
Zirconium	1600	720	No apparent attack		138
Hafnium	1600	720	No dissolution or attack noted		138
Ti-6Al-4V	750	500	No attack noted		137
Vanadium	1380	500	Became embrittled due to pickup of oxygen and nitrogen from cesium		140
Rhodium	1380	500	No attack		140
Palladium	1380	500	No attack		140
Rhenium	1380	500	No attack		140
	2500	100	No attack	TZM capsules	141
		1000	No attack	Ditto	141
	2800	100	No attack	"	141
		1000	No attack	"	141
	3100	100	No attack	"	141
		1000	Mass transfer of Mo	"	141
	3400	100	No attack	"	141
		1000	Mass transfer of Mo	"	141

6. REFERENCES

General

(1) Kelman, L. R., Wilkinson, W. D., and Yaggee, F. L., "Resistance of Materials to Attack by Liquid Metals", Report No. ANL-4417, Argonne National Laboratory, Lemont, Illinois, under USAEC Contract W-31-109-eng-38 (July, 1950).

(2) Epstein, L. F., and Weber, C. E., "Problems in the Use of Molten Sodium as a Heat Transfer Fluid", Report TID-70, J. Met. and Ceram. (January, 1951).

Sodium and NaK

(3) Mausteller, J. W., and Batutis, E. F., "Effect of Oxygen on the Mass Transport of Stainless Steel Components in Sodium", Technical Report No. 36, Mine Safety Appliances Co., Callery, Pennsylvania, under Contract NObs-65426 (March 16, 1955) (also designated as NP-5583).

(4) Davis, M., and Draycott, A., "Compatibility of Reactor Materials in Flowing Sodium", Proceedings of the Second United Nations International Conference on the Peaceful Uses of Atomic Engery, 7, pp 95-110 (1958).

(5) Trocki, T., and Nelson, D. B., "Liquid Metal Heat-Transfer System for Nuclear Power Plants", Mechanical Engineering, 75, pp 472-476 (June, 1953).

(6) Bowers, H. I., and Ferguson, W. E., "Structural Materials in LASL Liquid Sodium Systems", in IMD Special Report Series No. 12, Nuclear Metallurgy, AIME, Vol IX, 1963 (L. R. Kelman, Ed.); Also Report No. LADC-5783 (October 18, 1964).

(7) Dudek, R. F., "The Corrosion Testing of Various Materials in Sodium Part I;" "Part II", Ferguson K. M., Report No. BW-7020, The Babcock & Wilcox Co., Alliance, Ohio (April 26, 1957).

(8) Hetzler, F. J., and Young R. S., "Sodium Mass Transfer: II Screening Test Data and Analysis. Volume 2-Metallurgy", Report No. GEAP-3726 (Vol 2), General Electric Co., Atomic Power Equipment Dept., San Jose, California, under USAEC Contract AT(04-3)-189 (June, 1962).

(9) Lyashenko, V. S., Zotov, V. V., and Ivanov, B. A., "Resistance to Corrosion of Austenitic and Ferritic Steels in a Stream of Liquid Sodium at Temperatures of 600 and 700 C", Conference on Corrosion of Reactor Materials, Salzberg, Austria, June 4-9, 1962; Translated in Report No. FTD-MT-62-23.

(10) Frye, J. H., Jr., Manly, W. D., and Cunningham, J. E., "Metallurgy Division Semiannual Progress Report for Period Ending April 10, 1956", Report No. ORNL-2080, Oak Ridge National Laboratory, Oak Ridge, Tennessee, under USAEC Contract W-7405-eng-26 (November 2, 1956).

(11) Frye, J. H., Jr., Manly, W. D., and Cunningham, J. E., "Metallurgy Division Semiannual Progress Report for Period Ending October 10, 1956", Report No. ORNL-2217, Oak Ridge National Laboratory, Oak Ridge, Tennessee, under USAEC Contract W-7405-eng-26 (December 19, 1956).

(12) Frye, J. H., Jr., Manly, W. D., and Cunningham, J. E., "Metallurgy Division Annual Progress Report for Period Ending October 10, 1957", Report No. ORNL-2422, Oak Ridge National Laboratory, Oak Ridge, Tennessee, under USAEC Contract W-7504-eng-26 (December 13, 1957).

(13) Coyle, G. E., "Type 316 Stainless Steel Forced Convection Liquid Metal Corrosion Tests; NSSA-1A1, NSSA-2A2, NSSB-1A1, and NSSB-3A3", Report No. TIM-592, Pratt & Whitney Aircraft - CANEL, Division of United Aircraft Corp., under Contract AF 33(600)-40584 (December 16, 1958).

(14) Rieb, M. J., "Type 316 Stainless Steel Forced Convection NaK Corrosion Loop Tests, NSSC-1A1, -2A2", Report No. TIM-655, Pratt & Whitney Aircraft - CANEL, Division of United Aircraft Corp., Middletown, Connecticut, under Contract AF 33(600)-40548 (April 28, 1961).

(15) Perlow, M. A., "Snap 2 Primary Coolant Development", Report No. NAA-SR-6439, Atomics International, Canoga Park, California, under USAEC Contract AT(11-1)-GEN-8 (July 15, 1961).

(16) Holman, W. R., "Mass Transfer by High Temperature Liquid Sodium", Report No. AECU-4072, American Standard, Atomic Energy Division, Mountain View, California (1958).

(17) Grieser, D. R., Cocks, G. G., Hall, E. H., Henry, W. M., and McCallum, J., "Determination of Oxygen in Sodium at Concentrations Below 10 PPM", Report No. BMI-1538, Battelle Memorial Institute, Columbus, Ohio, under USAEC Contract W-7405-eng-92 (August 23, 1961).

(18) Horsley, G. W., "The Corrosion of Iron by Oxygen-Contaminated Sodium", British Report AERE-M/R-1441, Atomic Energy Research Establishment, Harwell, England (April, 1964).

(19) Weeks, J. R., "Heterometallic Phenomena", Proceedings of the NASA-AEC Liquid Metals Corrosion Meeting held at Lewis Research Center, Cleveland, Ohio, October 2-3, 1963, Volume I, Report No. NASA-SP-41 (1964).

(20) Baus, R. A., Bogard, A. D., Grand, J. A., Lockhart, L. B., Miller, R. R., and Williams, D. D., "The Solubility of Structural Materials in Sodium", Proceedings of the First United Nations International Conference on the Peaceful Uses of Atomic Energy, 9, pp 356-363 (1956).

(21) Rodgers, S. J., Mausteller, J. W., and Batutis, E. F., "Nickel and Iron Concentration in Sodium", Technical Report No. 27, Mine Safety Appliances Company, Callery, Pennsylvania, under Contract NObs-65426 (June 30, 1954).

(22) Epstein, L. F., "Preliminary Studies of the Solubility of Iron in Liquid Sodium", Science, 112, p 426 (1950).

(23) Drugas, P. G., and Kelman, L. R., "Equipment and Procedures for Studying the Equilibrium Solubility of Iron in NaK", Report No. ANL-5359, Argonne National Laboratory, Lemont, Illinois, under Contract W-31-109 Eng-38 (September 4, 1953).

(24) Kovacina, T. A., and Miller R. R., "The Solubility of Nickel in Sodium by a Tracer Technique", Nucl. Sci. Eng., 10, pp 163-166 (1961).

(25) Grand, J. A., Baus, R. A., Bogard, A. D., Williams, D. D., Lockhart, L. B., Jr., and Miller, R. R., "The Solubility of Tantalum and Cobalt in Sodium by Activation Analysis", J. Phys. Chem., 63, pp 1192-1194 (July, 1959).

(26) Preliminary information, Naval Research Laboratory, Washington, D. C.,.

(27) Lockhart, R. W., and Young, R. S., "General Electric Sodium Mass Transfer Program", Paper presented at the AEC Sodium Components Development Program Information Meeting, Chicago, Illinois, June 16, 1965.

(28) Anderson, W. J., and Sneesby, G. V., "Carburization of Austenitic Stainless Steel in Liquid Sodium", Report No. NAA-SR-5282, Atomics International, Canoga Park, California, under USAEC Contract AT(11-1)-GEN-8 (September 1, 1960).

(29) Leppard, J. A., "Carburization Potential in Sodium Systems", paper presented at the AEC Sodium Components Development Program, Hollywood, California, April 14-16, 1964.

(30) Gratton, J. G., "Solubility of Carbon in Sodium at Elevated Temperatures", Report No. KAPL-1807, Knolls Atomic Power Laboratory, Schenectady, New York, under USAEC Contract W-31-109 Eng-52 (June 30, 1957).

(31) Goldmann, K., and Minushkin, B., "Sodium Technology", in Reactor Technology, Link, L. E., (Ed.), Argonne National Laboratory, Selected Reviews, p 321 (1965); also Report No. TID-8541.

(32) Kelley, K. J., Hobart, E. W., and Bjork, R. G., "Studies Concerning the Chemical State of Carbon, Nitrogen, and Oxygen in Alkali Metals", Report No. CNLM-6337, Pratt & Whitney Aircraft - CANEL, Division of United Aircraft Corporation, Middletown, Connecticut, under Contract AT(30-1)-2789 (April 14, 1965).

(33) Pepkowitz, L. P., and Porter, J. T., "The Determination of Carbon in Sodium", J. Anal. Chem., 28 (10), 1606-1607 (October, 1958); also Report No. KAPL-1444 (1955).

(34) Luner, C., Johnson, I., Cosgarea, A., and Feder, H. M., Argonne National Laboratory, Chemical Engineering Division, Private Communication, March 11, 1966.

(35) Anderson, W. J., and Sneesby, G. V., "Carburization of Austenitic Stainless Steel in Liquid Sodium", Report No. NAA-SR-5282, Atomics International, Canoga Park, California, under USAEC Contract AT(11-1)-GEN-8 (September 1, 1960).

(36) Lyashenko, V. S., and Nevzorov, B. A., "Mechanism of Carbon Transfer in Liquid Sodium", USAEC Translation AEC-tr-5408 (translated from Paper No. CN-13/41 presented at the Conference on Corrosion of Reactor Materials, Salzburg, Austria, June 4-9, 1962).

(37) Savage, H. W., Compere, E. L., MacPherson, R. E., Huntley, W. R., and Taboada, A., "SNAP 8 Corrosion Program Quarterly Report for Period Ending May 31, 1964", Report No. ORNL-3671, Oak Ridge National Laboratory, Oak Ridge, Tennessee, under USAEC Contract W-7405-Eng-26 (July, 1964).

(38) Savage, H. W., Compere, E. L., MacPherson, R. E., Huntley, W. R., and Taboada, A., "SNAP 8 Corrosion Program Quarterly Report for Period Ending November 30, 1964", Report No. ORNL-3784, Oak Ridge National Laboratory, Oak Ridge, Tennessee, under USAEC Contract W-7405-Eng-26 (March, 1965).

(39) Peterson, S. (Comp. and Ed.), "Metals and Ceramics Division Annual Progress Report for Period Ending June 30, 1965", Report No. ORNL-3870, Oak Ridge National Laboratory, Oak Ridge, Tennessee, under USAEC Contract W-7405-Eng-26 (November, 1965).

(40) Andrews, R. C., and Barker, K. R., "Effect of High-Temperature Sodium on Austenitic Materials, Topical Report No. 2, Results of Physical Property Tests of 316 SS Specimens in 1200 F Sodium with Low Oxygen", Report No. MSAR 64-18, Mine Safety Appliances Company, Callery, Pennsylvania, under USAEC Contract AT (11-1)-765 (March, 1964).

(41) "Effect of High-Temperature Sodium on Austenitic and Ferritic Steels - Physical Properties of Materials, Quarterly Progress Report, April to June 1963", Report No. MSAR 65-96, Mine Safety Appliances Company, Callery, Pennsylvania, under USAEC Contract AT(11-1)-765 (August 6, 1965).

(42) "Effect of High-Temperature Sodium on Austenitic and Ferritic Steels - Physical Properties of Materials, Progress Report No. 53, January, 1965", Report No. MSAR-65-28, Mine Safety Appliances Company, Callery, Pennsylvania, under USAEC Contract AT(11-1)-765 (February 24, 1965).

(43) Andrews, R. C., and Tepper, F., "Mechanical Properties of Materials in Sodium", Proceedings of Sodium Component Development Program Information Meeting, Chicago, Illinois, June 16-17, 1965, pp 1-17; Report No. CONF-650620.

(44) Anstine, R. C., "The Combined Effects of a Sodium Environment and Extended Life on Type 316 Stainless Steel and Croloy 2-1/4 Alloy Steel Design Stresses", Report No. BW-67-3, The Babcock & Wilcox Company, Barberton, Ohio, under USAEC Contract AT(11-1)-1280 (September, 1964).

(45) Gill, J. J., and Bokros, J. C., "Nitriding of Type 304 Stainless Steel in a Sodium-Nitrogen System", Report No. NAA-SR-6162, Atomics International, Canoga Park, California, under USAEC Contract AT(11-1) -GEN-8 (May 30, 1961).

(46) Brush, E. G., and Rodd, C. R., "Preliminary Experiments on the Nitriding of Reactor Materials in Sodium", Report No. KAPL-M-EGB-21, Knolls Atomic Power Laboratory, Schenectady, New York, under USAEC Contract W-31-309-Eng-52 (1955).

(47) DiStefano, J. R., and Hoffman, E. E., "Corrosion Mechanisms in Refractory Metal-Alkali Metal Systems", Report No. ORNL-3424, Oak Ridge National Laboratory, Oak Ridge, Tennessee, under USAEC Contract W-7405-Eng-26 (September 16, 1963).

(48) Brush, E. G., and Koenig, R. F., "Evaluation of Ferritic Substitutes for the Austenitic Stainless Steels 1. Resistance to Attack by Sodium", Report No. KAPL-1103, Knolls Atomic Power Laboratory, Schenectady, New York, under USAEC Contract W-31-309-ENG-52 (April 22, 1954).

(49) Hayes, W. C., and Shepard, O. C., "Corrosion and Decarburization of Ferritic Chromium-Molybdenum Steels in Sodium Coolant Systems", Report No. NAA-SR-2973, Atomics International, Canoga Park, California, under Contract AT (11-1)-GEN-8 (December 1, 1958).

(50) Anderson, W. J., Sheffield, G. S., and Birkle, A. J., "Development of Ferritic Steels for High-Temperature Sodium Service, Part II", Report No. NAA-SR-7544, Atomics International, Canoga Park, California, under USAEC Contract AT (11-1)-GEN-8 (November 30, 1963).

(51) Andrews, R. C., and Barker, K. R., "Effects of High-Temperature Sodium on Austenitic and Ferritic Steels. Physical Properties of Materials, Topical Report No. 3, Results of Physical Property Tests of 2-1/4Cr-1Mo Steel Specimens in Sodium in High and Low Oxygen, Air, and Helium Environments at 1100 F", Report No. MSAR-64-81, MSA Research Corporation, Callery, Pennsylvania, under USAEC Contract AT(11-1)-765 (July, 1964).

(52) Savage, H. W., Compere, E. L., MacPherson, R. E., Huntley, W. R., and Taboada, A., "SNAP-8 Corrosion Program Quarterly Report for Period Ending February 28, 1965", Report No. ORNL-3823, Oak Ridge National Laboratory, Oak Ridge, Tennessee, under USAEC Contract W-7405-Eng-26 (June, 1965).

(53) Shaw, R. C., "Hastelloy X-Type 316 Stainless Steel Forced Convection Sodium Corrosion Loop Test", Report No. TIM-573, Pratt & Whitney Aircraft Division, United Aircraft Corporation, under USAEC Contract AT(11-1)-229 (September 23, 1958).

(54) Ellington, R. C., "Haynes Alloy No. 25 Forced Convection NaK Corrosion Loop Tests NHHA-1A1, -2A2, -3B1, and -5B2", Report No. TIM-654, Pratt & Whitney Aircraft - CANEL, Division of United Aircraft Corporation, Middletown, Connecticut, under Contract AF 33(600)-40548 (April 26, 1961).

(55) Jordan, W. H., Cromer, S. J., and Miller, A. J., "Aircraft Nuclear Propulsion Project Quarterly Progress Report for Period Ending March 31, 1957", Report No. ORNL-2274, Pt 1-5, Oak Ridge National Laboratory, Oak Ridge, Tennessee, under USAEC Contract W-7504-eng-26 (July 11, 1957).

(56) Oliver, R. B., Douglas, D. A., and DeVan, J. H., "Effect of Environment on Creep Properties of High-Temperature Alloys", paper presented at ANP-Materials Meeting, November 16-18, 1954; Report No. ORNL-2685, Oak Ridge National Laboratory, Oak Ridge, Tennessee, under USAEC Contract W-7405-Eng-26 (March 26, 1959).

(57) Lyashenko, V. S., Zotov, V. V., Andrew, V. E., Abramnovich, M. D., and Ivanov, V. I., "Corrosion Resistance of Steels in Sodium and Lithium", Conference on Corrosion of Reactor Materials, p 2194, Salzberg, Austria, June 4-9, 1962.

(58) Weir, J. R., Jr., Douglas, D. A., and Manly, W. D., "Inconel as a Structural Material for a High-Temperature Fused-Salt Reactor", Report No. ORNL-2264, Oak Ridge National Laboratory, Oak Ridge, Tennessee, under USAEC Contract W-7405-Eng-26 (June 18, 1957).

(59) Jackson, C. B. (Ed.), Liquid Metals Handbook - Sodium (NaK) Supplement, Report No. TID-5277 (July 1, 1955).

(60) Mackay, T. L., "Oxidation of Zirconium and Zirconium Alloys in Liquid Sodium", J. Electrochem. Soc., 110 (9), 960-964 (1963).

(61) "Proceedings of the French-American Conference on Graphite Reactors", held at Brookhaven National Laboratory, Upton, New York, November 12 to 15, 1957; Report No. BNL-489 (September, 1958):

(a) Eichelberger, R. L. (Atomics International), "Recent Information on Moderator Sheath Conversion in Liquid Sodium", pp 168-173.

(b) Carniglia, S. C. (Atomics International), "Interactions of Graphite with Liquid Sodium", pp 159-167.

(62) Koening, R. F., "Chapter IX-C, Corrosion of Beryllium in Liquid Metals" in The Metal Beryllium [D. W. White, Jr., and J. S. Burke (Eds.)], American Society for Metals, 1955.

(63) Bett, F. L., and Draycott, A., "The Compatibility of Beryllium With Liquid Sodium and NaK in Dynamic Systems", Proceedings of the Second United Nations International Conference on the Peaceful Uses of Atomic Energy, 7, pp 125-131 (1958).

(64) Kendall, W. W., "Corrosion of Beryllium in Flowing Sodium", Report No. GEAP-3333, General Electric Company, Atomic Power Equipment Department, under USAEC Contract AT(04-3)-189 PA No. 6 (January 15, 1965).

(65) Lymperes, C. J., Chapman, J. D., and Schenck, G. F., "Interactions in a Type 316 Stainless Steel - NaK - Cb-1Zr Alloy System", Report No. TIM-896, Pratt & Whitney Aircraft - CANEL, Division of United Aircraft Corporation, Middletown, Connecticut, under Contract AF 33(600)-40548 (June 23, 1965).

(66) Foote, F. G., Chiswik, H. H., and Macherey, R. E., "Annual Report for 1962 - Metallurgy Division", Report No. ANL-6677, Argonne National Laboratory, Argonne, Illinois, under USAEC Contract W-31-109-Eng-38.

(67) Foote, F. G., Chiswik, H. H., and Macherey, R. E., "Annual Report for 1963 - Metallurgy Division", Report No. ANL-6868, Argonne National Laboratory, Argonne, Illinois, under USAEC Contract W-31-109-Eng-38.

(68) Austin, G. W., "NaK Corrosion Investigation of Selected Bimetallic Systems", Report No. PWAC-342, Pratt & Whitney Aircraft - CANEL, Division of United Aircraft Corporation, Middletown, Connecticut, under Contract AF 33(600)-40548 (June 30, 1961).

(69) Hoffman, E. E., and Holowach, J., "Alkali Metal/Refractory Alloy Component and Compatibility Evaluation Tests", Trans. Am. Nucl. Soc., 8, pp 396-398 (1965).

(70) Winsche, W. E., and Miles, F. T., "Nuclear Engineering Department Annual Report, December 31, 1964", Report No. BNL-900, Brookhaven National Laboratory, Upton, New York, under USAEC Contract AT(30-2)-GEN-16 (April, 1965).

(71) Romano, A. J., Fleitman, A. H., and Klamut, C. J., "The Relative Agressiveness of Li, Na, K, Rb, and Cs Boiling and Condensing in Cb-1Zr Capsules", Trans. Am. Nucl. Soc., 8, p 391 (1965).

(72) DeVan, J. H., DiStefano, J. R., and Jansen, D. H., "Compatibility of Refractory Metals With Boiling Alkali Metals", Trans. Am. Nucl. Soc., 8, pp 390-391 (1965).

(73) Raines, G. E., Weaver, C. V., and Stang, J. H., "Corrosion and Creep Behavior of Tantalum in Flowing Sodium", Report No. BMI-1284, Battelle Memorial Institute, Columbus, Ohio, under USAEC Contract W-7504-Eng-92 (August 21, 1958).

(74) Kissel, J. W., Glaeser, W. A., and Allen, C. M., "Frictional Behavior of Sodium-Lubricated Materials in a Controlled High-Temperature Environment", Wear, 5, pp 446-457 (1962).

(75) Pearlman, H., "Corrosion of Uranium, Thorium, and Uranium Alloys in Sodium and Organics", paper presented at Fuel Elements Conference, Paris, France, November 18-23, 1957; included in Report No. TID-7546, Book 2 (March, 1958).

(76) Hoffman, E. E., "Compatibility of Dynamic Uranium-Sodium, Type 347 Stainless Steel System", ORNL Corrosion Report No. 167 (September 16, 1957).

(77) Hoffman, E. E., Patriarca, P., Leitten, C. F., Jr., and Slaughter, G. M., "An Evaluation of the Corrosion and Oxidation Resistance of High-Temperature Brazing Alloys", Report No. ORNL-1934, Oak Ridge National Laboratory, Oak Ridge, Tennessee, under Contract W-7405-Eng-26 (November 7, 1956).

(78) Lee, S. K., "An Investigation of Nickel-Base Brazing Alloys and Brazed Joints for Service in Liquid Sodium", Report No. NAA-SR-11326, Atomics International, Canoga Park, California, under USAEC Contract AT(11-1)-GEN-8 (December 15, 1965).

(79) Epstein, L. F., "Nonmetallic Solids", Proceedings of the NASA-AEC-Liquid-Metals Corrosion Meeting (held at Lewis Research Center, Cleveland, Ohio, October 2-3, 1963), Volume 1, Report No. NASA-SP-41, p 79 (1964).

(80) "Resistance of Barrier Materials to Sodium Jet Impingement", Report No. NDA-084-4, Nuclear Development Corporation of America, White Plains, New York, under USAEC Contract AT(30-3)-256 (February 26, 1958).

(81) Coultas, T. A., and Cygan, R., "Compatibility of Sodium, Graphite, and Stainless Steel", Report No. NAA-SR-258, Atomics International, Canoga Park, California, under USAEC Contract AT(11-1)-GEN-8 (October 4, 1953).

(82) Greening, W. J., and Davis, W. A., "The Compatibility of Sodium and Graphite", Report No. NAA-SR-Memo-1852, Atomics International, Canoga Park, California, under USAEC Contract AT(11-1)-GEN-8 (March 1, 1957).

(83) Collins, J. F., Unpublished Memorandum on Stability of Ceramic Materials in Liquid Sodium At Temperatures up to 2000 F, NEPA Division of Fairchild Engine and Aircraft Company, Oak Ridge, Tennessee (January 23, 1951).

(84) Gill, J. J., "Sodium-Graphite Interaction and Graphite Protective Coatings", Report No. NAA-SR-6094, Atomics International, Canoga Park, California, under USAEC Contract AT (11-1)-GEN-8 (May 1, 1961).

(85) Asher, R. C., and Wilson, S. A., "Lamellar Compound of Sodium With Graphite", Nature, 181, pp 409-410 (1958).

(86) Asher, R. C., "A Lamellar Compound of Sodium and Graphite", J. Inorg. Nucl. Chem., 10, pp 238-249 (1959).

(87) Davidson, R. H., "Moderator Element Failures in the Hallam Nuclear Power Facility", Trans. Am. Nucl. Soc., 8, Suppl., p 35 (1965).

(88) Cook, W. H., "Corrosion Resistance of Various Ceramics and Cermets to Liquid Metals", Report No. ORNL-2391, Oak Ridge National Laboratory, Oak Ridge, Tennessee, under USAEC Contract W-7405-Eng-26 (June 15, 1960).

(89) Basham, S. J., Stang, J. H., and Simons, E. M., "Corrosion Screening of Component Materials for NaK Heat-Exchange Systems", Chemical Engineering Symposium Series, 55 (23), 53-60 (1959).

(90) McCreight, L. R., "Ceramics for Nuclear Power Applications", Industrial and Engineering Chemistry, 46, 185 (January, 1954).

Potassium

(91) Cleary, R. E., Schenck, G. F., and Blecherman, S. S., "Solubility Studies in Alkali Metals", USAEC Report CNLM-6335, Pratt & Whitney Aircraft - CANEL, Division of United Aircraft Corporation, Middletown, Connecticut, under USAEC Contract AT(30-1)-2789 (April 21, 1965).

(92) Ginell, W. S., and Teitel, R. J., "Solubility of Transition Metals in Molten Potassium", Paper presented at AEC-NASA Liquid Metals Information Meeting, Gatlinburg, Tennessee, April 21-22, 1965, covering work done under IRAD Program by Douglas Aircraft Company, Inc., Santa Monica, California.

(93) American Nuclear Society 1965 Winter Meeting, Washington, D. C., November 15-18, 1965, Transactions, 8 (2):

(a) Hoffman, E. E., and Holowach, J., "Alkali Metal/Refractory Alloy Component and Compatibility Evaluation Tests", pp 396-398.

(b) Goldman, K., Hyman, N., Kostman, S., and McKee, J., "Carbon and Nitrogen Transfer in a Type 316 Stainless Steel - Cb-1% Zr, Liquid-Potassium System", p 396.

(c) Ginell, W. S., and Teitel, R. J., "Determination of the Solubility of Several Transition Metals in Molten Potassium", pp 393-394.

(d) Harrison, R. W., "Alkali Metal Corrosion Studies on Materials for Advanced Space Power Systems", pp 392-393.

(e) DeVan, J. H., DiStefano, J. R., and Jansen, D. H., "Compatibility of Refractory Metals with Boiling Alkali Metals", pp 390-391.

(f) Cunningham, C. W., De Van, J. H., Fuller, L. E., Jansen, D. H., and MacPherson, R. E., "Screening Tests of Turbine Nozzle and Blade Materials", p 401.

(g) Frank, R. G., "Bearing Materials for Use in Rankine Cycle Space Power Systems", pp 403-405.

(94) Litman, A. P., "The Effect of Oxygen on the Corrosion of Niobium by Liquid Potassium" (Thesis), Report No. ORNL-3751, Oak Ridge National Laboratory, Oak Ridge, Tennessee, under Contract W-7405-Eng-26 (July, 1965).

(95) Stang, J. H., "Corrosion by Liquid Metals", Reactor Materials, 8 (2), 90 (1965).

(96) Scheuerman, C. M., and Barrett, C. A., "Compatibility of Columbium and Tantalum Tubing Alloys With Refluxing Potassium", Report No. NASA TN D-3429, Lewis Research Center, Cleveland, Ohio (May, 1966).

(97) Engel, L. B., Jr., and Frank R. G., "Evaluation of High-Strength Columbium Alloys for Alkali Metal Containment", Interim Report No. 2 covering the period July 25, 1962, to July 10, 1964, Report No. NASA-CR-54226, General Electric Company, Space Power and Propulsion Section, Missile and Space Division, Cincinnati, Ohio, under Contract NAS3-2140.

(98) "Proceedings of the NASA-AEC Liquid Metals Corrosion Meeting", October 2-3, 1963, Volume I, Lewis Research Center, Cleveland, Ohio, Report NASA-SP-41 (1964):

(a) General Electric Company, Space Power and Propulsion Section, Cincinnati, Ohio, Capsule Results, pp 153-160.

(b) General Electric Company, Space Power and Propulsion Section, Cincinnati, Ohio, Loop Results, pp 189-197.

(c) United Nuclear Corporation, Development Division, Loop Results, pp 213-215.

(d) Battelle Memorial Institute, Columbus, Ohio, "Stress-Rupture of SAE-4340 Steel in Potassium Vapor", pp 233-235.

(e) Battelle Memorial Institute, Columbus, Ohio, "Fatigue of Mo-0.5Ti in Potassium Vapor", pp 226-229.

(f) Battelle Memorial Institute, Columbus, Ohio, "Stress-Rupture of Mo-0.5Ti in Potassium Vapor", pp 230-232.

(99) Jansen, D. H., and Hoffman, E. E., "Niobium - 1% Zirconium, Natural Circulation, Boiling-Potassium Corrosion Loop Test", Report No. ORNL-3603, Oak Ridge National Laboratory, Oak Ridge, Tennessee, under USAEC Contract W-7405-Eng-26 (May, 1964).

(100) "Metals and Ceramics Division Annual Progress Report for Period Ending June 30, 1965", Report No. ORNL-3870, Oak Ridge National Laboratory, Oak Ridge, Tennessee, under Contract W-7405-Eng-26 (November, 1965).

(101) Kelly, K. J., Blecherman, S. S., and Hodel, J. E., "Corrosion Studies of Refractory Metal Alloys in Boiling Potassium and Liquid NaK", USAEC Report No. CNLM-6246, Pratt & Whitney Aircraft - CANEL, Division of United Aircraft Corporation, Middletown, Connecticut, under USAEC Contract AT(30-1)-2789 (April 22, 1965).

(102) Salley, R., and Kovacevich, E., "Materials Investigation, SPUR Program Part IV. Fatigue Evaluation of Cb-1Zr", Technical Documentary Report No. ASD-TDR-63-270, Part IV, Battelle Memorial Institute, Columbus, Ohio, under Contract AF 33(657)-8954 (February, 1964).

(103) Carlson, R. G., Miketta, D. N., Frank, R. G., and Semmel, J. W., Jr., "Evaluation of a High Strength Columbium Alloy (AS-55) for Alkali Metal Containment", Interim Report covering the period November 25, 1961, to July 25, 1962, Report No. GE62FPD365, General Electric Company, Space Power and Propulsion Section, Missile and Space Division, Cincinnati, Ohio under Contract NAS3-2140.

(104) "NASA-AEC Liquid Metals Corrosion Meeting", December 14-15, 1961, Brookhaven National Laboratory, USAEC Report TID-7626 (Pt 1) (April, 1962):

(a) Chandler, W. T., "Alkali-Metal Corrosion Studies at Rocketdyne", pp 42-62.

(b) Kovacevich, E. A., "Potassium Corrosion Studies", AiResearch Manufacturing Company of Arizona, pp 63-68.

(c) Semmel, J. W., Jr., "Liquid Metal Investigations", General Electric Company, Flight Propulsion Laboratory Department, pp 69-86.

(105) Harrison, R. W., "Studies of Alkali Metal Corrosion on Materials for Advanced Space Power Systems", Quarterly Progress Report No. 3 for Quarter Ending March 26, 1965, Report No. NASA-CR-54390, General Electric Company, Space Power and Propulsion Section, Missile and Space Division, Cincinnati, Ohio, under Contract NAS3-6012.

(106) Goldmann, K., Hyman, N., Kostman, S., and McKee, J., "Carbon and Nitrogen Transfer in a Type 316 Stainless Steel, Cb-1%Zr, Liquid Potassium System", Report No. UNC-SPLM-94, under Contract AT(30-1)-3078, presented at Symposium on Materials Technology for Large Alkali-Metal Rankine Space Power Systems, ANS Annual Meeting, Washington, D. C. (November 17, 1965).

(107) Hoffman, E. E. (Ed.), "Potassium Corrosion Test Loop Development", Quarterly Progress Report 6, Covering the period October 15, 1964, to January 15, 1965, Report No. NASA-CR-54344, General Electric Company, Space Power and Propulsion Section, Missile and Space Division, Cincinnati, Ohio, under Contract NAS3-2547 (March 12, 1965).

(108) Blecherman, S. S., Corliss, J. E., and Cleary, R. E., "Solubility of Refractory Metals in Lithium and Potassium", Report No. TIM-850, Pratt & Whitney Aircraft - CANEL, Division of United Aircraft Corporation, Middletown, Connecticut, under Contract AT(30-1)-2789 (November, 1965).

(109) Basham, S. J., Allen, C. M., and Rieder, W. G., "Development of a Long-Life Contact Seal for a High-Speed Rotating Shaft in Liquid-Metal Dynamic Power Systems", Technical Report AFAPL-TR-65-97, Battelle Memorial Institute, Columbus, Ohio, under Contract AF 33(657)-10961 (May, 1965).

(110) Salley, R. L., and Kovacevich, E. A., "Materials Investigation, SNAP 50/SPUR Program, Part I. Creep-Rupture Properties of Stress-Relieved TZM Alloy", Technical Documentary Report No. APL-TDR-64-116, Part I, AiResearch Manufacturing Company of Arizona, Phoenix, Arizona, under Contract AF 33(657)-10922 (October, 1964).

(111) Simons, E. M., and Lagedrost, J. F., "Materials Investigation, SNAP 50/SPUR Program, Part III. Mass-Transfer of TZM by Potassium in Boiling-Refluxing Capsules", Technical Documentary Report No. APL-TDR-64-116, Part III, Battelle Memorial Institute, Columbus, Ohio, for AiResearch Manufacturing Company of Arizona, Phoenix, Arizona, under Contract AF 33(615)-2289 (May, 1965).

(112) Kovacevich, E. A., and Salley, R. L., "Mass-Transfer Tests With Two-Phase Flow", Technical Documentary Report No. APL-TDR-64-119, AiResearch Manufacturing Company of Arizona, Phoenix, Arizona, under Contract AF 33(657)-8954 (November 20, 1964).

(113) Salley, R. L,, and Kovacevich, E. A., "Materials Investigation SPUR Program, Part II. Creep-Rupture Properties of Mo+0.5Wt. % Ti", Technical Documentary Report No. ASD-TDR-63-270, Part II, AiResearch Manufacturing Company Arizona, Phoenix, Arizona, under Contract AF 33(657)-8954 (November, 1963).

(114) Salley, R., and Kovacevich, E., "Materials Investigation, SPUR Program, Part III. Fatigue Evaluation of Mo+0.5Wt.% Ti", Technical Documentary Report No. ASD-TDR-63-270, Part III, AiResearch Manufacturing Company of Arizona, Phoenix, Arizona, under Contract AF 33(657)-8954 (December, 1963).

(115) Litman, A. P., and Prados, J. W., "The Partitioning of Oxygen Between Zirconium and Liquid Potassium", Report ORNL-TM-1039, Oak Ridge National Laboratory, Oak Ridge, Tennessee, under Contract W-7405-Eng-26 (April 1965); also Electrochem. Tech., 3 (9-10), 228-33 (September - October, 1965).

(116) Swisher, J. H., "Solubility of Iron, Nickel, and Cobalt in Liquid Potassium and Effect of Oxygen Gettering Agents on Iron Solubility", NASA Technical Note NASA TN D-2734, National Aeronautics and Space Administration, Lewis Research Center, Cleveland, Ohio (March, 1965).

(117) McKisson, R. L., and Eichelberger, R. L., "Solubility and Diffusion Studies of Ultra Pure Transition Elements in Ultra Pure Alkali Metals", Status Summary presented at AEC-NASA Liquid Metals Information Meeting, Gatlinburg, Tennessee, April 21-22, 1965, covering work done by Atomics International, Canoga Park, California, under Contract NAS3-4163.

(118) "NASA-AEC Liquid-Metals Corrosion Meeting", December 7-8, 1960, Washington, D. C., Technical Note NASA-TN-D-769 (February, 1961):

(a) Hoffman, E. E., Oak Ridge National Laboratory Boiling Alkali Metal and Related Studies, pp 15-24.

(b) Rosenblum, L., National Aeronautics and Space Administration, Lewis Research Center, "Liquid Metals Research Program", pp 65-72.

(119) Jansen, D. H., and Hoffman, E. E., "Type 316 Stainless Steel, Inconel, and Haynes Alloy No. 25 Natural-Circulation Boiling-Potassium Corrosion Test Loops", Report No. ORNL-3790, Oak Ridge National Laboratory, Oak Ridge, Tennessee, under Contract W-7405-Eng-26 (June, 1965).

(120) Woodward, C. E., Potts, J. R., Lymperes, C. J., and Schenck, G. F., "Posttest Examination of Type 316 Stainless Steel Pump Impeller RI 7C3", Report No. TIM-842, Pratt & Whitney Aircraft - CANEL, Division of United Aircraft Corporation, Middletown, Connecticut, under Contract NAS3-2541 (December 30, 1964).

(121) "Materials Investigation SPUR Program, Part I. Creep-Rupture Properties of SAE 4340 Steel", Technical Documentary Report No. ASD-TDR-63-270, Part I, AiResearch Manufacturing Company of Arizona, Phoenix, Arizona, under Contract AF 33(657)-8954 (April, 1963).

(122) Simons, E. M., and VanEcho, J. A., "Creep of H-11 Steel in Liquid Potassium at 800 and and 1000 F", Topical Report, Battelle Memorial Institute, Columbus, Ohio, under AiResearch Contract AF 33(657)-10922 (June 30, 1964).

(123) Sawitke, D. W., "Metallographic Examination of H-11 Steel Creep Specimens", Report WAED-64.64E, Westinghouse Electric Corporation, Aerospace Electrical Division, Lima, Ohio, under Contract AF 33(615)-1551 (November, 1964).

(124) Semmel, J. W., Jr., Young, W. R., and Kearns, W. H., "Alkali Metals Boiling and Condensing Investigations, Volume II. Materials Support", Final Report covering the period January 1, 1961, to June 30, 1962, Report No. GE63APD66, General Electric Company, Space Power and Propulsion Section, Missile and Space Division, Cincinnati, Ohio, under Contract NAS5-681 (January 14, 1963).

(125) Frank, R. G., (Ed.), "Materials for Potassium-Lubricated Journal Bearings", Quarterly Progress Report No. 7 covering the period October 22, 1964, to January 22, 1965, Report No. NASA-CR-54345 (or N65-28354), General Electric Company, Space Power and Propulsion Section, Missile and Space Division, Cincinnati, Ohio, under Contract NAS3-2534.

(126) Kissel, J. W., Glaeser, W. A., and Allen, C. M., "Frictional Behavior of Sodium-Lubricated Materials in a Controlled High-Temperature Environment", ASME Paper No. 61-LUBS-16, Battelle Memorial Institute, Columbus, Ohio, under Contract W-7405-Eng-92 (May, 1961).

Lithium

(127) Leavenworth, H., Cleary, R. E., and Bratton, W. D., "Solubility of Structural Metals in Lithium", Report No. PWAC-356, Pratt & Whitney Aircraft Division, United Aircraft Corporation, under USAEC Contract AT(11-1)-229 (June, 1961).

(128) DeStefano, J. R., "Corrosion of Refractory Metals by Lithium", Report No. ORNL-3551, Oak Ridge National Laboratory, Oak Ridge, Tennessee, under USAEC Contract W-7405-eng-26 (March, 1964).

(129) Freed, M. S., and Kelly, K. J. (Eds.), "Corrosion of Columbium Base and Other Structural Alloys in High Temperature Lithium", Report No. PWAC-355, Pratt & Whitney Aircraft - CANEL, Division of United Aircraft Corporation, under USAEC Contract AT(11-1)-229 (June 30, 1961). Declassified in June, 1965.

(130) DeStefano, J. R., and Hoffman, E. E., "Relation Between Oxygen Distribution and Corrosion in Some Refractory Metal-Lithium Systems", Report No. ORNL-TM-327, Oak Ridge National Laboratory, Oak Ridge, Tennessee, under USAEC Contract W-7405-Eng-26 (October, 1962).

(131) Hoffman, E. E., "Effects of Oxygen and Nitrogen on the Corrosion Resistance of Columbium to Lithium at Elevated Temperatures", Report No. ORNL-2675, Oak Ridge National Laboratory, Oak Ridge, Tennessee, under USAEC Contract W-7405-Eng-26 (January, 1959).

(132) Kelly, K. J., unpublished information (July, 1965).

(133) Cleary, R. E., "Corrosion Studies of Refractory Metals in Lithium", paper presented at AEC-NASA Liquid Metals Information Meeting, Gatlinburg, Tennessee, April 21-22, 1965; also Report No. CNLM-6348.

(134) DeVan, J. H., and Sessions, C. E., "Compatibility of Some Refractory Alloys in Flowing Nonisothermal Lithium", Trans. Am. Nucl. Soc., 8 (2), 394 (November, 1965).

(135) Sessions, C. E., "Corrosion of Advanced Refractory Alloys in Lithium", paper presented at AEC-NASA Liquid Metals Information Meeting, Gatlinburg, Tennessee, April 21-22, 1965.

(136) DeMastry, J. A., and Griesenauer, N. M., "Investigation of High-Temperature Refractory Metals and Alloys for Thermionic Converters", Report No. AFAPL-TR-65-29, Battelle Memorial Institute, Columbus, Ohio, under Contract AF 33(657)-10404 (April, 1965).

Cesium

(137) Winslow, P. M., "Synopsis of Cesium Compatibility Studies", presented at AEC-NASA Liquid Metal Symposium, Gatlinburg, Tennessee, April 21-22, 1965.

(138) Chandler, W. T., and Hoffman, N. J., "Effects of Liquid and Vapor Cesium on Container Metals", Report No. ASD-TDR-62-965, Rocketdyne, Division of North American Aviation, Inc., Canoga Park, California, under Contract AF 33(616)-8435 (March, 1963).

(139) Levinson, D. W., "Stress-Dependent Interactions Between Cesium and Other Materials", Report No. IITRI-B215-22, Illinois Institute of Technology Research Institute, Chicago, Illinois, under Contract Nonr 3441(00) (November, 1964).

(140) Hall, W. B., and Kessler, S. W., "Cesium Compatibility of Thermionic Converter Structural Materials", Radio Corporation of America, under Contract NObs-84823.

(141) DeMastry, J. A., and Griesenauer, N. M., "Investigation of High-Temperature Refractory Metals and Alloys for Thermionic Converters", Report No. AFAPL-TR-65-29, Battelle Memorial Institute, Columbus, Ohio, under Contract AF 33(657)-10404 (April, 1965).

(142) Tepper, F., and Greer, J., "Factors Affecting the Compatibility of Liquid Cesium With Containment Metals", Report No. AFML-TR-64-327, MSA Research Corporation, Callery, Pennsylvania, under Contract AF 33(657)-9168 (November, 1964).

(143) Rigney, D. V., Unpublished internal memorandum summarizing cesium corrosion data (July 15, 1965), Pratt & Whitney Aircraft - CANEL, Division of United Aircraft Corporation, under USAEC Contract AT(30-1)-2289.

(144) Tepper, F., and Greer, J., "Factors Affecting the Compatibility of Liquid Cesium With Containment Metals", Report No. ASD-TDR-63-824, Part I, MSA Research Corporation, Callery, Pennsylvania, under Contract AF 33(657)-9168 (September, 1963).

Unclassified
Security Classification

DOCUMENT CONTROL DATA - R&D

(Security classification of title, body of abstract and indexing annotation must be entered when the overall report is classified)

1. ORIGINATING ACTIVITY (Corporate author) Battelle Memorial Institute Defense Metals Information Center 505 King Avenue, Columbus, Ohio 43201	2a. REPORT SECURITY CLASSIFICATION Unclassified 2b. GROUP

3. REPORT TITLE
Compatibility of Liquid and Vapor Alkali Metals With Construction Materials

4. DESCRIPTIVE NOTES (Type of report and inclusive dates)
DMIC Report

5. AUTHOR(S) (Last name, first name, initial)
Stang, J. H., Simons, E. M., De Mastry, J. A., and Genco, J. M.

6. REPORT DATE	7a. TOTAL NO. OF PAGES	7b. NO. OF REFS
April 15, 1966	112	144

8a. CONTRACT OR GRANT NO.	9a. ORIGINATOR'S REPORT NUMBER(S)
AF 33(615)-3408	DMIC Report 227
b. PROJECT NO.	
c.	9b. OTHER REPORT NO(S) (Any other numbers that may be assigned this report)
d.	

10. AVAILABILITY/LIMITATION NOTICES Copies of this report may be obtained, while the supply lasts, from DMIC at no cost by U. S. Government agencies, contractors, subcontractors, and their suppliers. Qualified requestors may also obtain copies from the Defense Documentation Center (DDC), Alexandria, Virginia 22314

11. SUPPLEMENTARY NOTES	12. SPONSORING MILITARY ACTIVITY
	U. S. Air Force Materials Laboratory Research and Technology Division Wright-Patterson Air Force Base, Ohio 45433

13. ABSTRACT

This report presents the highlights of what has been ascertained about the interactions of liquid and vapor sodium, NaK, potassium, lithium, and cesium with solid materials of potential use in practical liquid-metal systems. Data for inclusion were selected by the authors on the basis of their practical utility to designers and research workers. There has been an accelerating interest in alkali metals as (1) coolants for fast-breeder nuclear reactors, (2) coolants in space power plants, (3) Rankine-cycle working fluids in high-temperature nuclear reactors, (4) propellants in ion-propulsion engines, (5) seeding materials in magnetohydrodynamic generators, (6) space-charge dissipating media in thermionic generators, and (7) high-temperature hydraulic fluids. Prominent among the liquid-metals research efforts are studies directed toward finding the best containment material for a given alkali under a given set of operating conditions.

DD FORM 1 JAN 64 1473

Unclassified
Security Classification

Unclassified
Security Classification

14 KEY WORDS	LINK A		LINK B		LINK C	
	ROLE	WT	ROLE	WT	ROLE	WT
Compatibility	8	3				
Liquid metals	9	3				
Sodium	9	3				
NaK	9	3				
Potassium	9	3				
Lithium	9	3				
Cesium	9	3				
Containment	8	3				
Light metals	9	3				
Refractory metals	9	3				
Nickel-base alloys	9	3				
Iron-base alloys	9	3				
Cobalt-base alloys	9	3				
Superalloys	9	3				
Stainless steel	9	3				
Steel	9	3				
Chromium-alloy steels	9	3				
Zirconium	9	3				
Zirconium alloys	9	3				
Beryllium	9	3				
Columbium	9	3				
Columbium-base alloys	9	3				
Vanadium	9	3				
Vanadium-base alloys	9	3				
Tantalum	9	3				
Tantalum-base alloys	9	3				
Molybdenum	9	3				
Tungsten	9	3				
Uranium	9	3				
Thorium	9	3				
Braze alloys	9	3				
Graphite	9	3				
Cermets	9	3				
Ceramic materials	9	3				
Bearing materials	9	3				